Cheiron School, SPring-8, Japan
October 2, 2012

Studies on atoms and molecules using synchrotron radiation and free electron lasers

Kiyoshi Ueda
Institute of multidisciplinary research for advanced materials
Tohoku University, Sendai 980-8577, Japan

Introduction of myself

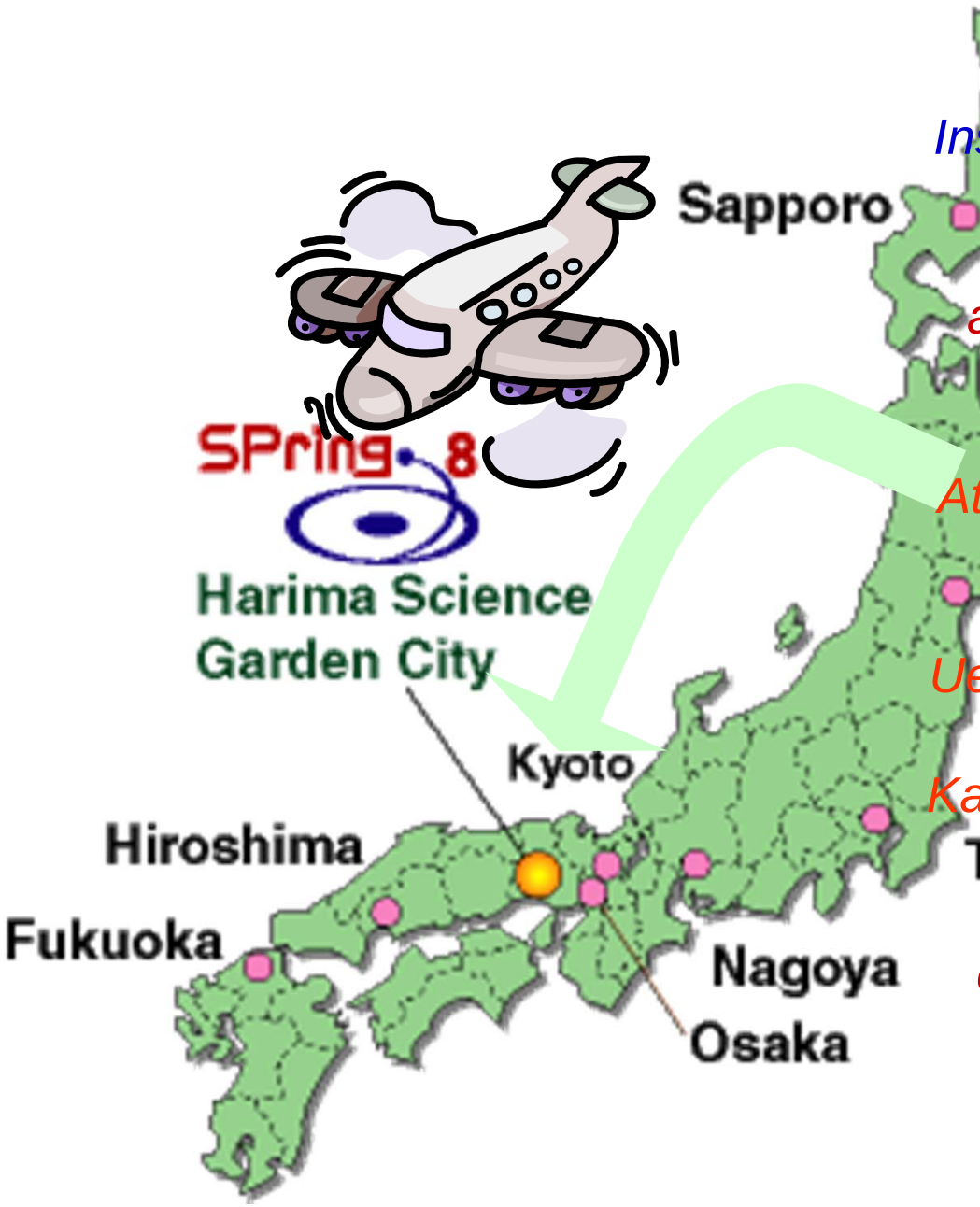

Prof. Kiyoshi Ueda
at
Tohoku University（Sendai）
Institute of multidisciplinary research for advanced materials
Leading
a research group for electron and molecular dynamics

Atomic and molecular science using Synchrotron Radiation
Ueda, JPB 36, R1 (2003);
Ueda & Eland, JPB 38, S839 (2005);
Ueda, JPSJ 75, 032001 (2006);
Kabachnik et al. PR 451, 155 (2007).

Application of the SR-based experimental techniques to laser experiments
(femtosecond laser and FEL)

Outline

1. Introduction to quantum world

2. Atomic resonant photoemission spectroscopy

- Introduction to the quantum interference

3. Vibrationally-resolved core-level photoelectron spectroscopy

- Adiabatic approximation and Franck-Condon analysis

- Young's double-slit experiments

4. Multiple-ion momentum imaging

- Snapshots of molecular deformation within a few fs

5. Electron-ion momentum imaging

- Molecular-frame photoelectron angular distributions

6. Interatomic Coulombic decay

7. Characteristic properties of free electron lasers

8. Atomic multi-photon processes by FEL: from EUV to X

Photoelectric effect

When matter is shined by the light, electron is emitted from the surface.

(i) Frequency of the light needs to be larger than ν_0.
(ii) Kinetic energy of the electron is determined by the frequency of the light.
(iii) Number of electrons is proportional to the intensity of the light.

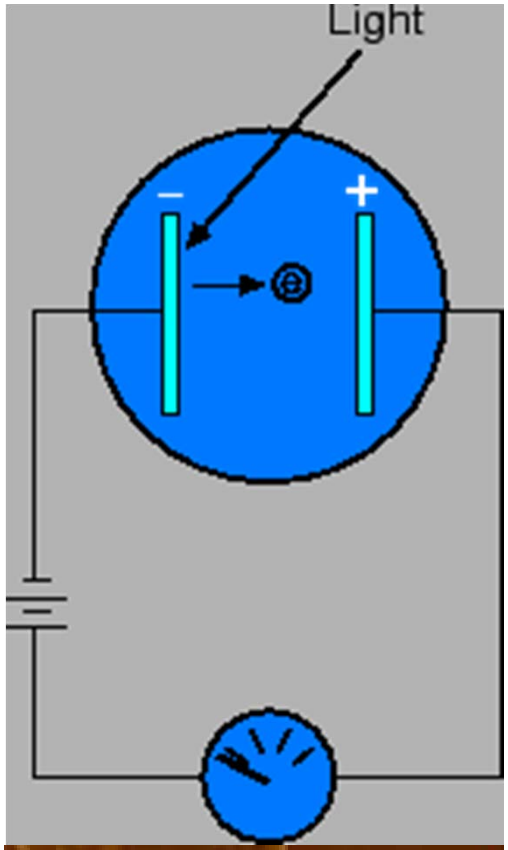

Einstein's explanation

Light at frequency of ν is considered to be a group of particles (photons) and each photon has energy $h\nu$.
An electron gets the energy $h\nu$ when it absorb one photon.
The electron in the matter is bound. For the electron to be emitted from the matter, the electron needs to receive the energy more than the work function *W.*
Then the kinetic energy *KE* of the emitted electron can be given as $KE = h\nu - W$.

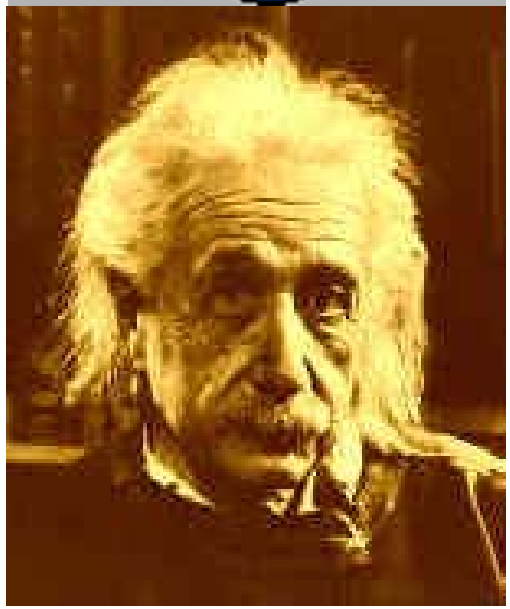

Photoelectron spectroscopy (UPS, XPS)

Precision measurements for kinetic energies of photoelectrons emitted via Einstein's photoelectric effects

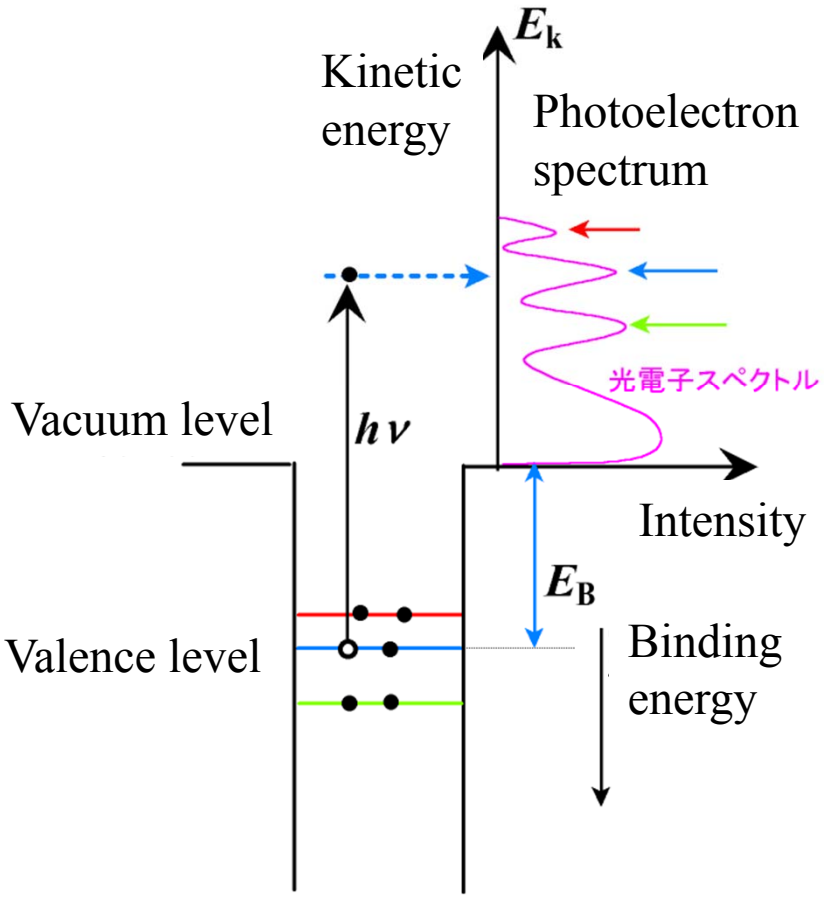

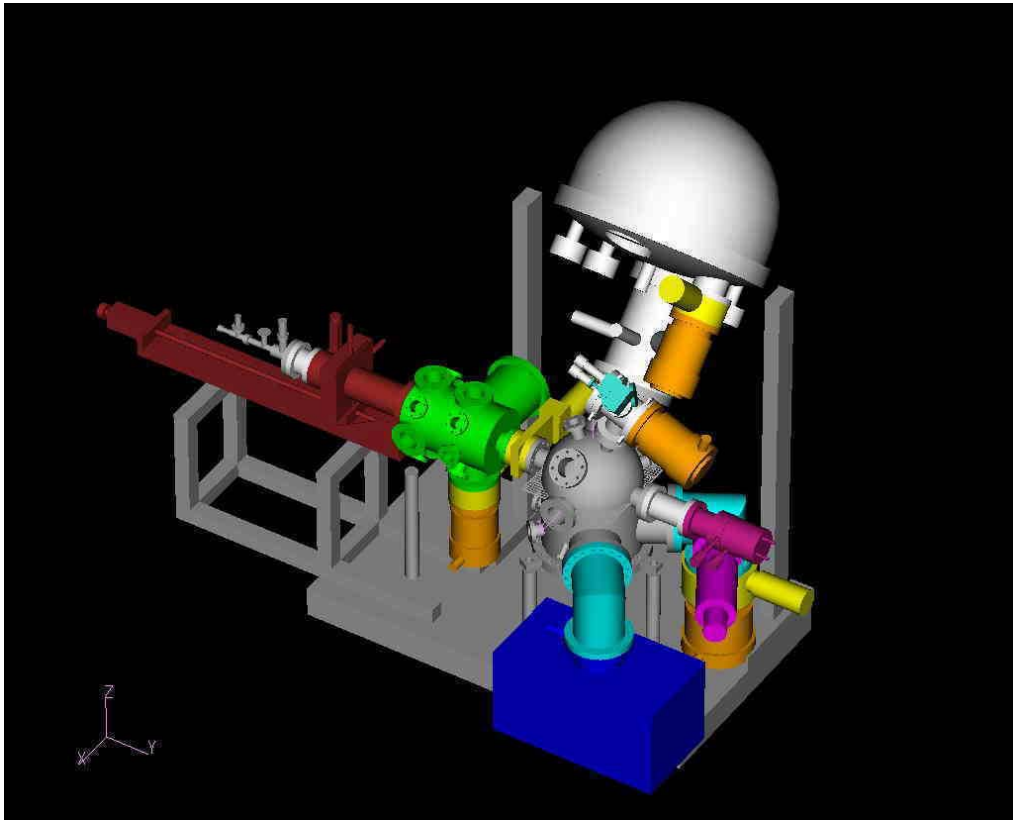

Balmer and Rydberg formulae

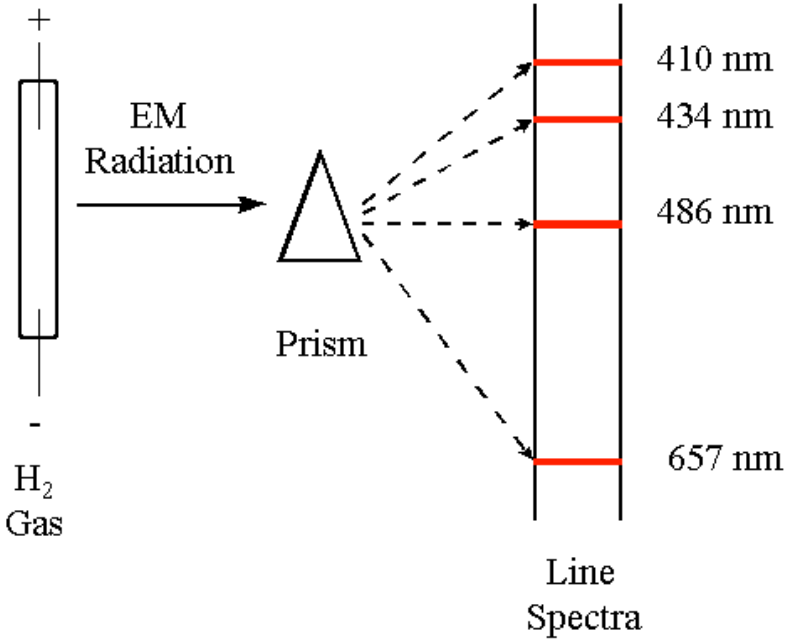

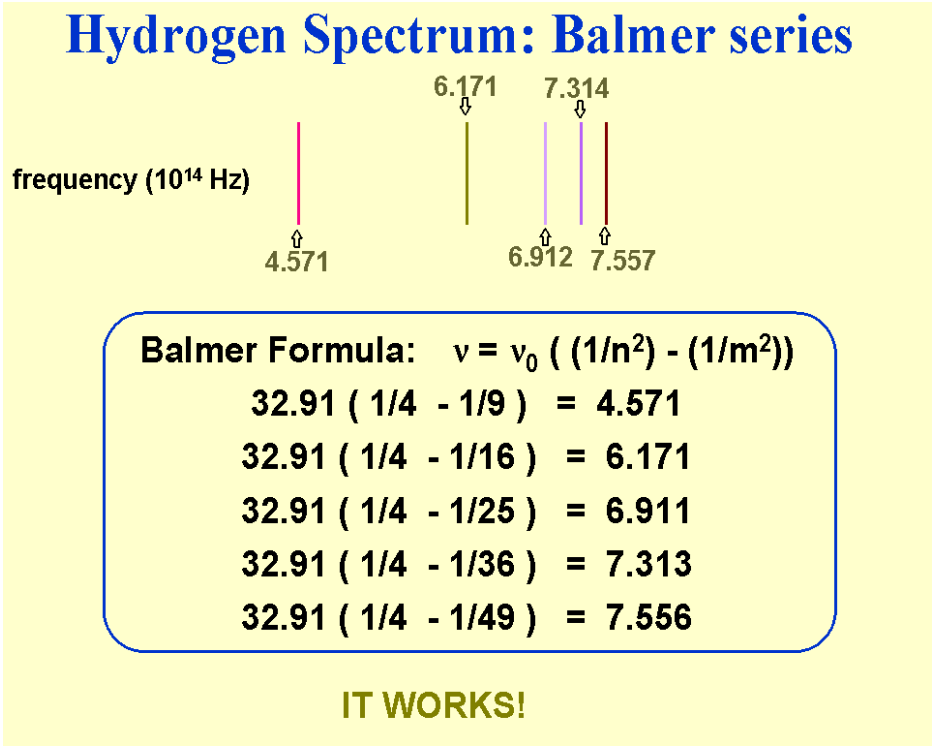

Balmer found beautiful regularity in the H spectrum!

Rydberg formula : $$\frac{\nu}{c} = \frac{1}{\lambda} = R\left(\frac{1}{n^2} - \frac{1}{n'^2}\right)$$

c, speed of light; λ, wavelength; *R*, Rydberg constant (*R* =109737.309 cm^{-1})

Bohr's atomic model

Electron orbits exist only when the classical orbits satisfy the following condition of quantization:

$$\int_0^{2\pi} p_\varphi \, \mathrm{d}\varphi = nh$$

φ, angle of rotation; $p_\varphi = m_e r^2 d\varphi / \mathrm{d}t$, angular momentum; r, radius; m_e, electron mass

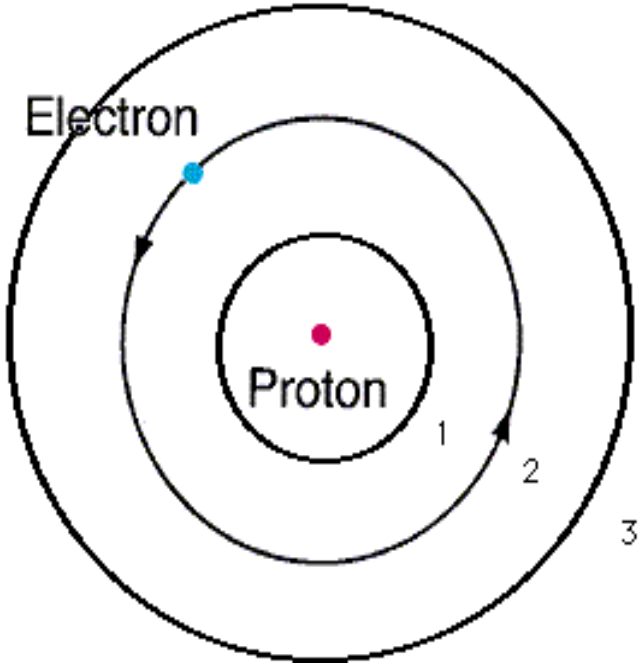

The electron binding energies are discrete:

$$\bar{E}_n = -hcR/n^2$$

De Broglie's matter wave and Bohr's model

$$Quantization\ :\ \int_0^{2\pi} p_\varphi \, \mathrm{d}\varphi = nh$$

$\lambda = h/p$ $\qquad$ $2\pi r_n = n\lambda = nh/p = nh/mv$

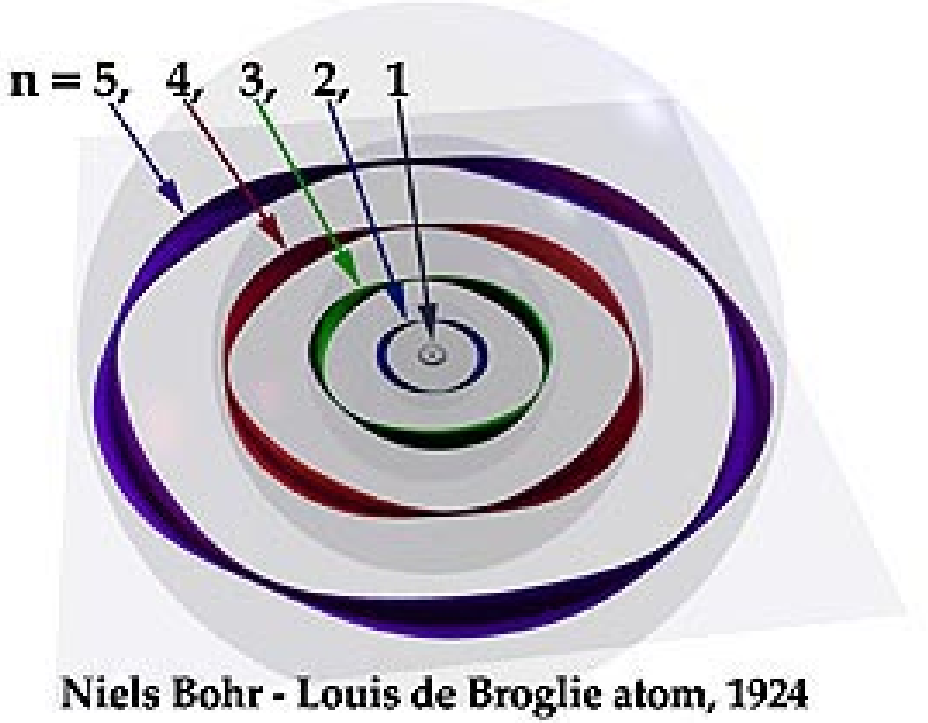

Niels Bohr - Louis de Broglie atom, 1924

Schrödinger equation of H atom (in atomic units)

$$H\Psi(r) = E\Psi(r)$$

$$H = T + U(r)$$ Hamiltonian

$$T = \frac{p^2}{2} = -\frac{1}{2}\frac{\partial^2}{\partial r^2}$$ kinetic energy

$$p = i\frac{\partial}{\partial r}$$ momentum

$$U(r) = -\frac{1}{r}$$ potential energy

$$E_n = -\frac{1}{2n^2}$$

Ψ: wave function
complex number (with phase!)

Atomic and molecular science now

Target: single atom or molecule; size: ~ 1 Å (= 0.1 nm = 10^{-10} m)

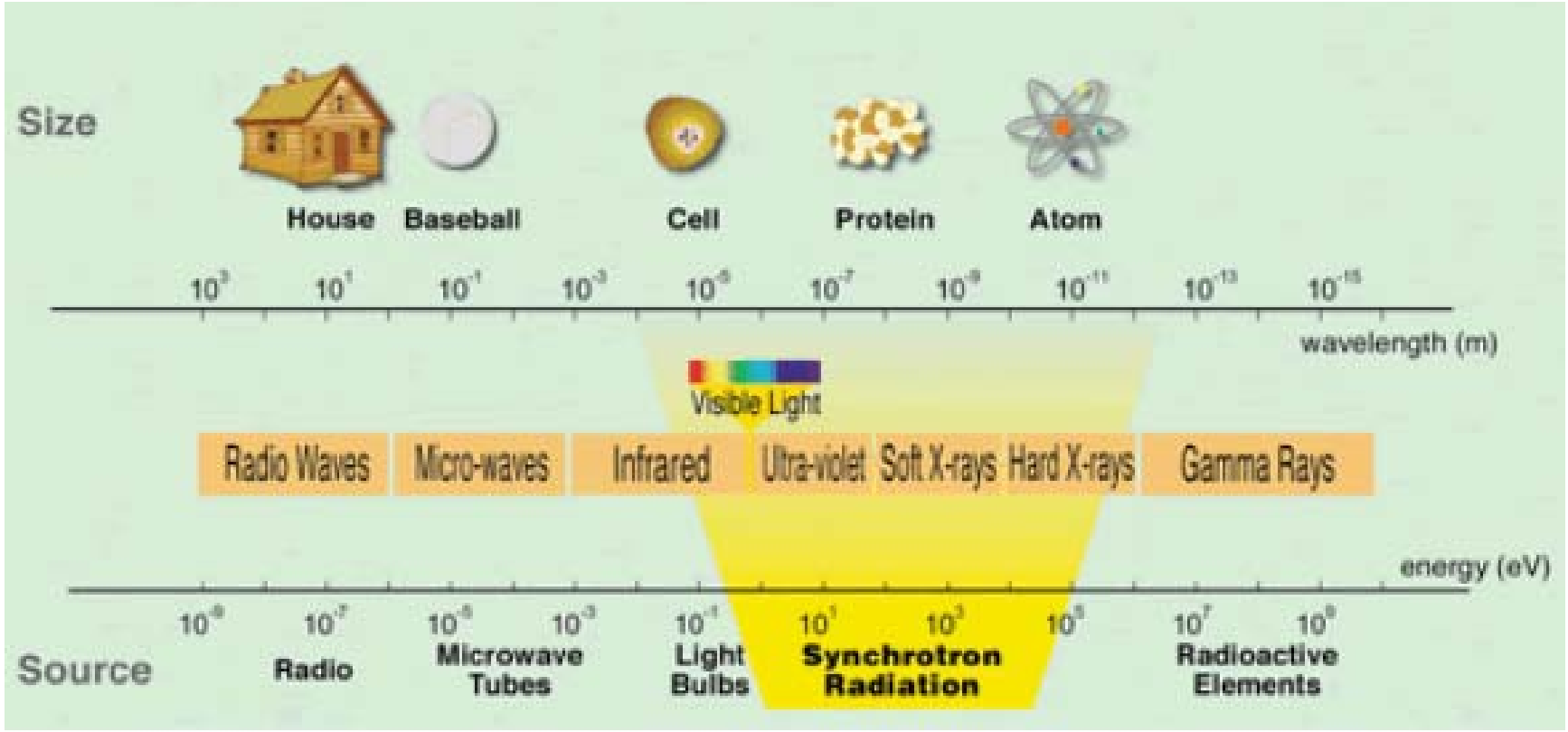

How to use synchrotron radiation to study atoms and molecules

We use monochromatic synchrotron radiation to excite atoms and molecules and to study their electronic structures as well as electron and nuclear dynamics in the excited states.

A single photon should be absorbed by a single atom or molecule first!

What photon energies to be used

Electron binding energies (eV) *Vacuum ultraviolet light!*

Element	K 1s	L_1 2s	L_2 $2p_{1/2}$	L_3 $2p_{3/2}$
1 H	13.6			
2 He	24.6*			
3 Li	54.7*			
4 Be	111.5*			
5 B	188*			
6 C	284.2*			
7 N	409.9*	37.3*		
8 O	543.1*	41.6*		
9 F	696.7*			
10 Ne	870.2*	48.5*	21.7*	21.6*

The experiments need to be in the vacuum!

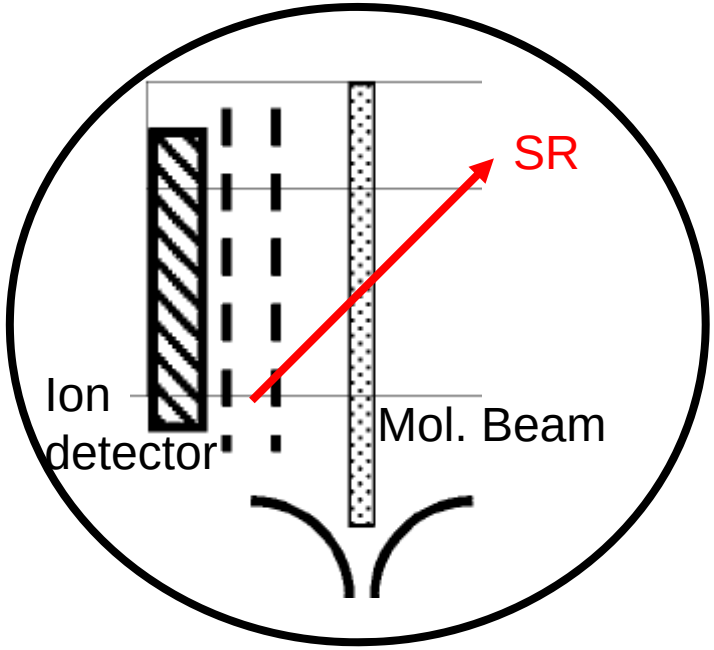

The easiest experiment: ion yield spectroscopy

SPring-8 BL27SU

Figure-8 undulator

- Linearly polarized light
- Horizontal polarization (1st)
- Vertical polarization (0.5th)

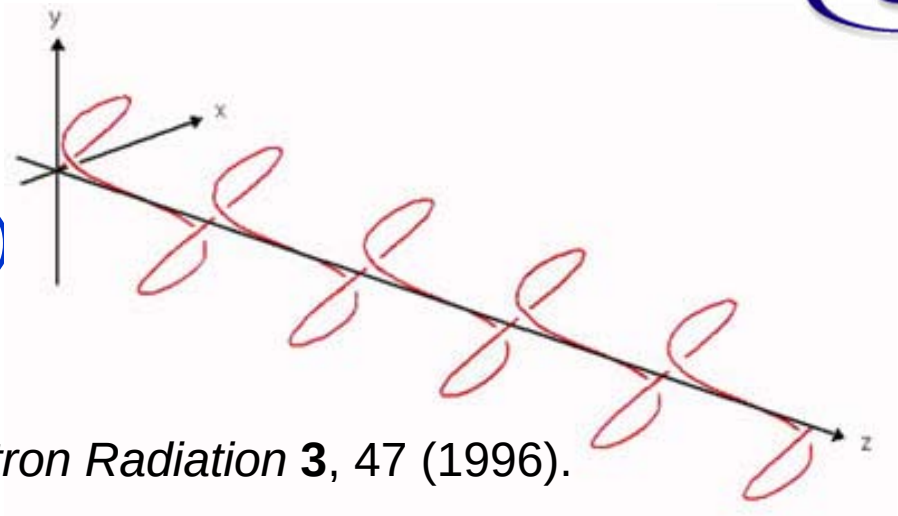

T. Tanaka and H. Kitamura, *J. Synchrotron Radiation* **3**, 47 (1996).

Soft X-ray monochromator

Hettrick type: varied line spacing plane grating

Energy range	0.15 ~ 2.5 keV
Photon Flux	> 10^{11} photon/s
Energy resolution	10000 - 20000

H. Ohashi, Y. Tamenori, E. Ishiguro *et al*. *Nucl. Instr. Methods A* **467**, 533 (2001).

Ne 1s total ion yield spectrum

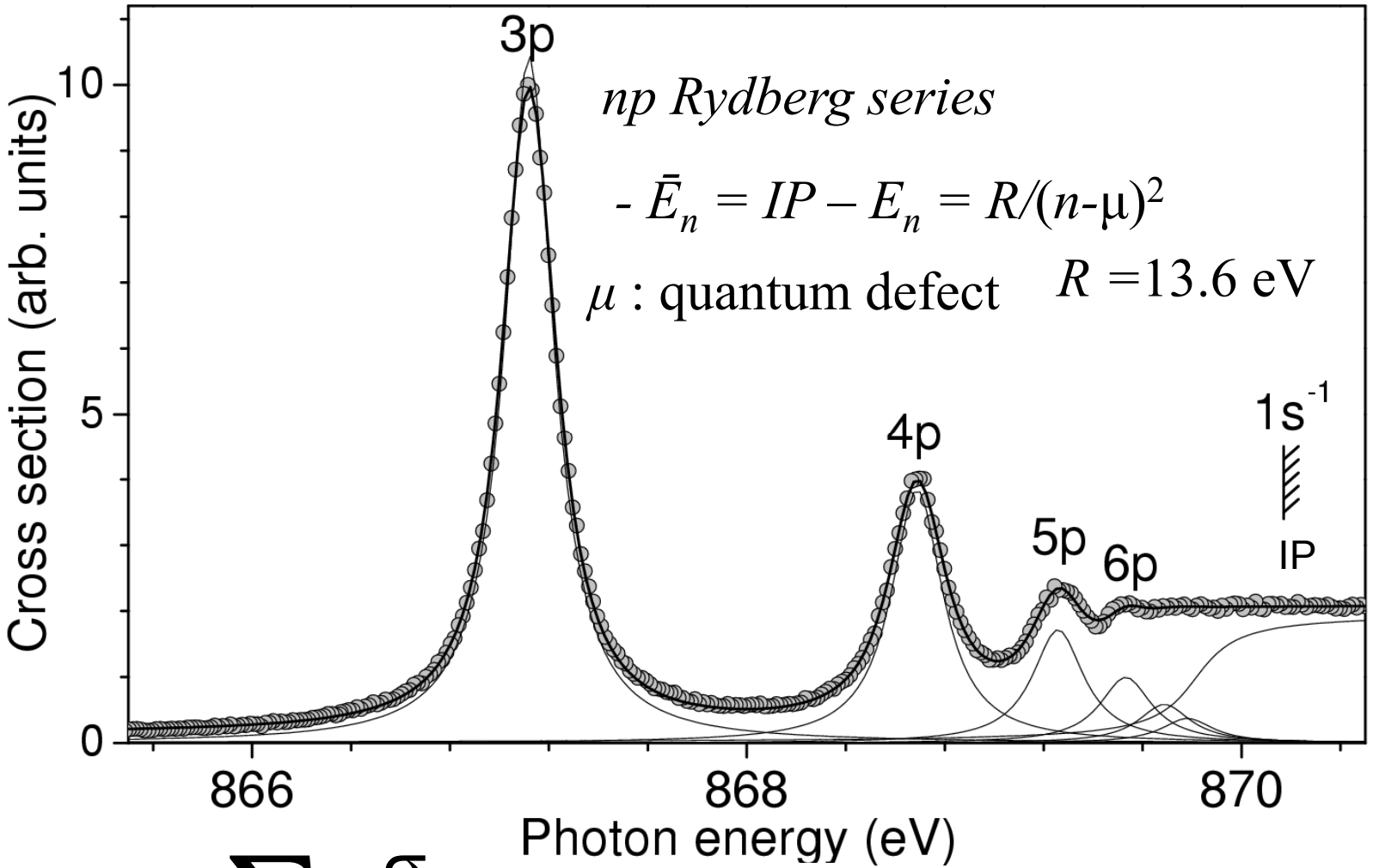

$$\sigma = \sigma_{dir} + \sum_n \frac{\sigma_n}{1+\varepsilon_n^2} + \sigma_{1s} \qquad \varepsilon = (h\nu - E_n)/(\Gamma_n/2)$$

$$\sigma_n \propto 1/(n-\mu)^3 \qquad \Gamma_n = \text{const!}$$

Auger decay and Auger electron spectroscopy

(a) Core ionization

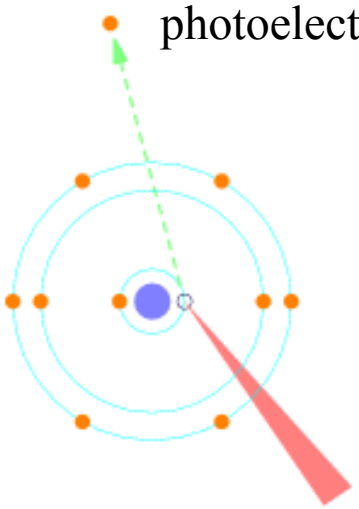

(b) Auger decay:

Core hole lifetime
defines the line width!

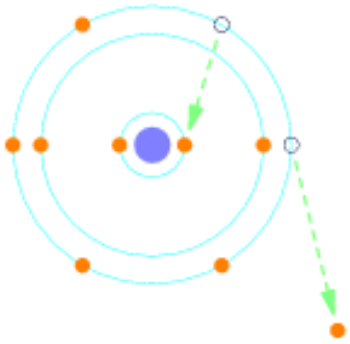

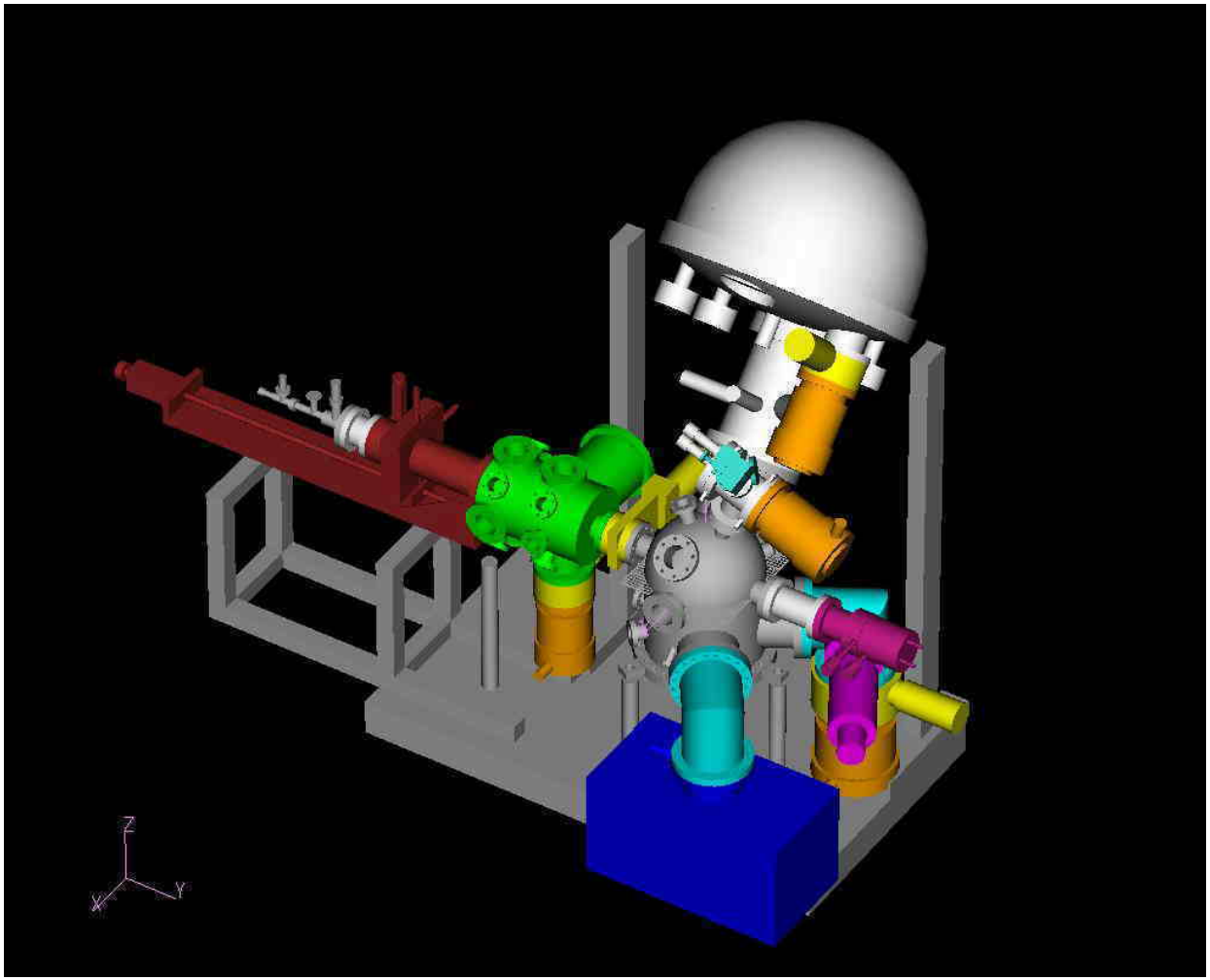

SES2002 analyzer

- Electrostatic hemispherical analyzer
  - Mean radius 200 mm
  - ΔE/PE=1/1600

  (66 meV at pass 100 eV)
  - **MCP+CCD camera**

  or MCP+Delay line anode

  - **Gas cell system**

  or Doppler-free molecular beam source

  Ueda *et al. PRL* . **90**, 153005 (2003)

  or effusive beam + momentum resolved ion spectrometer

  Prümper *et al.* PRA **71**, 052704, (2005).

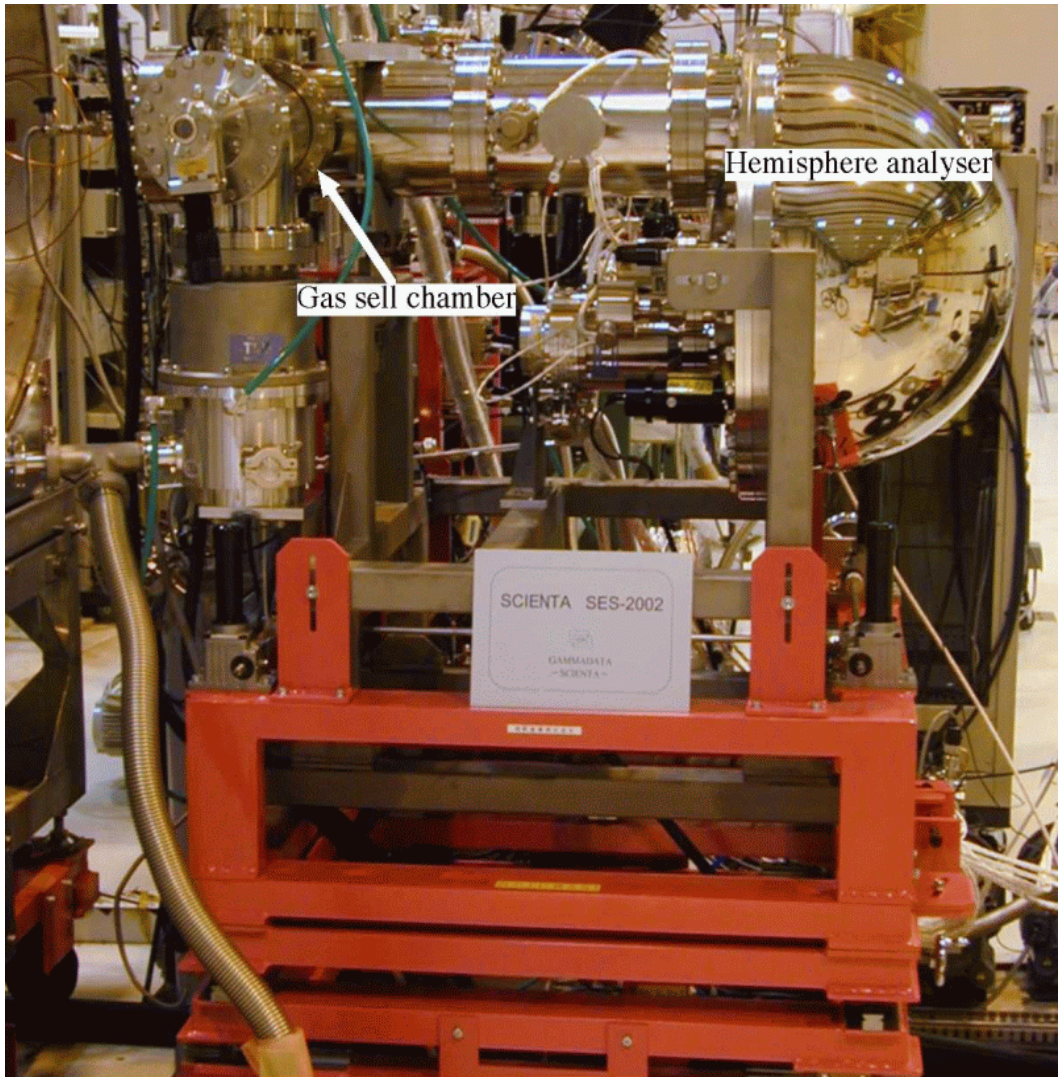

Angle-resolved resonant Auger spectra of Ne at 1s -> 3p excitation

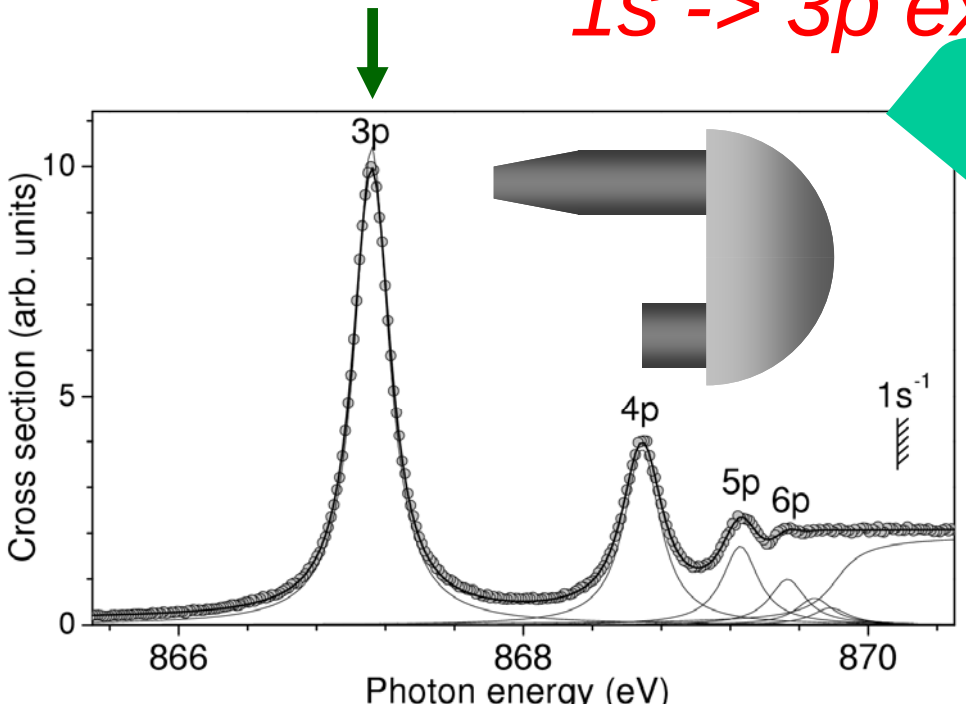

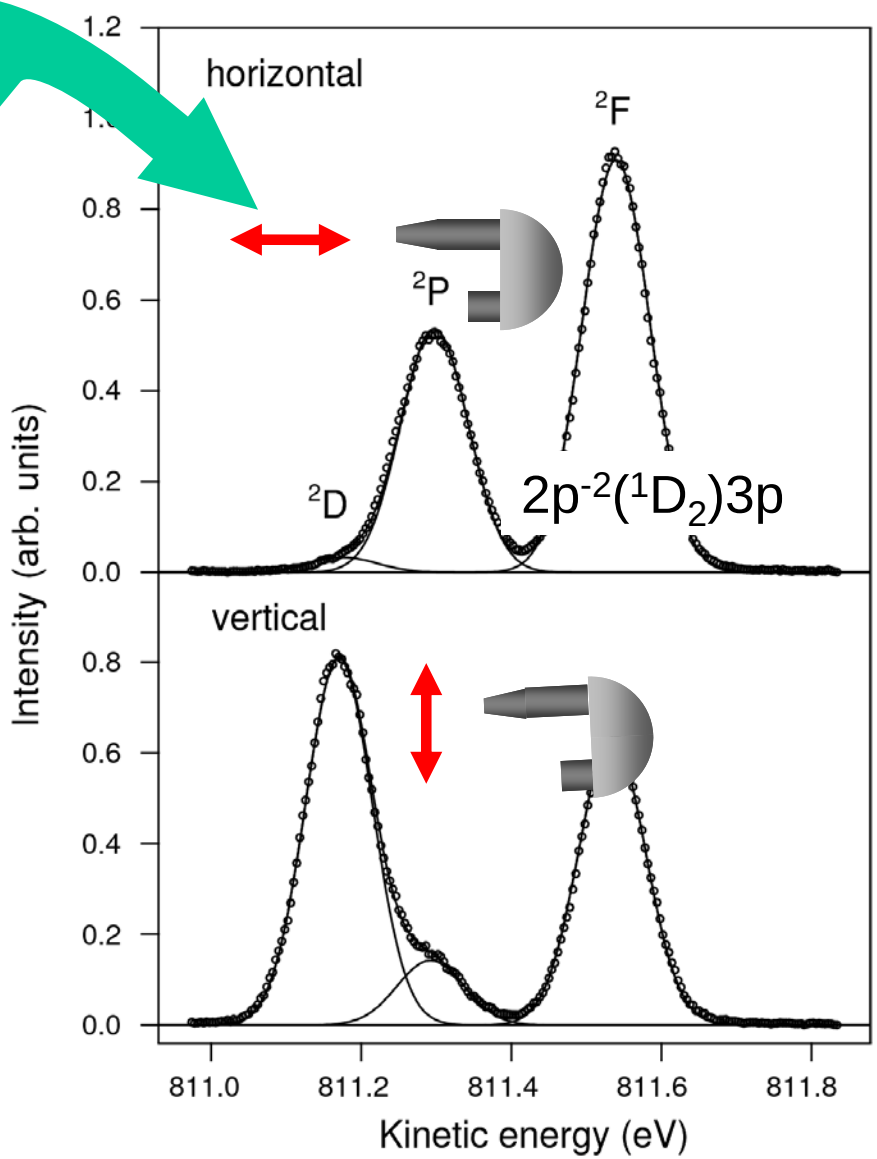

$$\frac{d\sigma}{d\theta} = \frac{\sigma}{4\pi}[1 + \beta P_2(\cos\theta)]$$

$$P_2(\cos\theta) = [3\cos\theta - 1]/2$$

β: asymmetry parameter

Measured angular distributions tell us how the angular momenta are coupled in the atom , allowing us the spectroscopic assignment !

Resonant Auger spectra of Ne "between" 1s -> 3p and 1s -> 4p excitations

$$\frac{d\sigma}{d\theta} = \frac{\sigma}{4\pi}[1 + \beta P_2(\cos\theta)] \qquad \sigma \propto I(0) + 2 \times I(90)$$

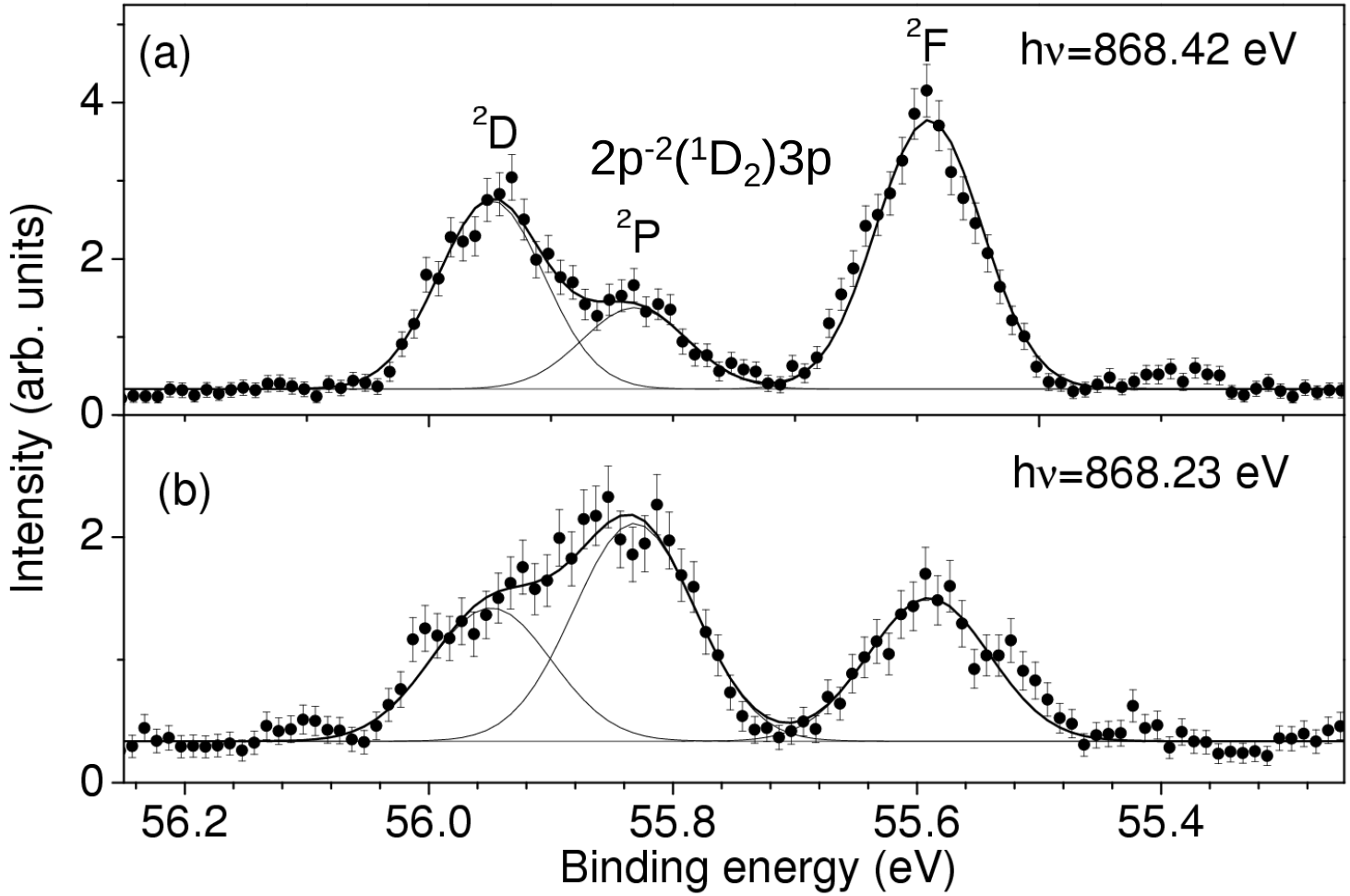

Interference effects between the two paths

$$A_\alpha = d_\alpha + \sum_n \frac{D_{n\alpha}}{i+\varepsilon_n}$$

$$\sigma_\alpha = |A_\alpha|^2$$

$$\varepsilon_n = (h\nu - E_n)/(\Gamma_n/2)$$

$$d_\alpha = \langle g|r|\alpha\rangle$$

$$D_{n\alpha} = \langle g|r|i_n\rangle\langle i_n|v|\alpha\rangle$$

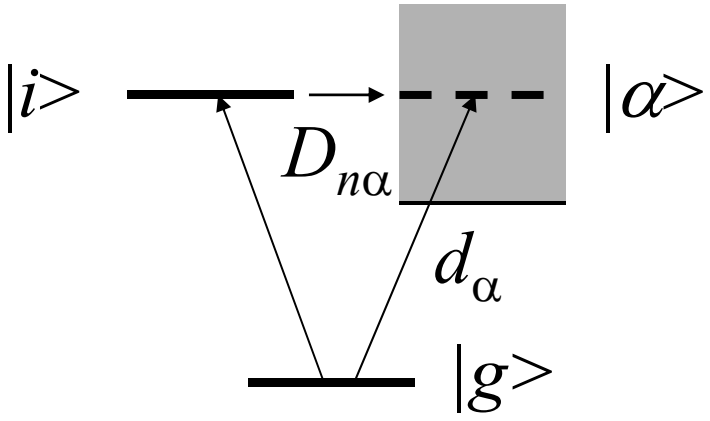

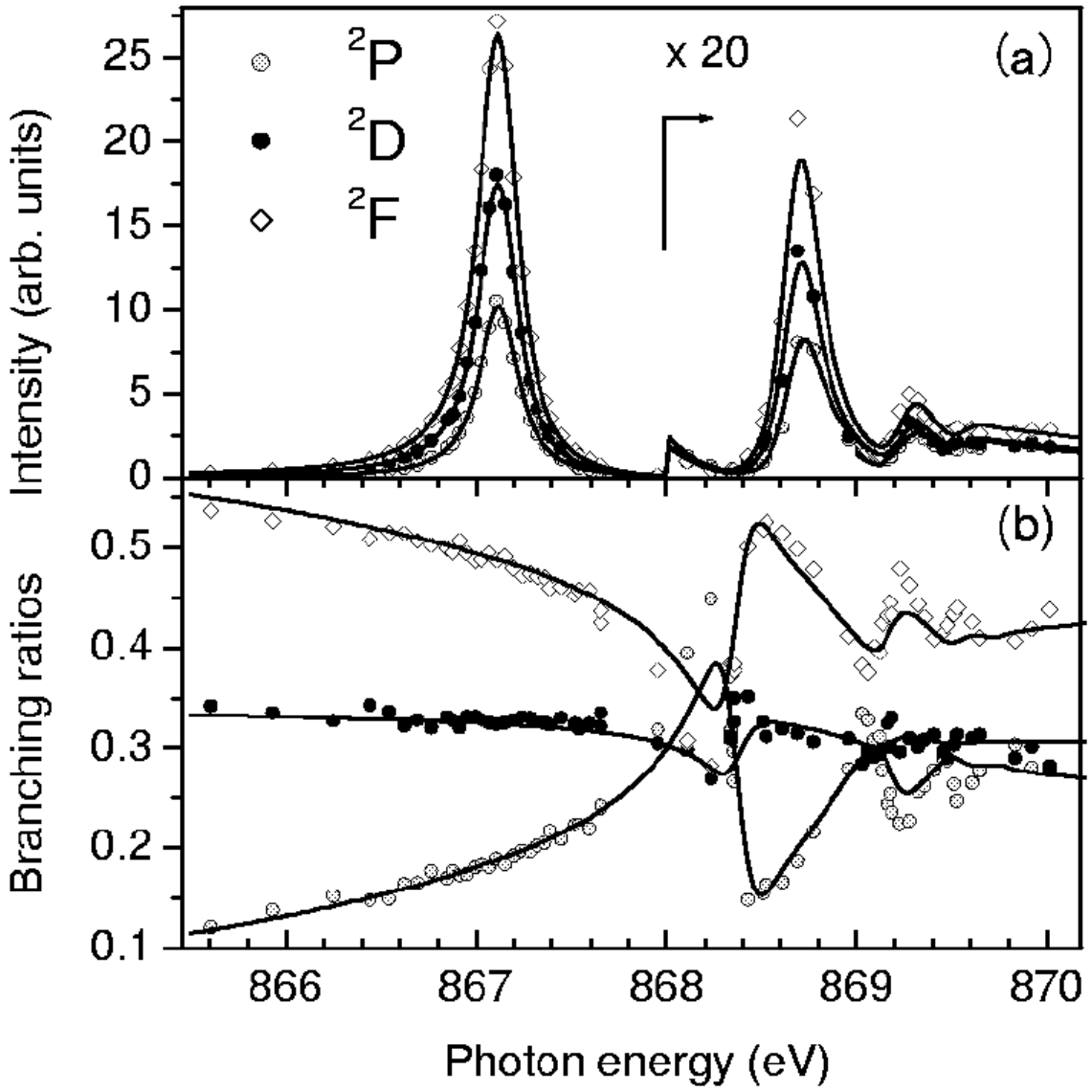

De Fanis *et al.* Phys. Rev. Lett. **89**, 023006 (2002).

Sendai City


Jozenji Street


Statue of Load Date

Introduction of molecular world

$$H\Psi(R,r) = E\Psi(R,r) \qquad H = T_R + T_r + V(r,R)$$

$$T_R = -\frac{\hbar}{2}\sum_k \frac{\partial^2}{M_k \partial R_k^2} \quad \text{KE of nucleus} \qquad T_r = -\frac{\hbar}{2m}\sum_j \frac{\partial^2}{\partial r_j^2} \quad \text{KE of electrons}$$

$$H = H_0 + T_R \qquad H_0 = T_r + V(r,R)$$

$$[H_0 - \varepsilon_n(R)]\varphi(R,r) = 0$$

$\varepsilon_n(R)$: adiabatic potential energy

$$\Psi(R,r) = \sum_n \Phi_n(R)\varphi_n(R,r)$$

$$[T_R + \varepsilon_m(R)]\Phi^0_{mv}(R) = E^0_{mv}\Phi^0_{mv}(R)$$

Nuclear motion is within the adiabatic potential energy surface!

Born-Oppenheimer approximation

Franck-Condon approximation for photoionization

$$\sigma^{+}_{iv'}(E) \sim \left| \int X^{*}_{iv'}(R) D_E(R) X_0(R) dR \right|^2$$

$X^{*}_{iv'}(R), X_0(R)$: Vibrational wavefunctions of ionic *iv'* and ground 0 states

$$D_E(R) = \int \varphi^{*}_{E}(r,R)\, r\, \varphi_{\text{core}}(r,R)\, \mathrm{d}r$$

$\varphi_E(r,R), \varphi_{\text{core}}(r,R)$: Electronic wavefunctions of the continuum *E* and core orbitals

Assume that the dipole moment $D_E(R)$ does not depend on R

$$\sigma^{+}_{iv'}(E) \sim \left| D_E(R_e) \right|^2 F(v'0)$$

$$F(v'0) = \left| \int X^{*}_{iv'}(R) X_0(R) \mathrm{d}R \right|^2$$ Franck-Condon factor

Vibrational intensity distribution in the photoelectron spectrum is determined by the Franck-Condon factors

Franck-Condon analysis based on harmonic approximation
Linear coupling model

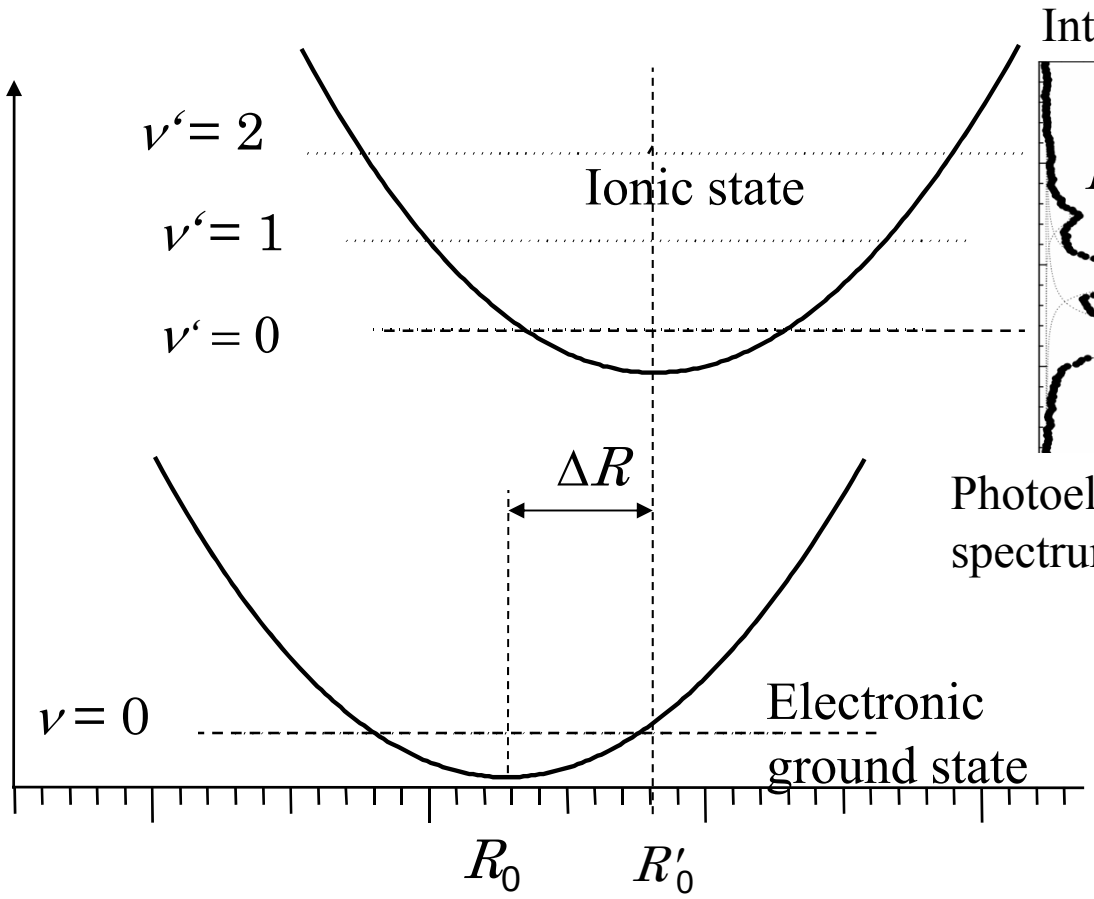

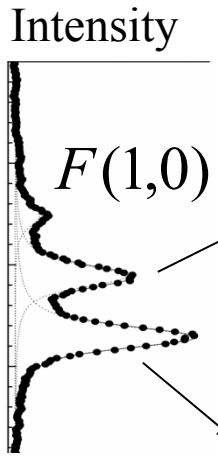

$$F(1,0) = \frac{\alpha(\Delta R)^2}{2}\exp\left(-\frac{\alpha(\Delta R)^2}{2}\right)$$

$$\alpha = \mu\omega/\hbar$$

$$F(0,0) = \exp\left(-\frac{\alpha(\Delta R)^2}{2}\right)$$

$$\frac{F(1,0)}{F(0,0)} = \frac{\alpha(\Delta R)^2}{2}$$

One can extract ΔR from photoelectron spectroscopy!

Franck-Condon analysis for the vibrational structure of the C 1s and O 1s mainlines of CO

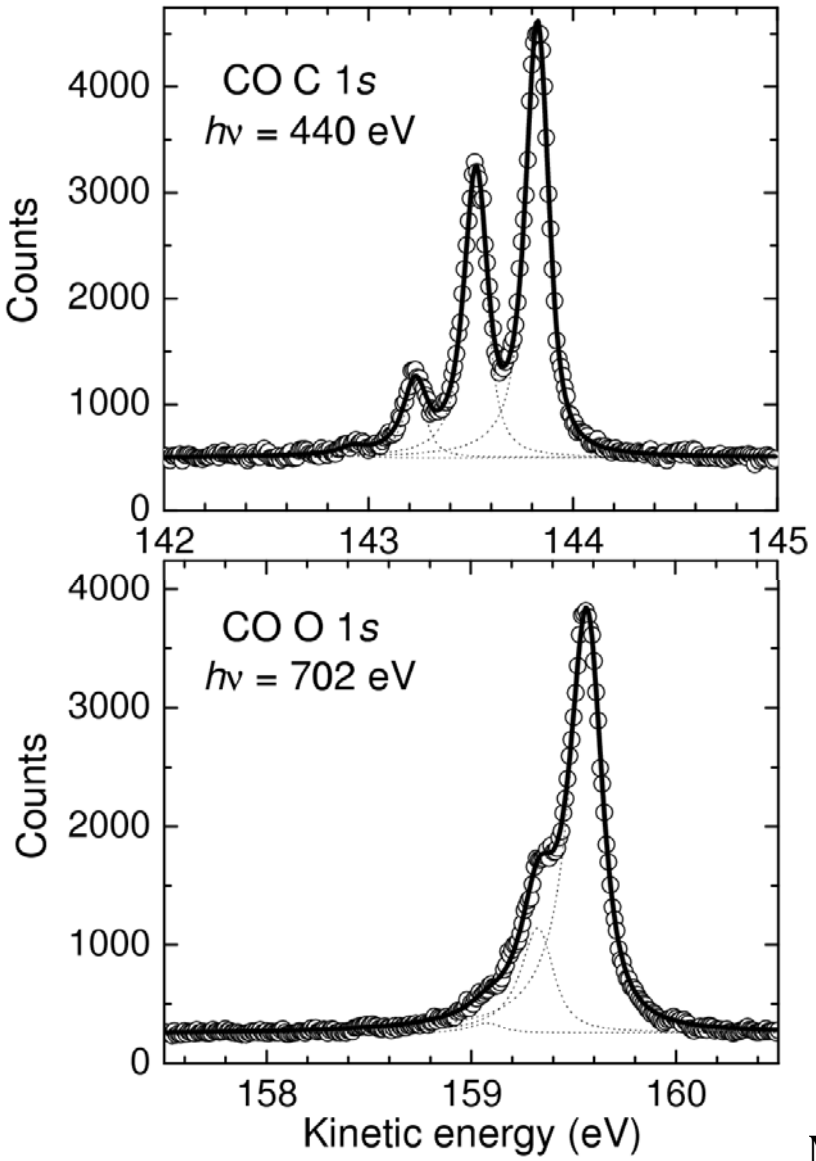

$I \sim |\langle \psi^{+}_{v} | \psi_0 \rangle|^2$: FC factor

ψ_0: v=0 vibrational wave function in the ground state

ψ^{+}_{v}: v-th vibrational wave function in the core-ionized state

Stable geometry of the core-ionized state extracted from the vibrational structure

	Exper.	Theory
C $1s^{-1}$		
ΔR_e (Å)	-0.051 (1)	-0.051
O $1s^{-1}$		
ΔR_e (Å)	0.037(2)	0.028

Matsumoto *et al.* Chem. Phys. Lett. **417**, 89-93 (2006).

Satellite spectrum in core-level photoemission in CO

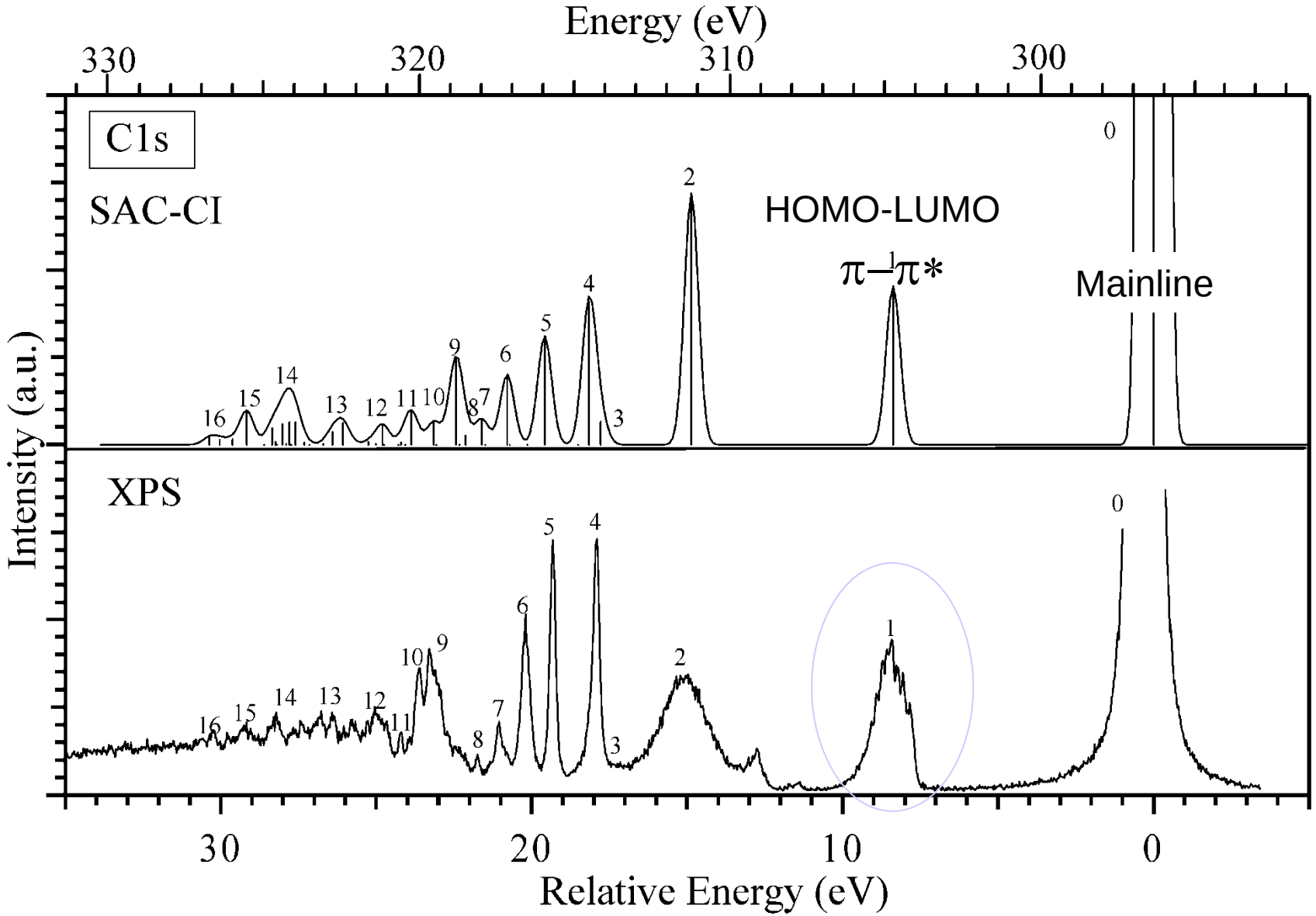

Ehara *et al.* J. Chem. Phys. **125**, 114304 (2006).

Franck-Condon analysis of the vibrational structure in the symmetry-resolved C 1s satellite bands of CO

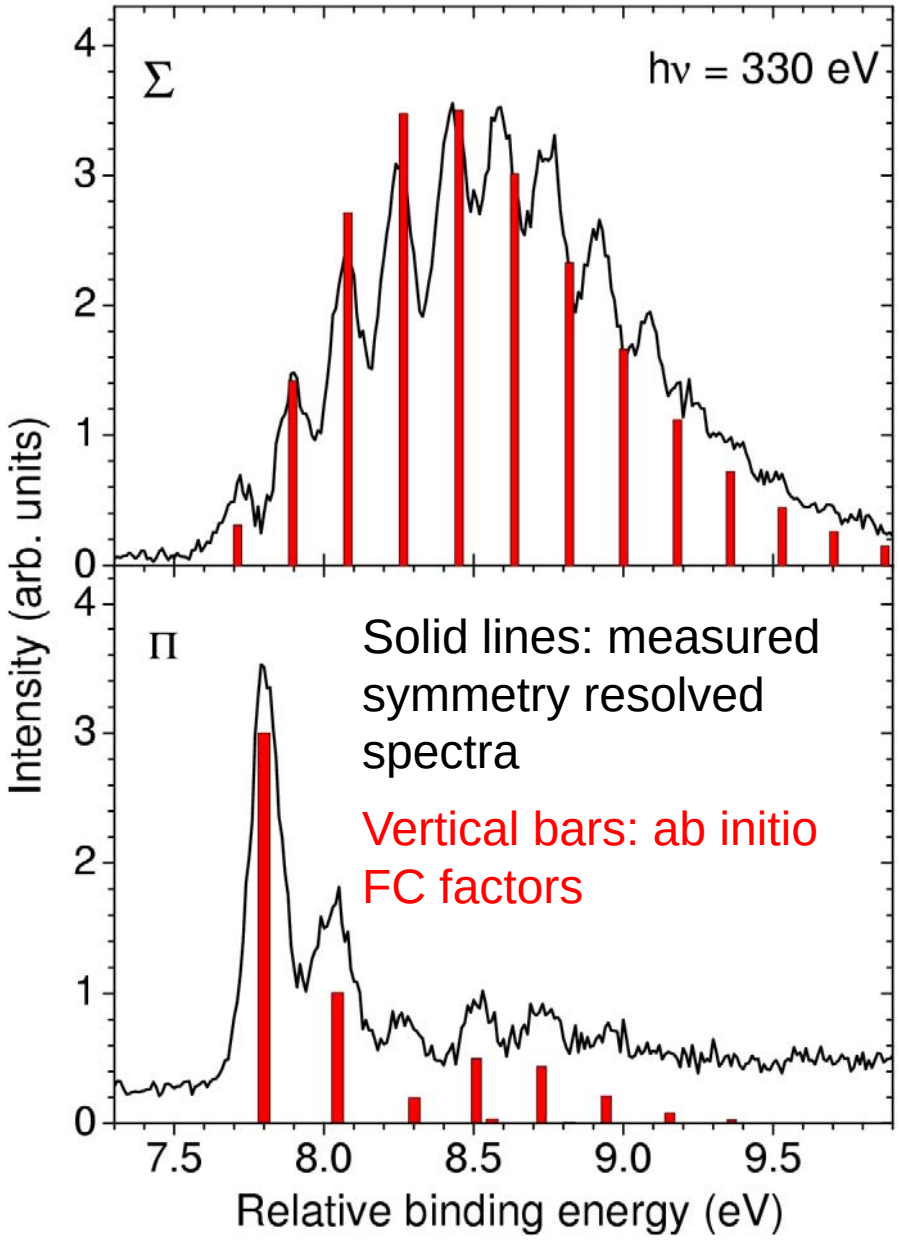

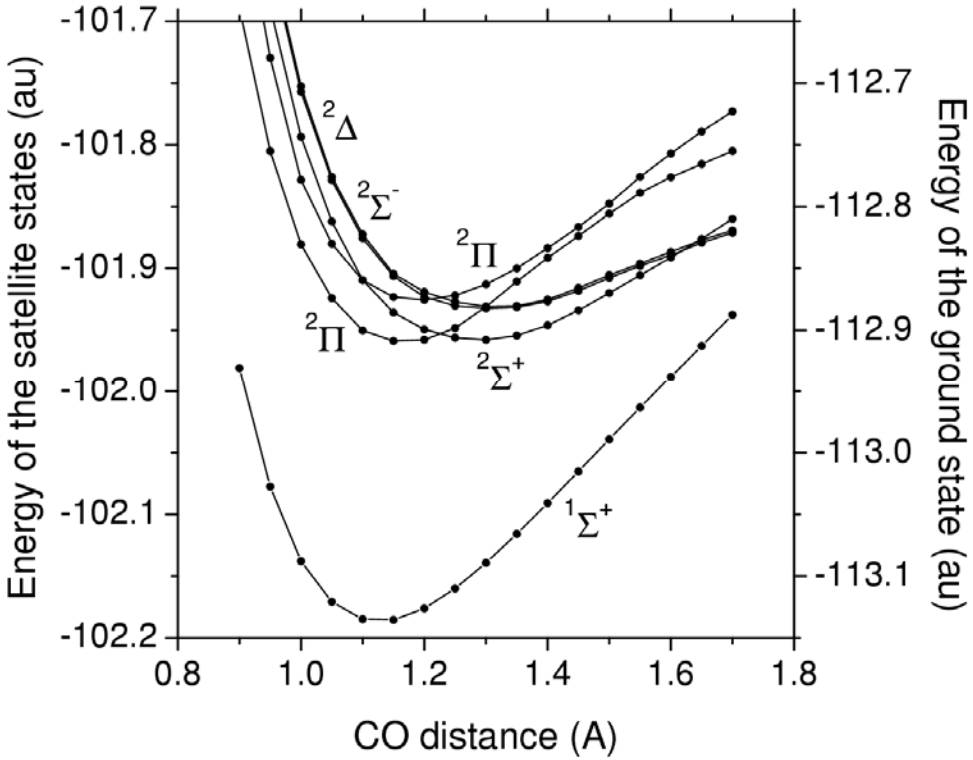

Ab initio potential curves

Ab initio FC factors reproduce the measured vibrational distributions.

Ueda *et al.*, Phys. Rev. Lett. **94**, 243004 (2005).

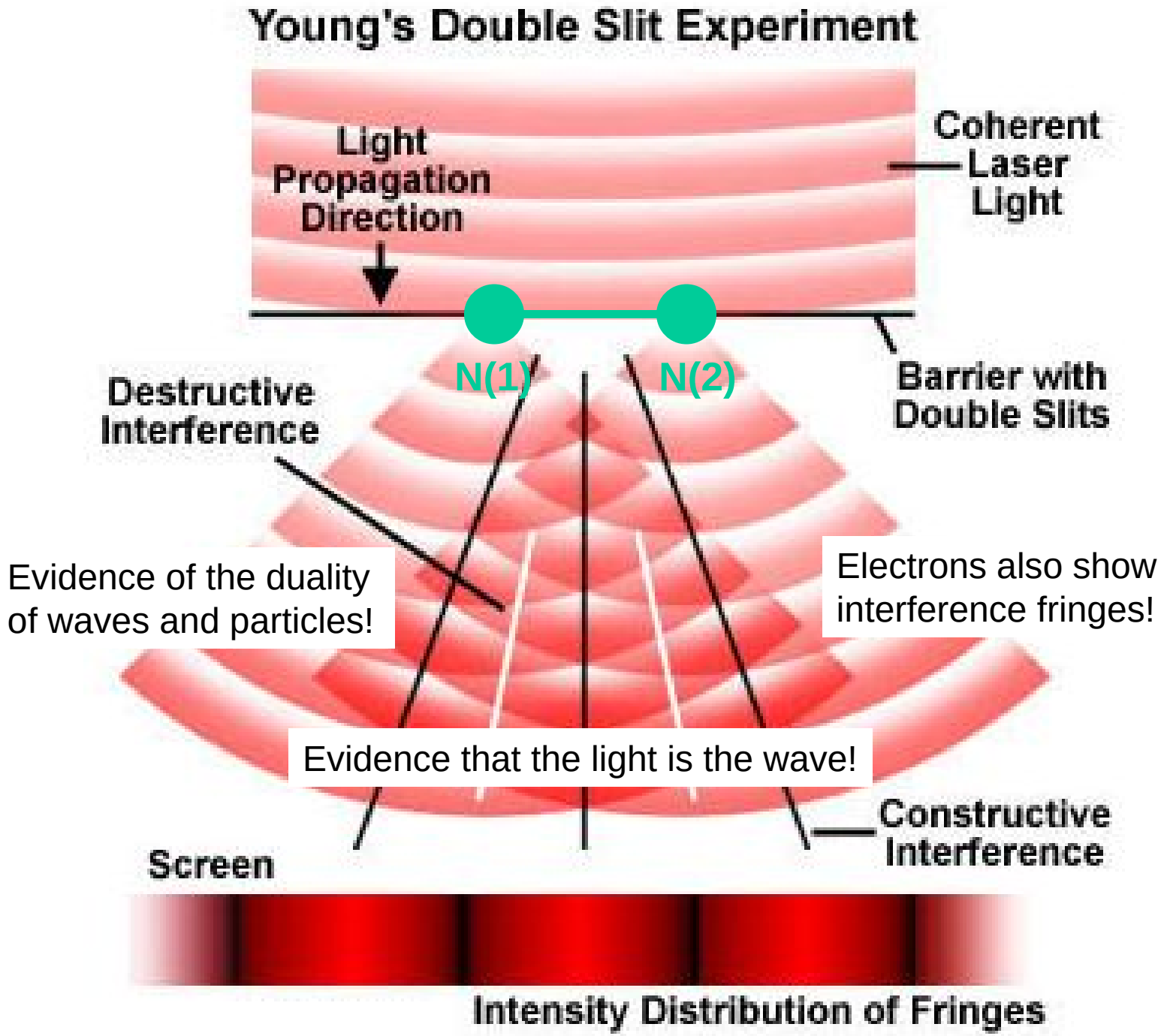
Young's Double Slit Experiment
Light Propagation Direction
Coherent Laser Light
N(1)
N(2)
Barrier with Double Slits
Destructive Interference
Evidence of the duality of waves and particles!
Electrons also show interference fringes!
Evidence that the light is the wave!
Constructive Interference
Screen
Intensity Distribution of Fringes

Franck-Condon analysis for the vibrational structure of the N 1s $1\sigma_u$ and $1\sigma_g$ mainlines of N_2

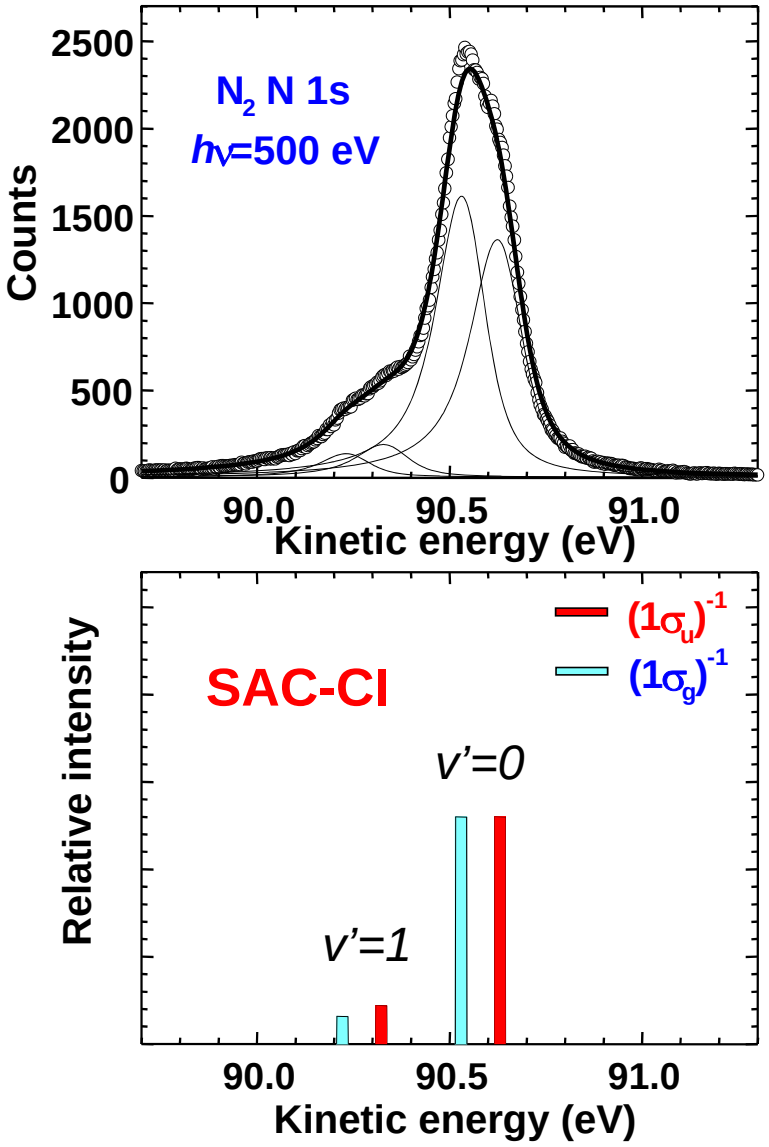

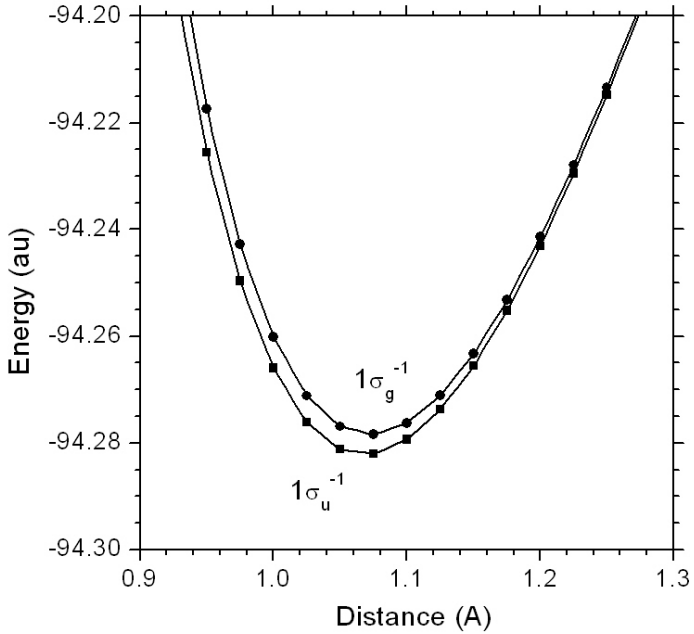

Equilibrium geometries of the core-ionized states extracted from the vibrational structure

	Exper.	Theory
N $1\sigma_u^{-1}$		
ΔR_e (Å)	-0.023(1)	-0.021
N $1\sigma_g^{-1}$		
ΔR_e (Å)	-0.018(1)	-0.017

Ehara *et al.* JCP **124**, 124311 (2006)

Cohen-Fano two-center interference

Two 1s ortibals in N_2 correspond to Young's double slits.

Molecular core-level ortibals: $1\sigma_{g,u} = \dfrac{1s_1 \pm 1s_2}{\sqrt{2}}$.

Core-level photoemission from fixed-in-space N_2:

$$\sigma_{g,u}(\omega) \propto \frac{1}{2}\left|e^{i\mathbf{k}\cdot\mathbf{R}_1} \pm e^{i\mathbf{k}\cdot\mathbf{R}_2}\right|^2 = 1 \pm \cos(\mathbf{k}\cdot\mathbf{R}) \ ,$$

Two center photoelectron wave — *Interference fringe*

where k: photoelectron momentum; R_1,R_2: position vectors of N (1) and N(2)

$\mathbf{R} = \mathbf{R}_1 - \mathbf{R}_2.$

Orientational average: Cohen-Fano formula

$$\sigma_{g,u}(\omega) = \sigma_0(\omega)\left[1 \pm \chi_{\mathrm{CF}}(k)\right] \ , \ \ \chi_{\mathrm{CF}}(k) = \frac{\sin kR}{kR}$$

Interference oscillatory structure becomes much smaller but remains!

H.D. Cohen and U. Fano, Phys. Rev. **150**, 30 (1966).

Ab initio N 1s $1\sigma_u$ and $1\sigma_g$ photoionization cross sections of N_2

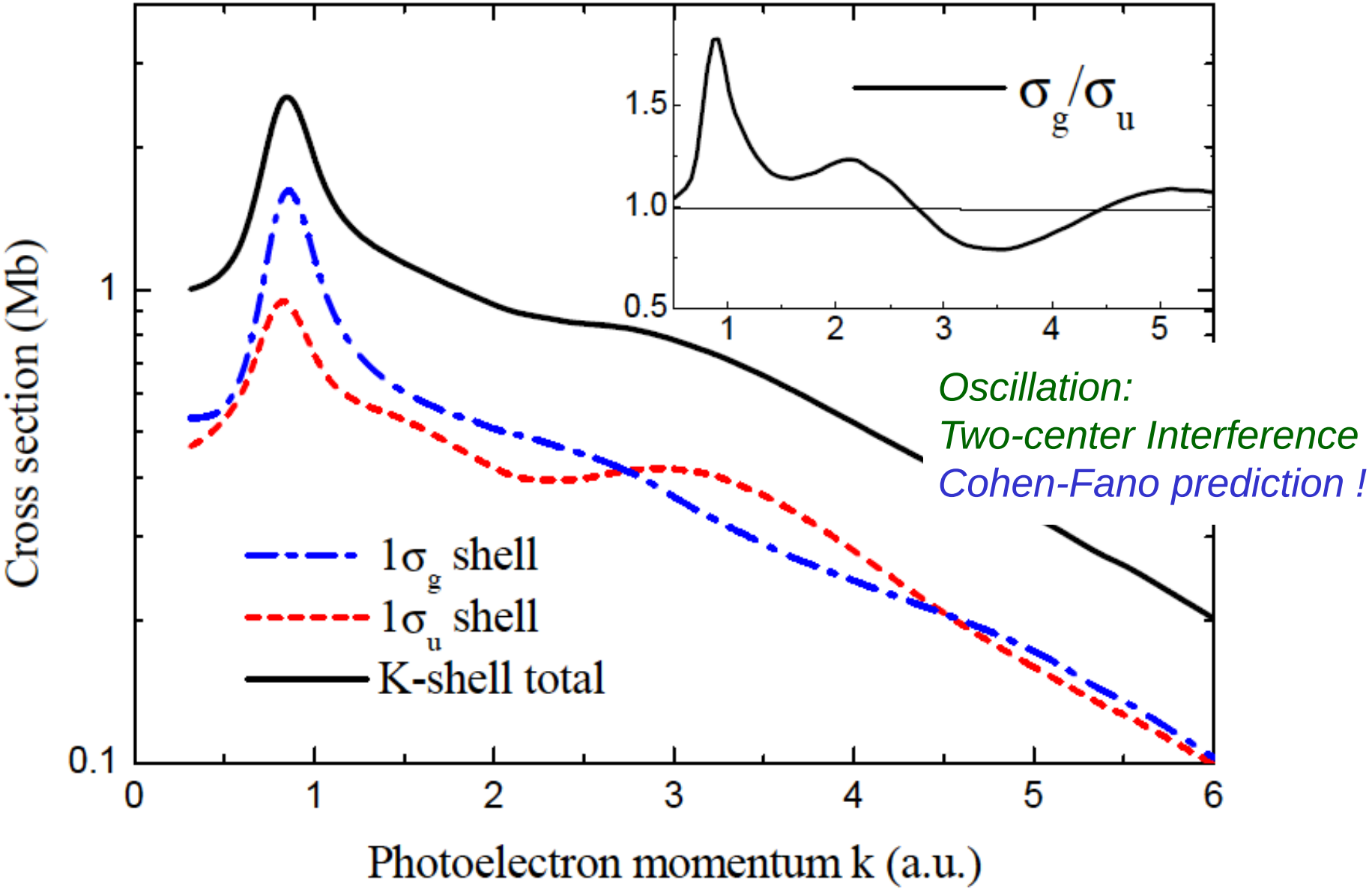

Semenov *et al*., J. Phys. B: At. Mol. Opt. Phys. 39, L261 (2006)

σ_g/σ_u ratio: experiment vs ab initio and Cohen-Fano

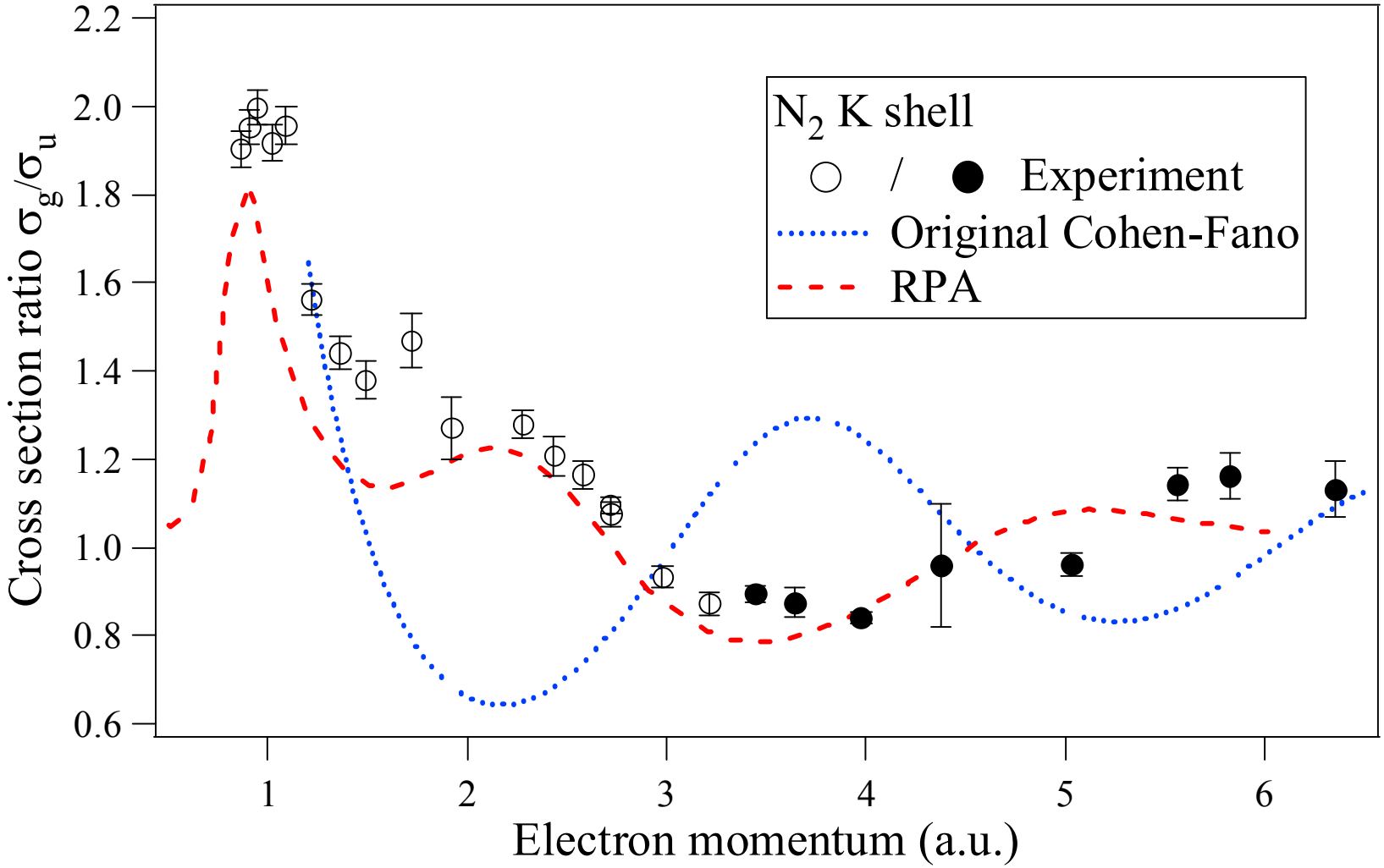

Both experimental and ab initio interference fringes shift from the prediction by Cohen-Fano formula!

Liu *et al.*, J. Phys. B. **39,** 4801-4817 (2006); JESRP **156-158**, 73-77 (2007).

Photoelectron scattering by the neighboring N atom

The amplitude of the photoelectron wave from one center:

$$\psi_1 = \underbrace{\hat{\mathbf{k}} e^{i\mathbf{k}\cdot\mathbf{R}_1}}_{A_1} + \underbrace{\hat{\mathbf{R}} \frac{e^{ikR}}{R} f(\vartheta) e^{i\mathbf{k}\cdot\mathbf{R}_2}}_{B_1} .$$

$$\psi_2 = A_2 + B_2$$

The amplitude of the photoelectron wave from two centers: $\psi_1 \pm \psi_2$

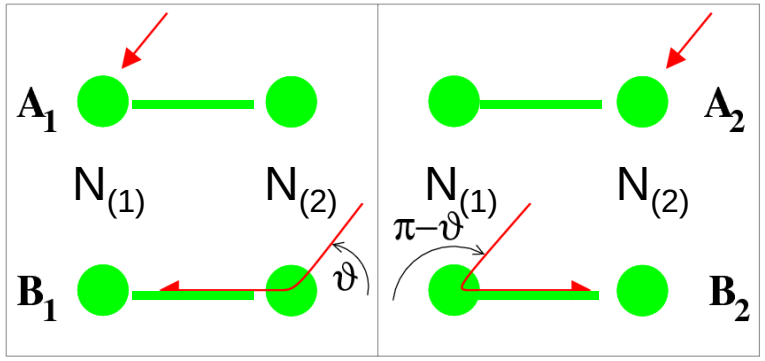

Cohen-Fano interference
A_1A_2 interference term

$$\chi_{CF}(k) = \frac{\sin kR}{kR}$$

The cross section~ $|\psi_1 \pm \psi_2|^2 = |(A_1+B_1) \pm (A_2+B_2)|^2$

$$\frac{\sigma_{g,u}(\omega)}{\sigma_0(\omega)} = 1 - \frac{1}{kR^2} \mathrm{Im}\left\{ f(\pi) e^{2i[kR+\delta_1(k)]} \right\} \pm \chi(k) ,$$

0

A_1B_1 and A_2B_2 one-center interference terms

$$\chi(k) = \frac{1}{kR} \sin\left[kR + 2\delta_1(k)\right]$$

δ_1(k): scattering phase

CF A_1A_2 interference term

A_1B_2 and A_2B_1 two-center interference terms !

Sendai
in summer

Tanabata festival

Multiple-ion coincidence imaging setup

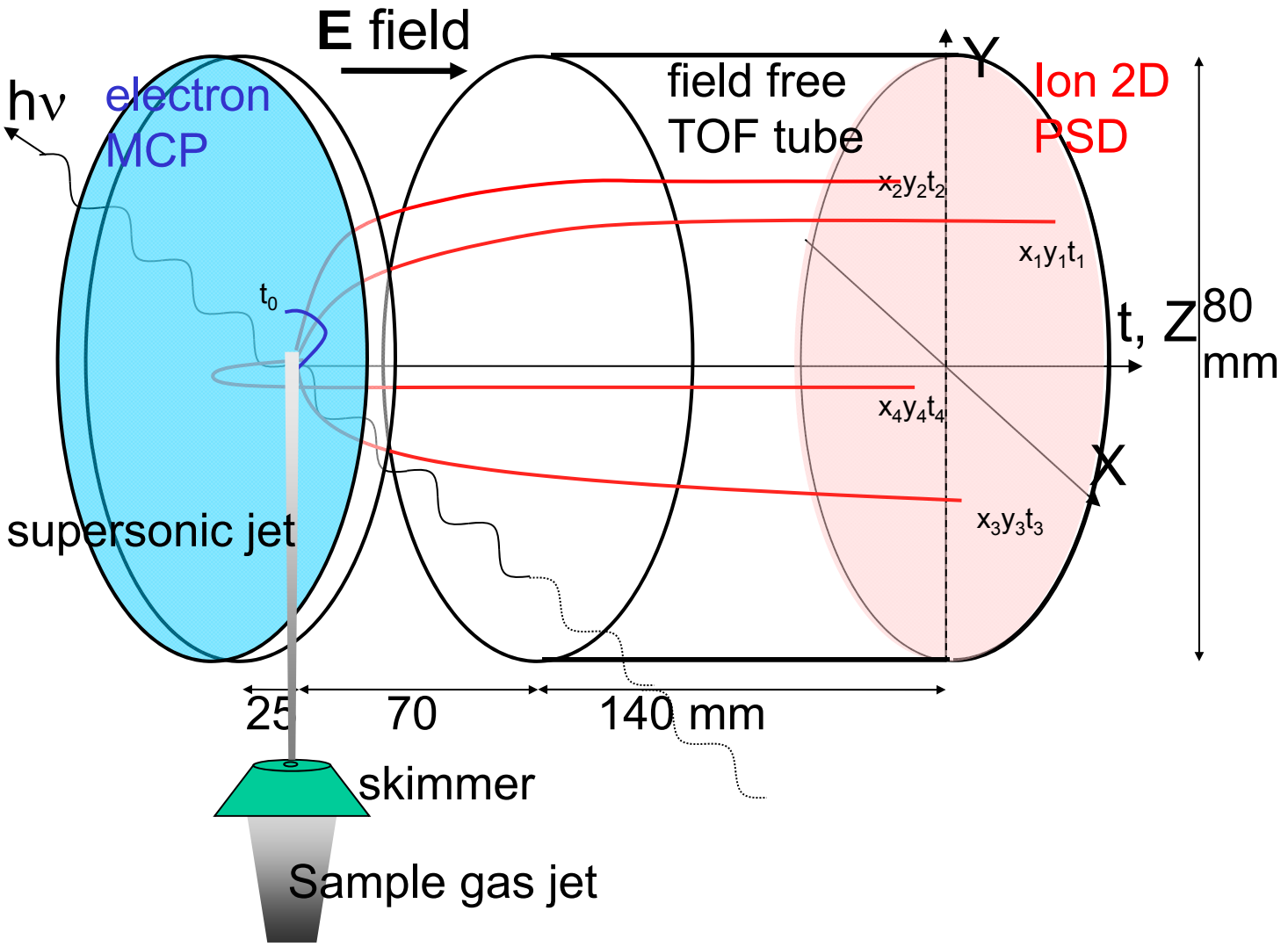

position & time of flight (x,y,t) → *3D momentum of each particle*

How to obtain 3D momentum

$$p_x = \frac{m(x - x_0)}{t}, \quad p_y = \frac{m(y - y_0)}{t}, \quad p_z = qE(t - t_0)$$

t: ion time-of-flight

t_o: ion TOF at rest

x, y: arrival position on the detector.

x_0, y_0 : initial position of the ion

m : ion mass

q: ion charge

E: electric field in the acceleration region

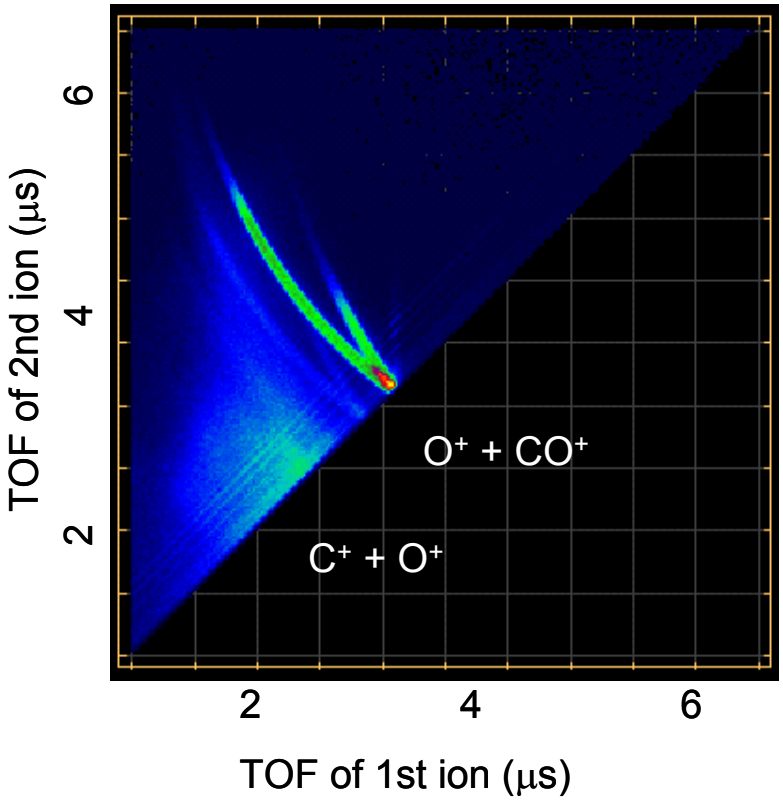

To be exact Pz becomes nonlinear → Iterative procedure

Total electron yield spectrum of CO_2 in the C1s excitation region

CO_2 ground state configuration:

$$\underbrace{1\sigma_g^{\,2}1\sigma_u^{\,2}}_{\text{O1s}}\underbrace{2\sigma_g^{\,2}}_{\text{C1s}}\underbrace{3\sigma_g^{\,2}2\sigma_u^{\,2}}_{\text{O2s}}\underbrace{4\sigma_g^{\,2}}_{\text{C2s}}$$

$$3\sigma_u^{\,2}1\pi_u^{\,4}1\pi_g^{\,4}(^1\Sigma_g^{\,+});\ 2\pi_u^{\,0}5\sigma_g^{\,0}4\sigma_u^{\,0}$$

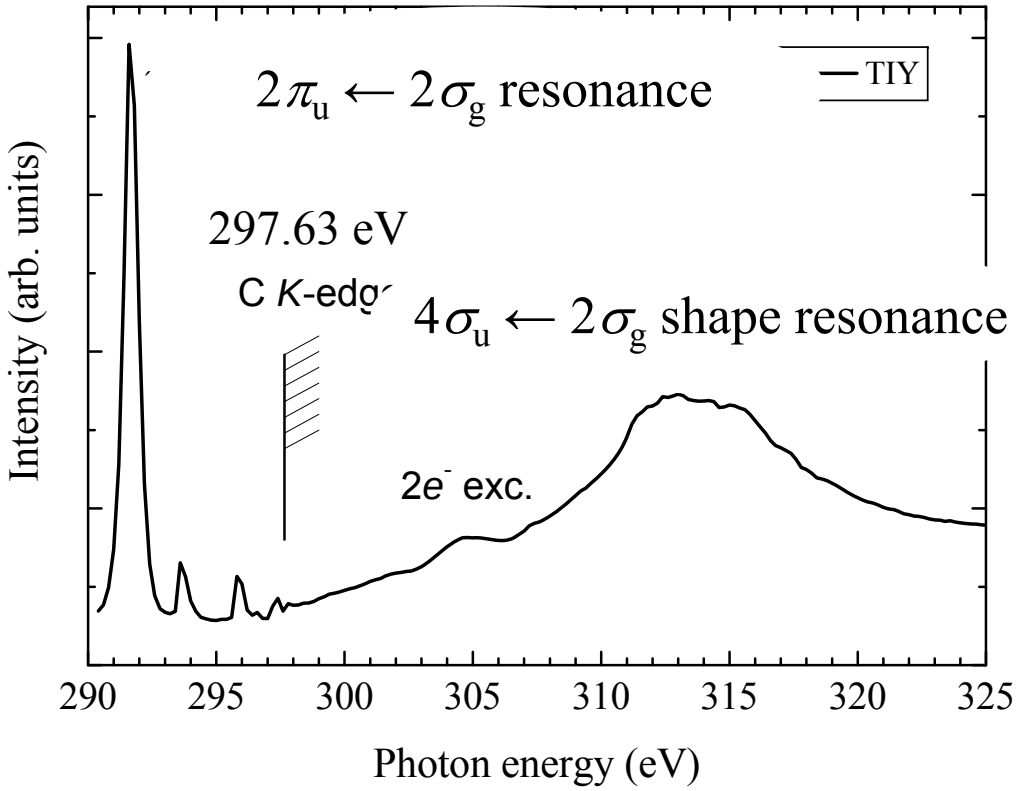

Renner-Teller splitting of CO_2

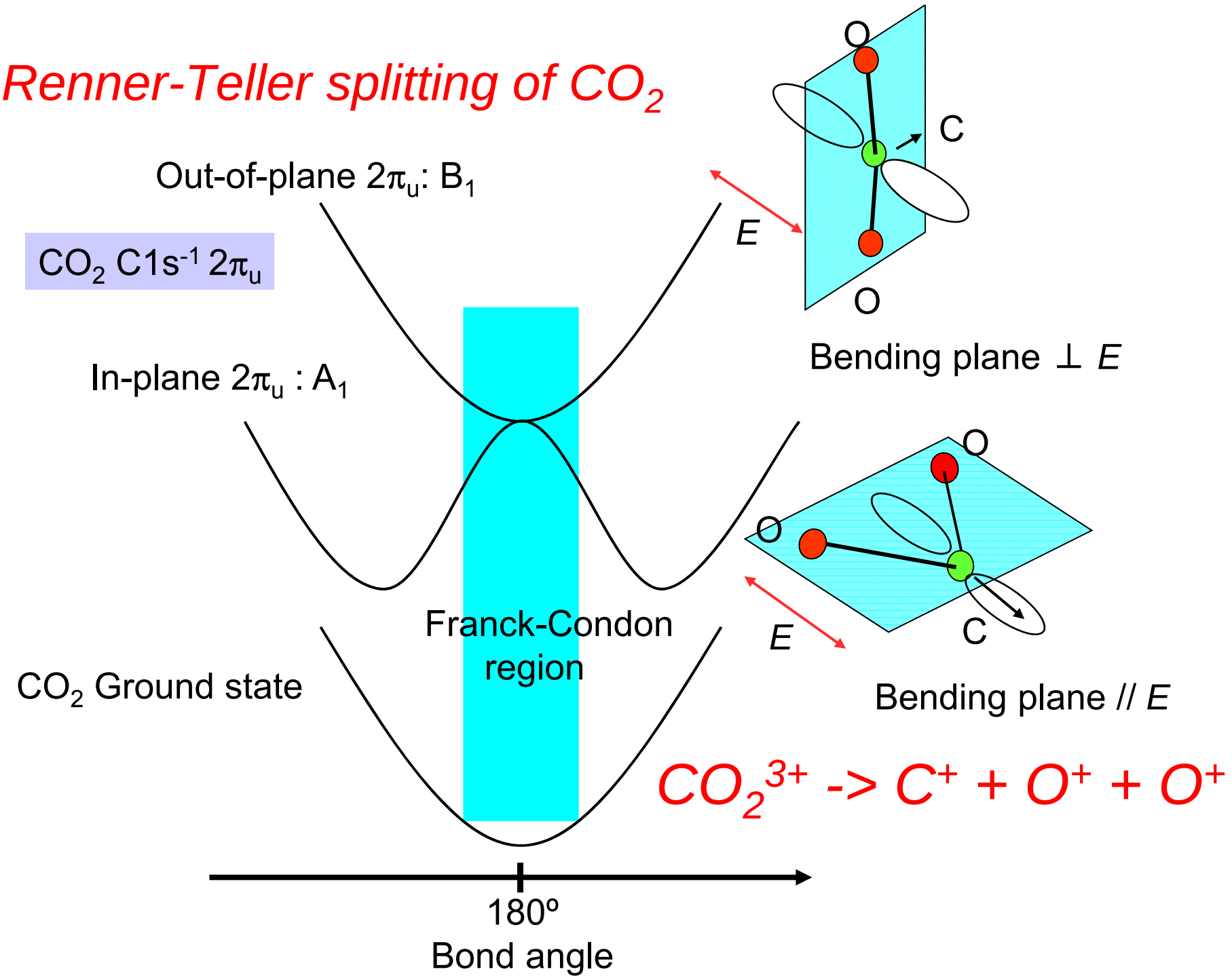

CO_2^{3+} -> C^+ + O^+ + O^+

Snapshot of the bending motion in the core-exited state with a liftetime ~7 fs

Newton Diagram

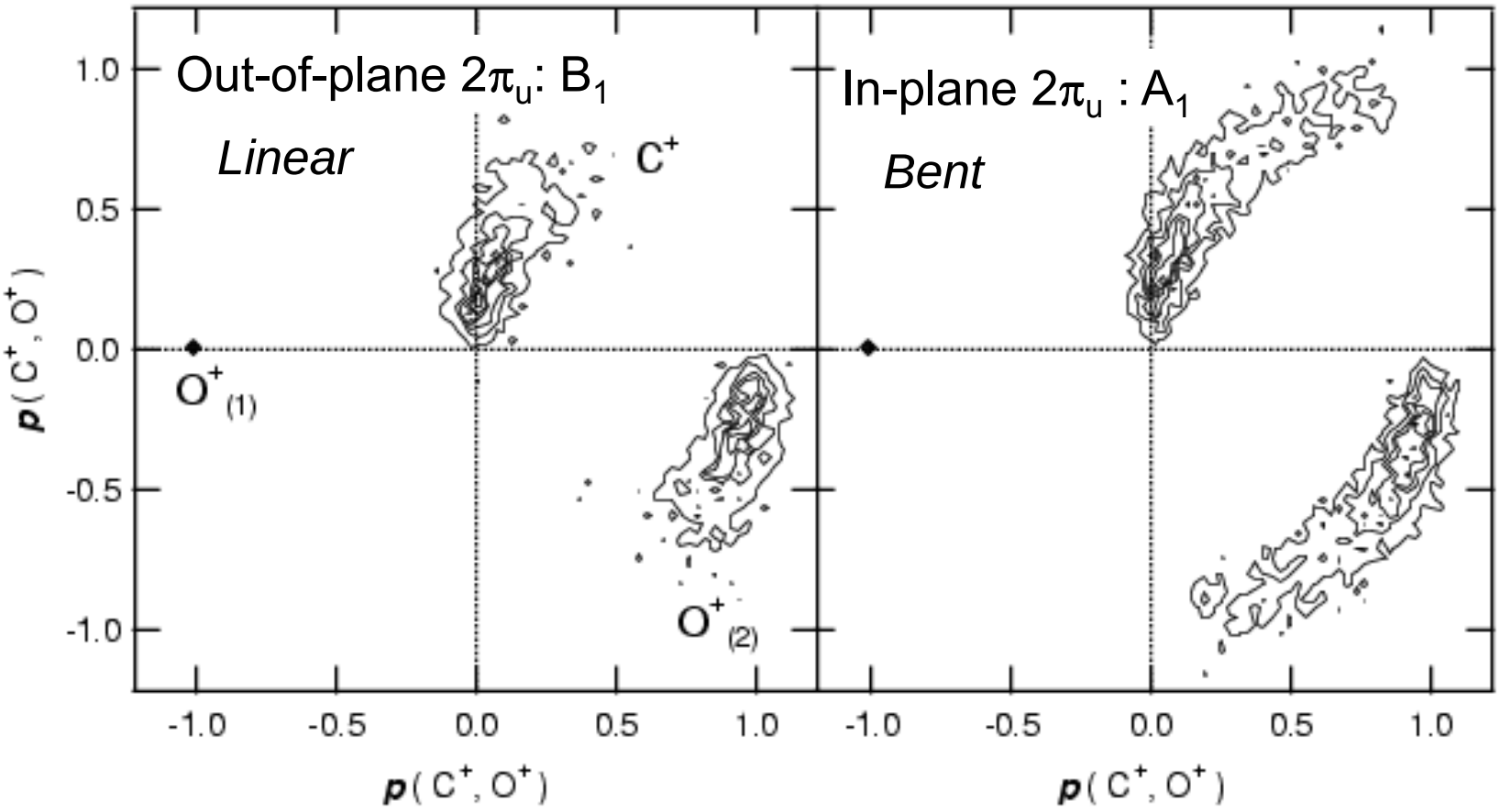

Muramatsu et al. Phys. Rev. Lett. 88, 133002 (2002).

Electron-ion coincidence momentum imaging

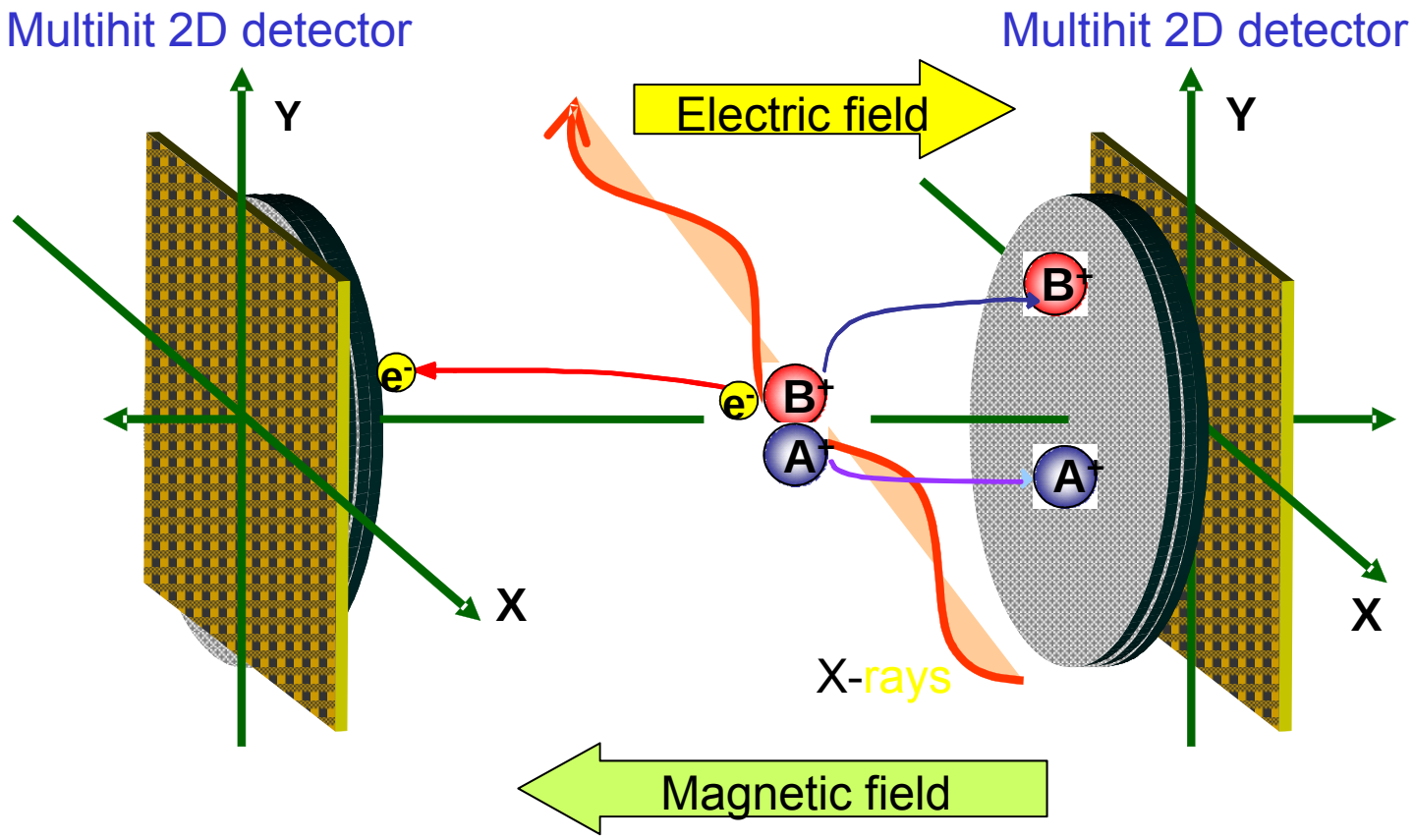

Ion-ion coincidence → *Molecular axis*

Ion momentum conservation → *Retrieval of the source point*

Electron-ion-ion coincidence → *Molecular-frame e^- angular distribution*

Towards photoelectron diffraction measurement

Total electron yield spectrum of CO_2 in the C1s ionization region

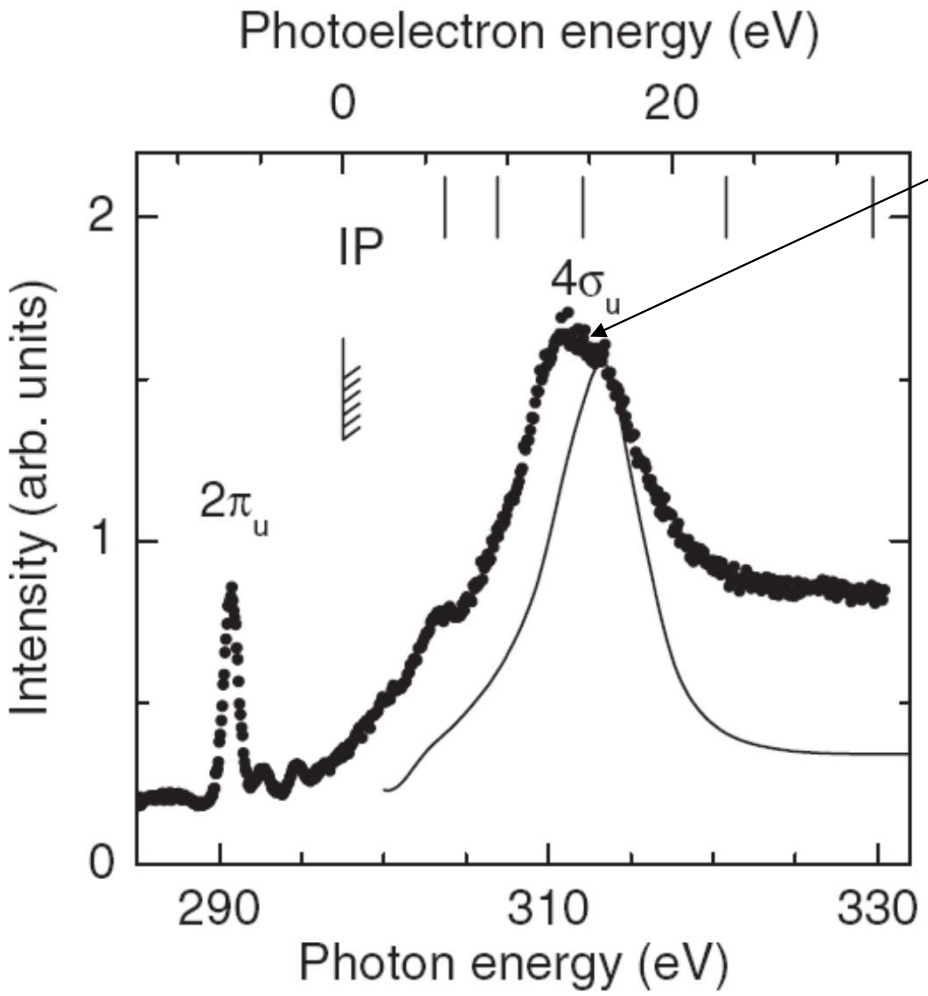

$4\sigma_u \leftarrow 2\sigma_g$ shape resonance

CO_2 ground state configuration:

$$\underbrace{1\sigma_g^{\,2}1\sigma_u^{\,2}}_{\text{O1s}}\;\underbrace{2\sigma_g^{\,2}}_{\text{C1s}}\;\underbrace{3\sigma_g^{\,2}2\sigma_u^{\,2}}_{\text{O2s}}\;\underbrace{4\sigma_g^{\,2}}_{\text{C2s}}$$

$$3\sigma_u^{\,2}1\pi_u^{\,4}1\pi_g^{\,4}(^1\Sigma_g^{\,+});\; 2\pi_u^{\,0}5\sigma_g^{\,0}4\sigma_u^{\,0}$$

C 1s threshold
297.63 eV

N. Saito *et al.*, J. Phys. B, **36** L25 (2003).

Reaction plane

Reaction plane ＝plane define by the E vector and molecular axis

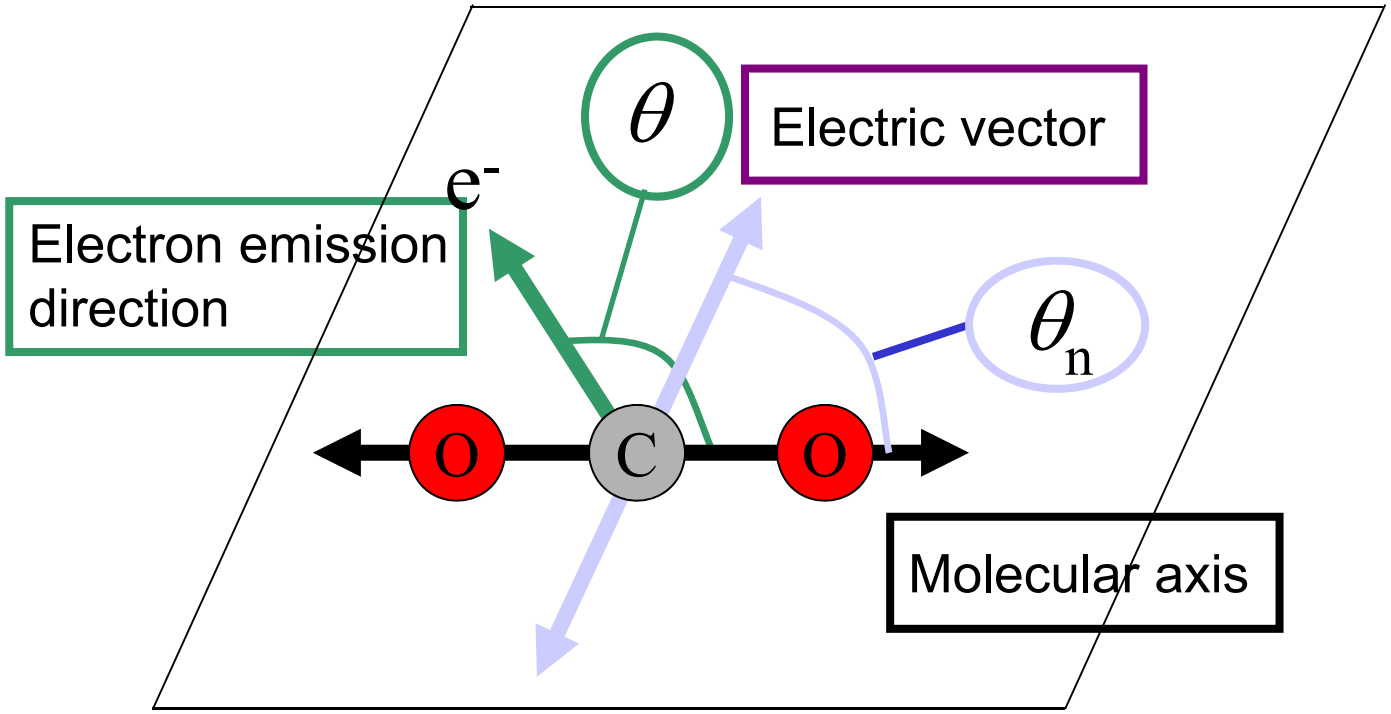

We focus on the electron emission within this reaction plane

C1s photoelectron diffraction (MFPAD) of CO_2: comparison between experiment and theory

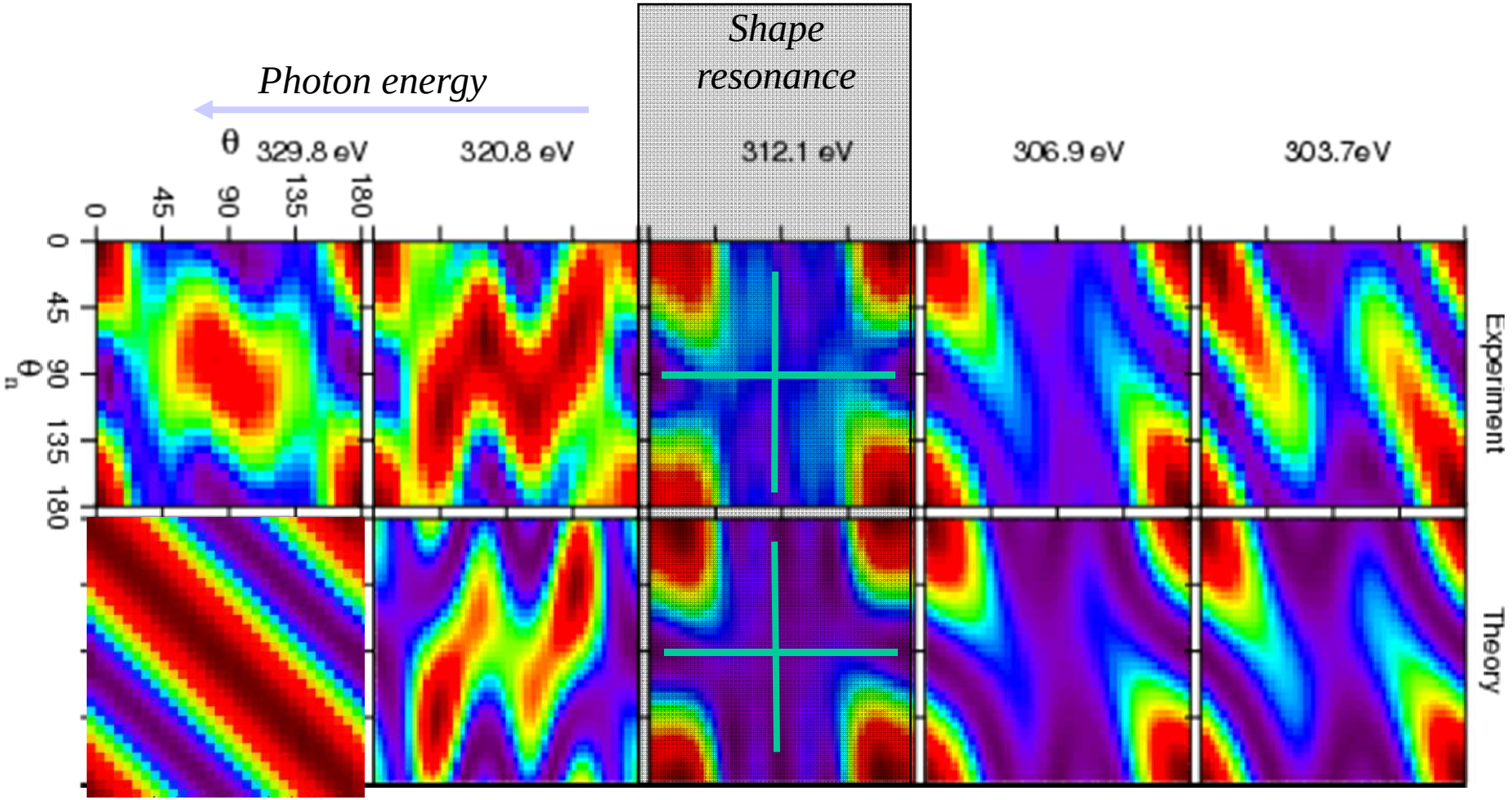

The general agreement between experiment and theory is reasonable.

At the shape resonance, the intensity drops at $\theta_n = 90°$ *i.e.* Σ-Σ *parallel transition. The intensity drops at* $\theta = 90°$, *i.e.,* σ_u *photoelectron wave !*

Near Sendai

Motsu-ji

Chuson-ji

Auger vs Interatomic Coulombic Decay (ICD)

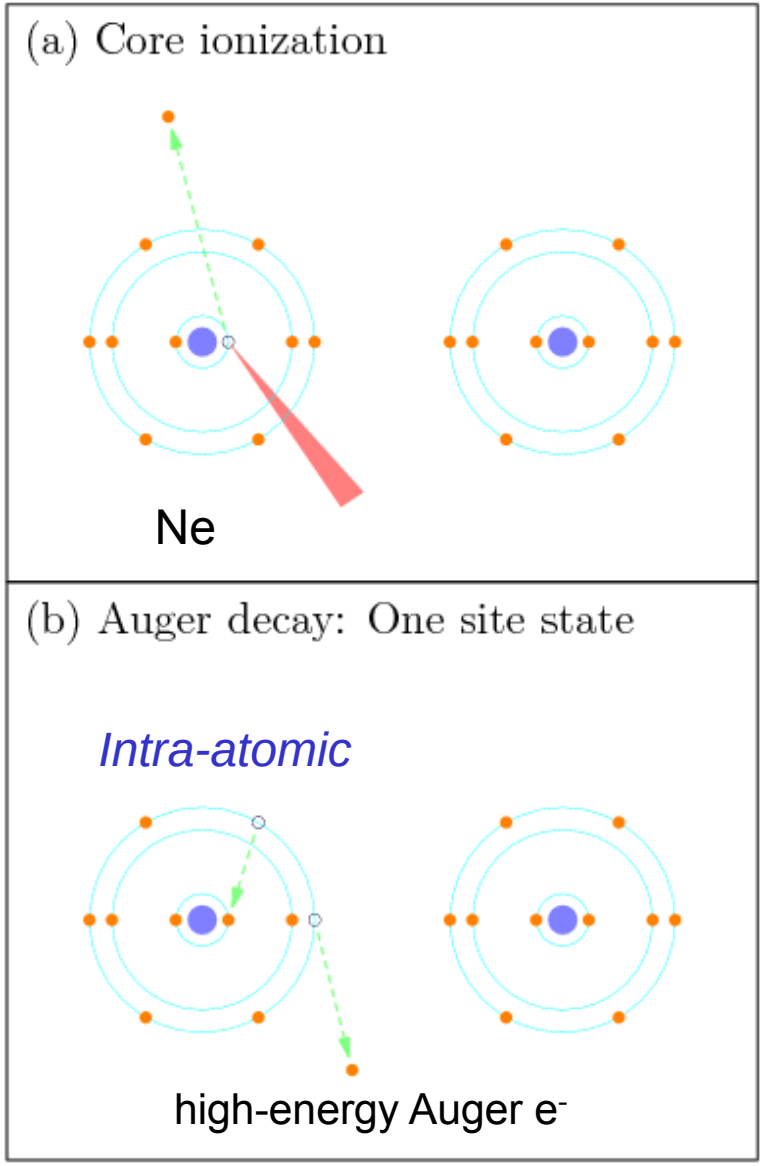

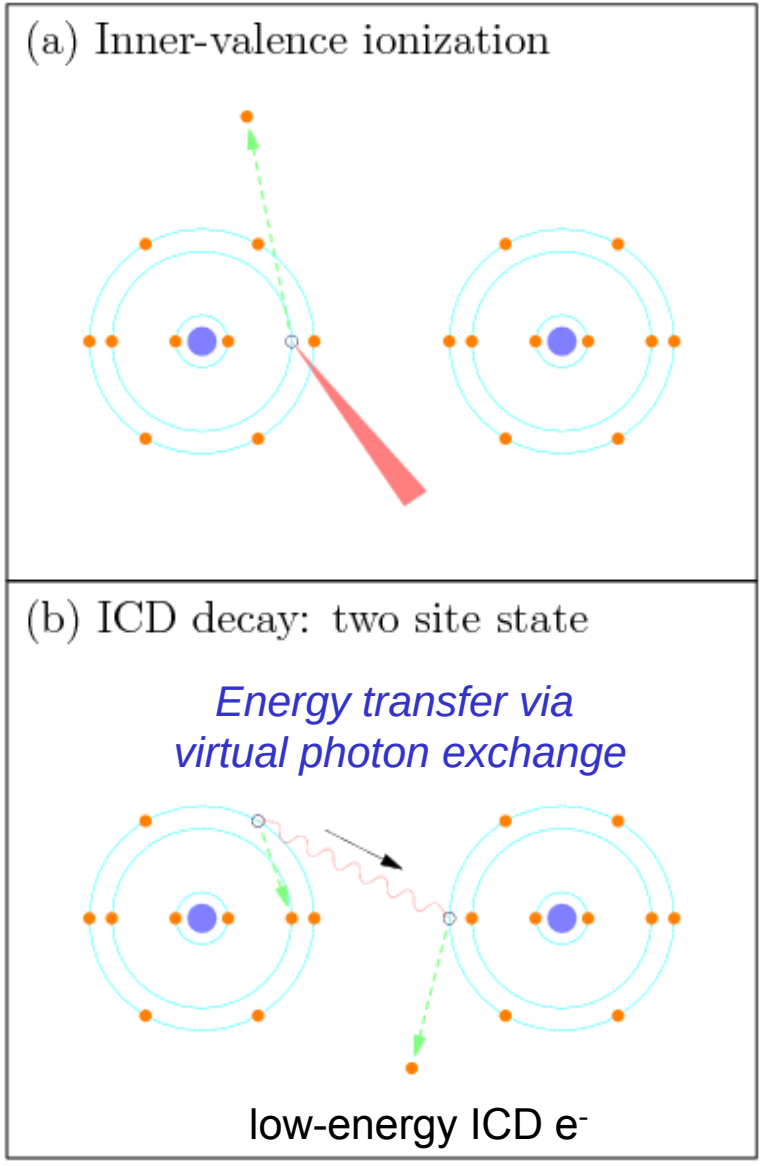

ICD rate is R dependent!

Why is ICD important?

ICD: electronic decay where the environment plays a role!

ICD takes place in van der Waals clusters, in hydrogen bonding clusters, in metallofullerenes, in bio-molecules in the living cell, etc

ICD is everywhere!

ICD is one of the key players in energy and charge transfer in these systems.

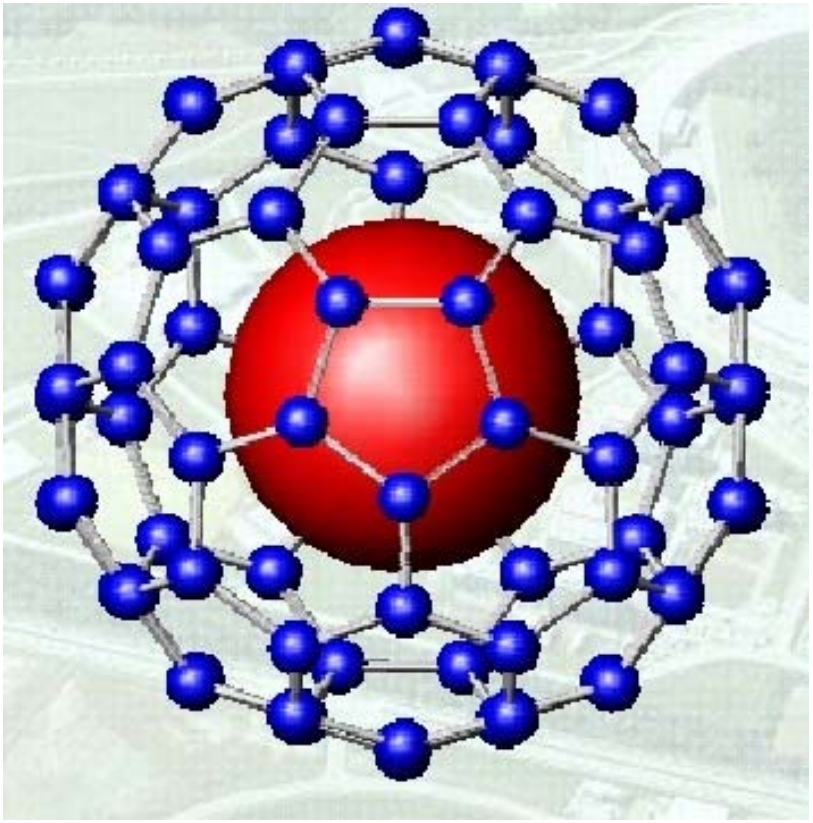

Metal atom in C_{60}

Interatomic Coulombic Decay (ICD)

Theoretical

First prediction - HF cluster:
L.S. Cederbaum, J. Zobeley, and F. Tarantelli, Phys. Rev. Lett. 79, 4778 (1997).

Prediction - Ne dimer:
R. Santra, J. Zobeley, L.S. Cederbaum *et al*., Phys. Rev. Lett. 85, 4490 (2000).

Experimental

First observation - Ne cluster:
U. Hergenhahn and coworkers, Phys.Rev. Lett. 90, 203401 (2003).

Cluster-size-dependent lifetime:
G. Öhrwall *et al*., Phys. Rev. Lett. 93, 173401 (2004).

Ne_2 e-ion-ion coincidence:
R. Dörner and coworkers, Phys. Rev. Lett. 93, 163401 (2004).

Observation of ICD in Ne_2 by Frankfurt group

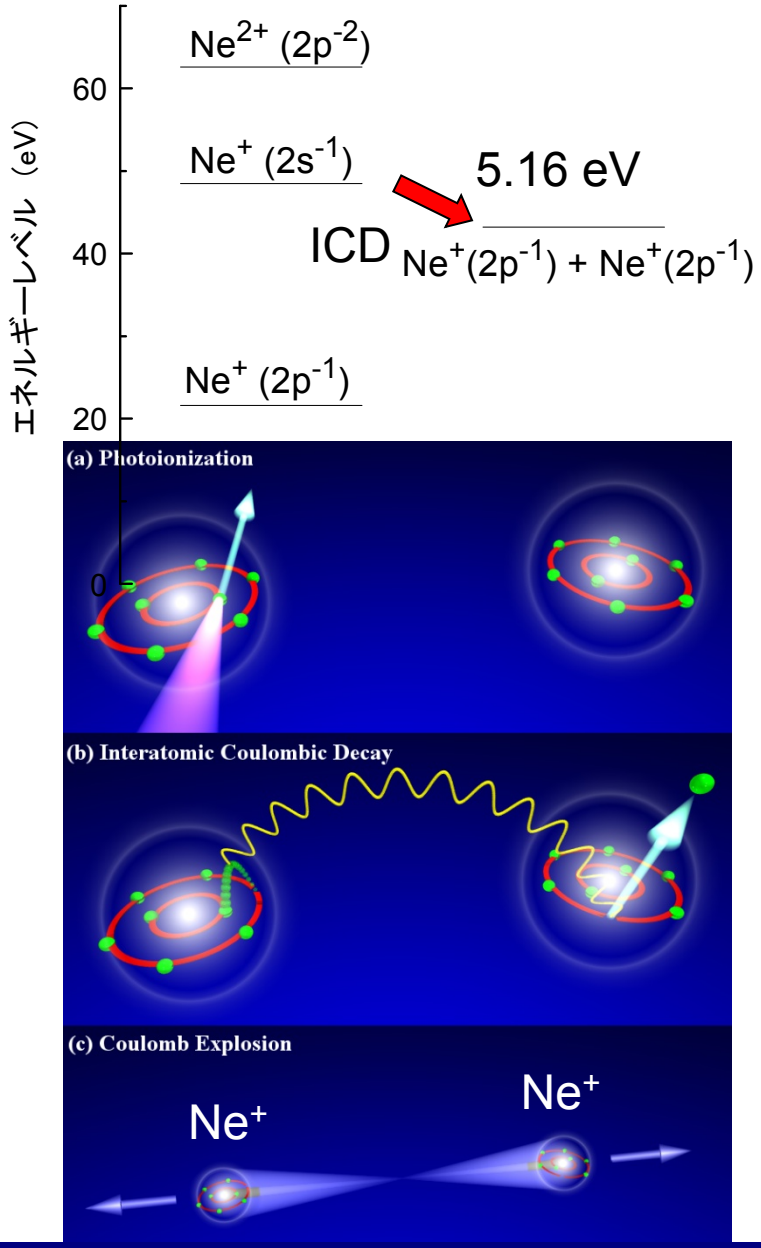

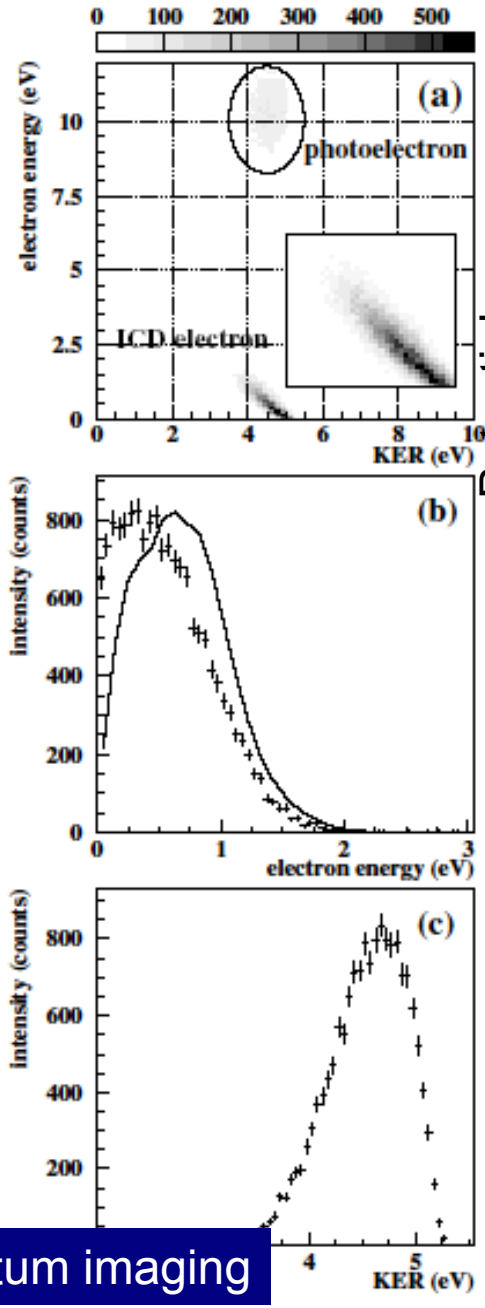

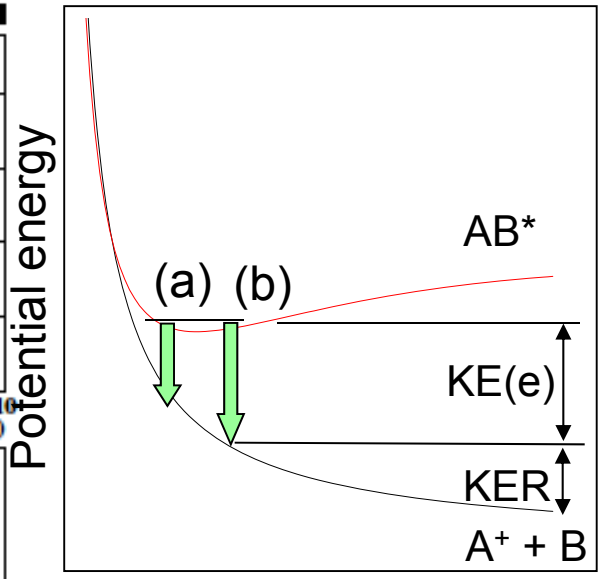

KE(e)+KER = 5.16 eV

T. Jahnke *et al.*
Phys. Rev. Lett.
93, 163401 (2004)

Electron-ion-ion coincidence momentum imaging

Interatomic Coulombic Decay after Auger decay

Prediction - ICD from Auger final states in Ne dimer:

R. Santra and L.S. Cederbaum, Phys. Rev. Lett. ***90****, 153401 (2003).*

Why is ICD after Auger decay interesting and important?

Radiation damage caused in bio-molecules in the living cell

Radiation damage, caused by e.g., X-ray radiation, is initiated by core ionization.

Radiation damage is known to be caused by low energy electron collisions, not high energy Auger electrons.

ICD is one of the important mechanisms to produce low energy electrons after Auger decay!

Labeling electron emission site via the ionic charge state

$$[A^{+}(core^{-1})\text{-}A] + e^{-}_{Photo} \rightarrow [A^{2+} - A] + e^{-}_{Auger} \rightarrow [A^{2+} + A^{+}] + e^{-}_{ICD}$$

Is the ICD electron ejected from the A^{+} *site or* A^{2+} *?*

Can the A^{+} *or* A^{2+} *be which-way information of the double slit experiment ?*

We can experimentally answer to this very basic question!

Experimental evidence of interatomic Coulombic decay from the Auger final states in argon dimers

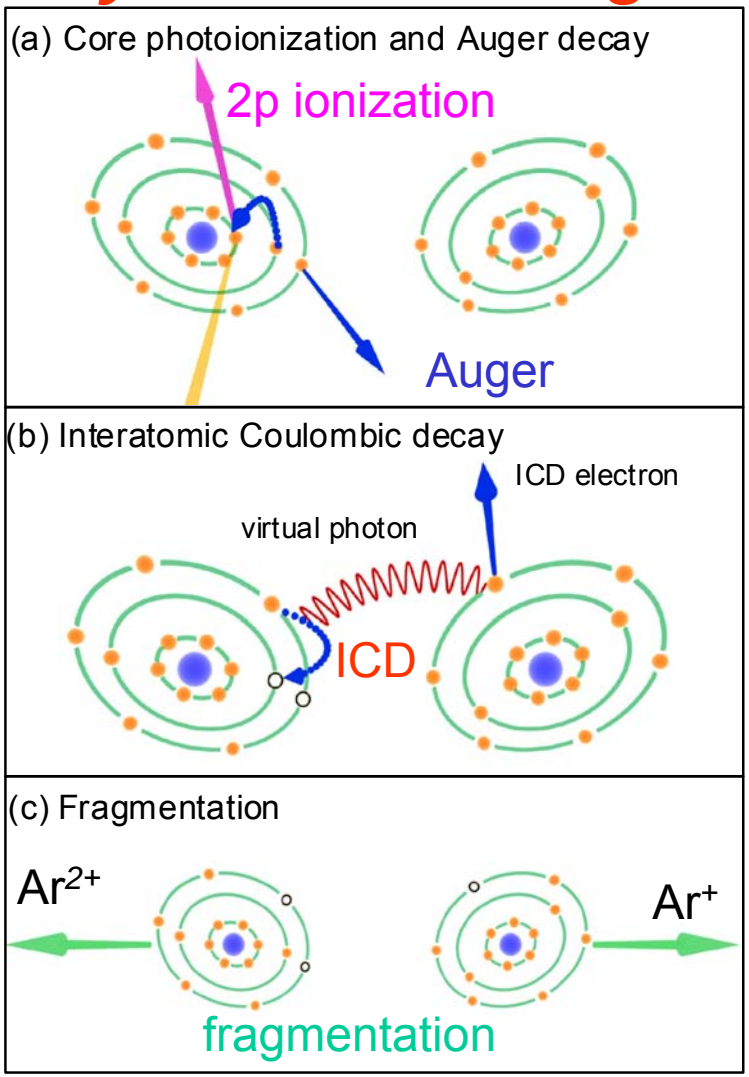

Morishita *et al.* Phys. Rev. Lett. **96**, 243402 (2006).

We detect ICD electrons in coincidence with Ar^{+} and Ar^{2+} using e-i-i coincidence momentum spectroscopy

Multiple coincidence momentum imaging

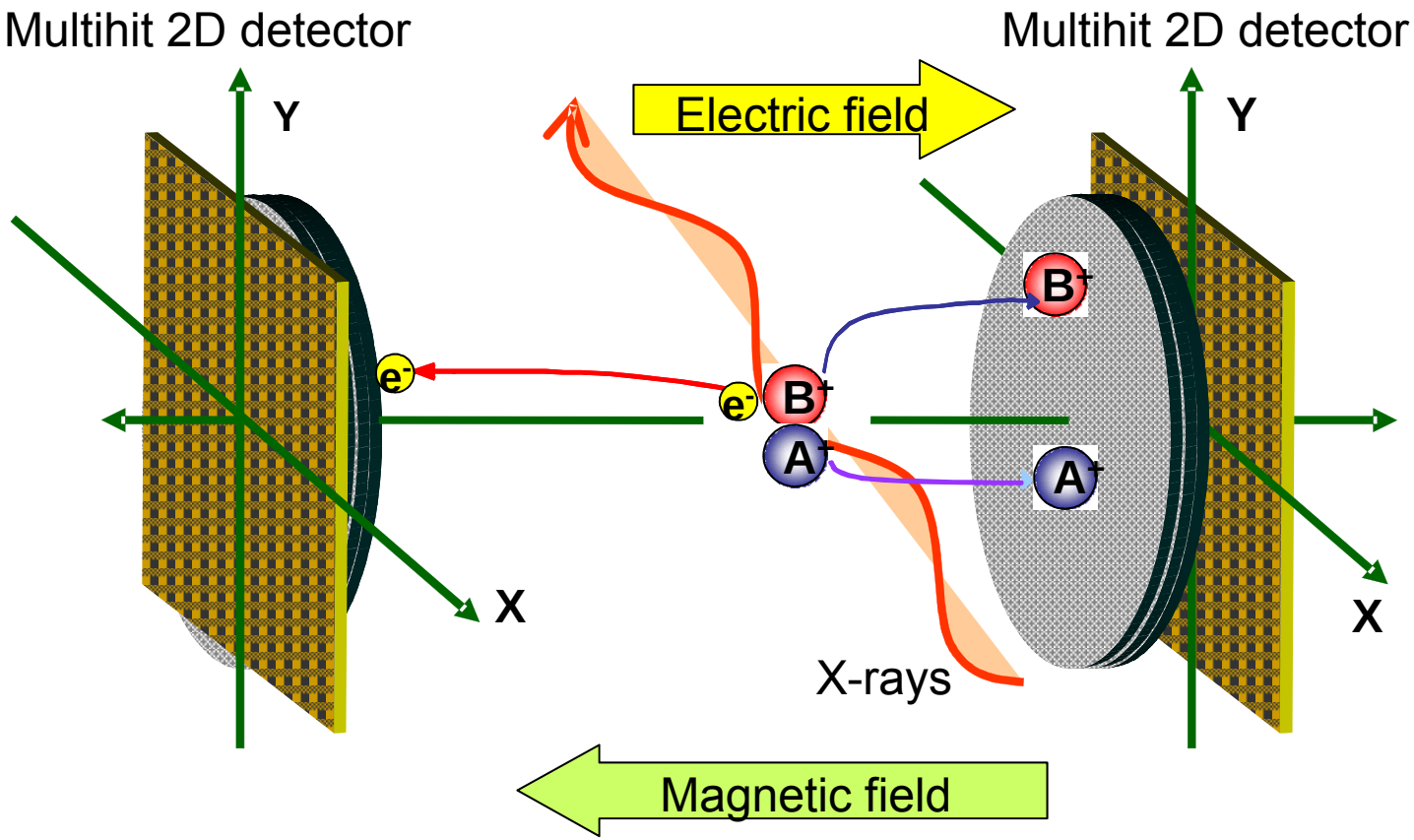

position & time of flight (x,y,t) → *3D momentum of each particle*

Multiple coincidence → *Momentum correlation among the particles*

Momentum conservation → *Selection of Dimer from others !*

Ar_2 PIPICO spectrum

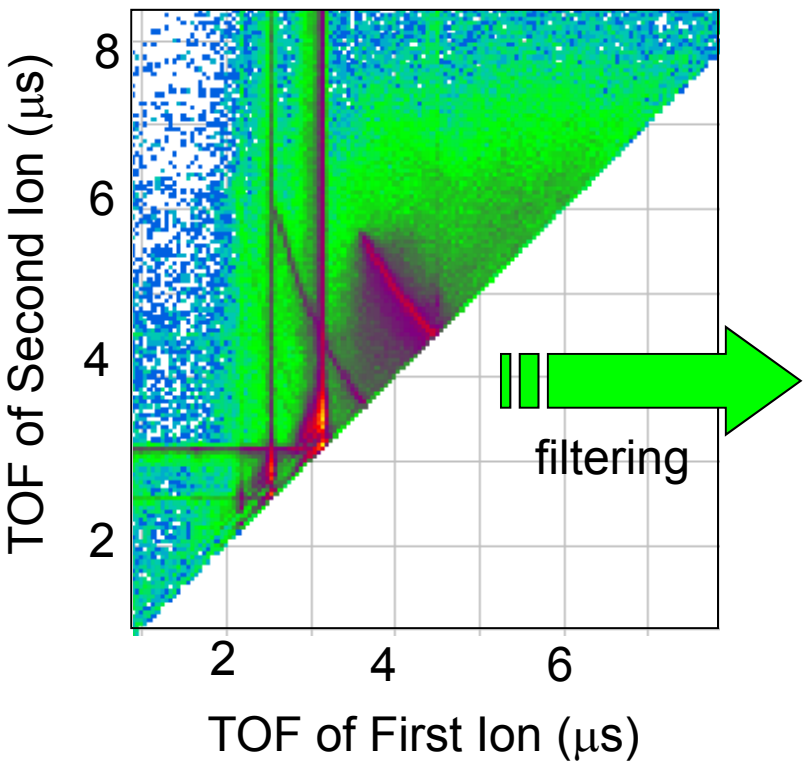

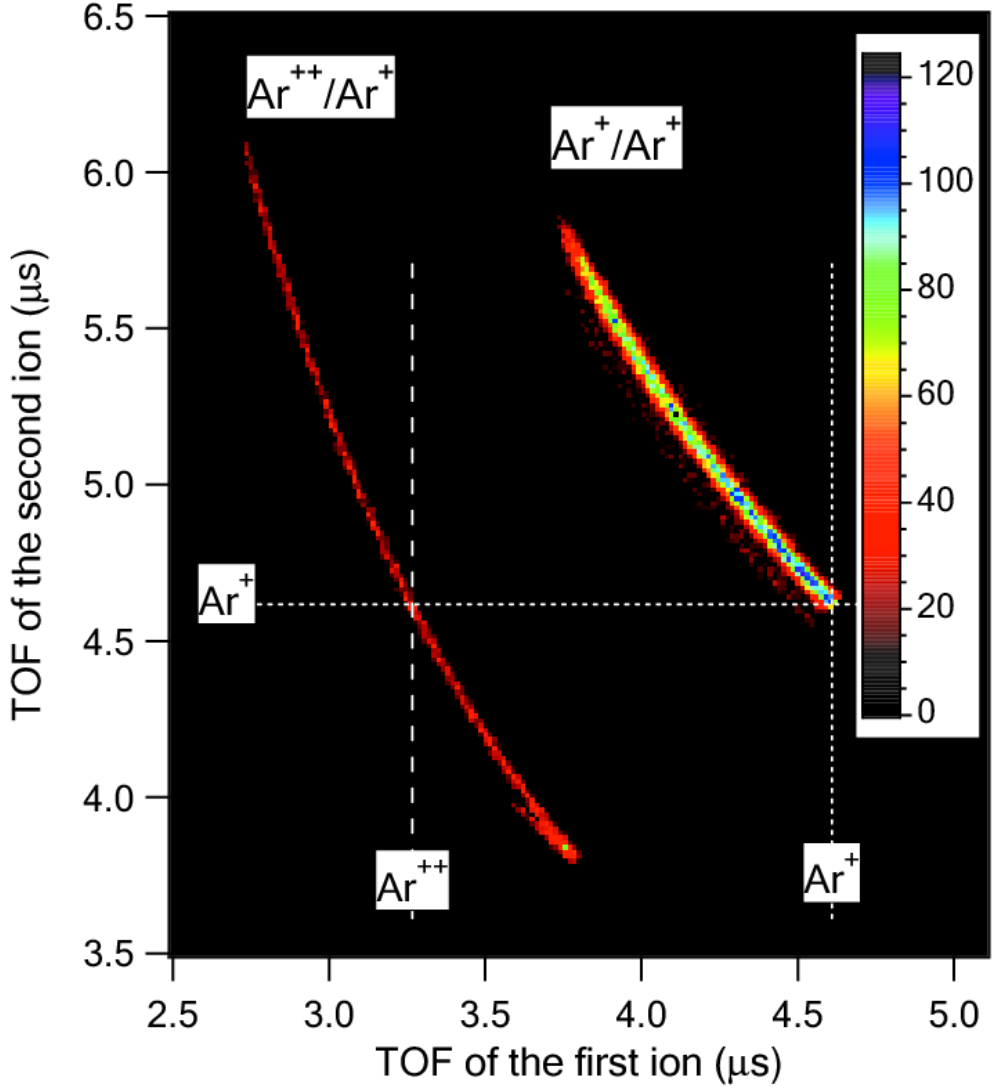

Filter conditions:

Ar^+/Ar^+: the sum of the momentum of Ar^+ and Ar^+ ~ 0

Ar^{++}/Ar^+: the sum of the momentum of Ar^{++} and Ar^+ ~ 0

Ar^{++}/Ar^+ comes from ICD !?

Electron spectrum, KER, and their correlation

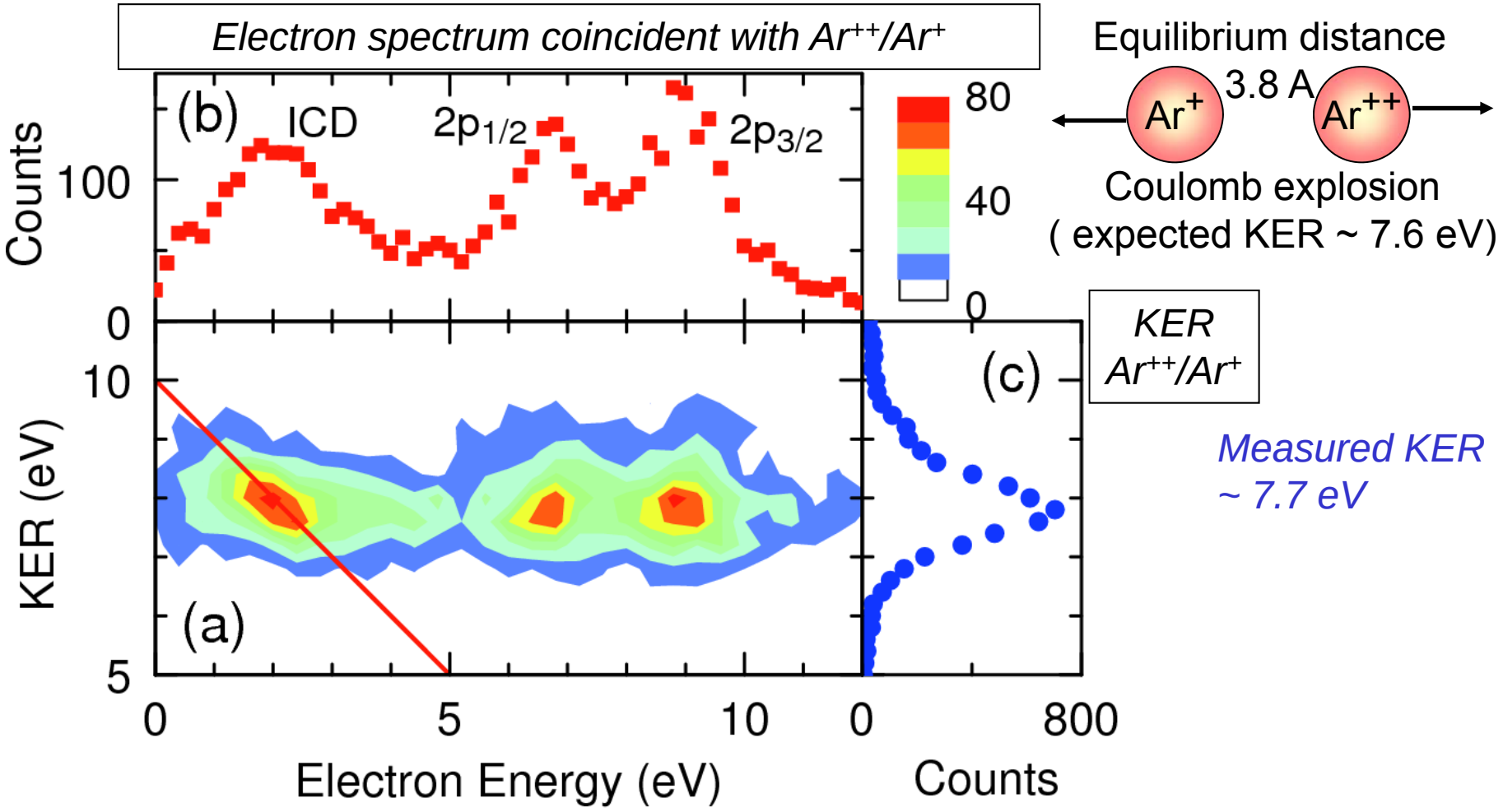

Measured KER ~ 7.7 eV

ICD: KER + KE(ICD electron) ~ constant

Islands of slope -1 are ICDs !

Breakup following ICD takes place almost instantaneously.

ICD is very fast!

Energy diagram of the ICD process in Ar_2

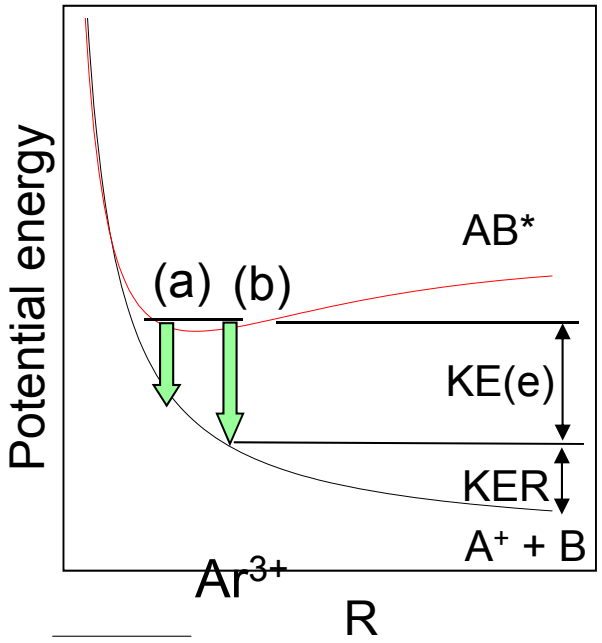

KER
+ ICD electron
= 10 eV

Photoelectron ejection
(13.4 and 11.3 eV)

$2p^{-1}$

Auger decay

hv=262 eV
photoionization

Binding Energy (eV)

70
60
50
40

$3s^{-2}$

$3p^{-3}3d(^1P)$

CI

$3s^{-1}3p^{-1}(^1P)$

ICD &
fragmentation

10eV

$3p^{-1}$ & $3p^{-2}$ (^1D)

$3p^{-2}$

Ar Ar^+

Ar Ar^{2+}

Ar^+ Ar^{2+}

*ICD from the Auger final states in **Ne** dimer*

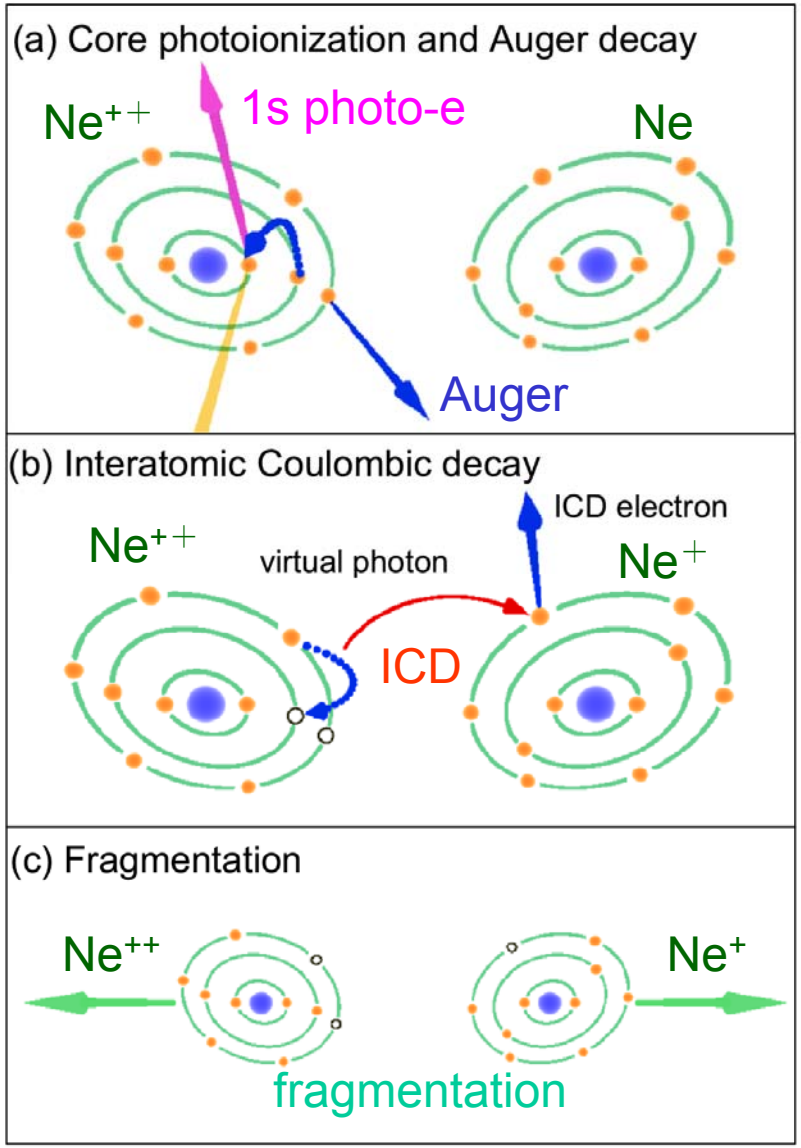

*Kreidi et al. J. Phys. B. **41**, 101002 (2008).*

We detect ICD electrons in coincidence with Ne^{+} and Ne^{2+}using e-i-i coincidence momentum spectroscopy

Variants of ICD

'direct' ICD

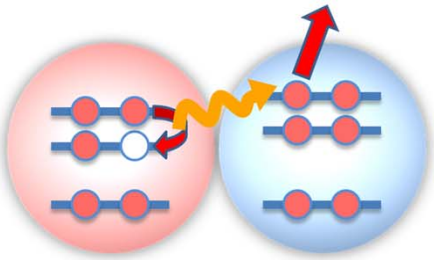

'exchange' ICD

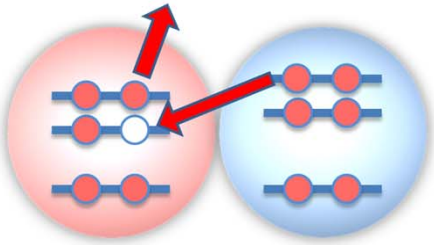

Kreidi et al.
J. Phys. B. ***41****, 101002 (2008).*

ETMD

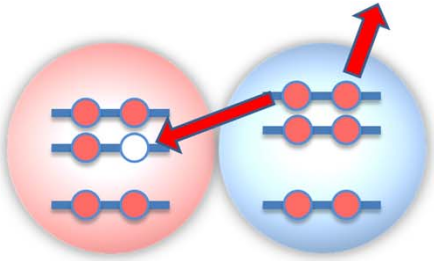

Sakai et al
Phys. Rev. Lett. ***106****, 033401 (2011).*

<u>ICD after Auger decay</u>

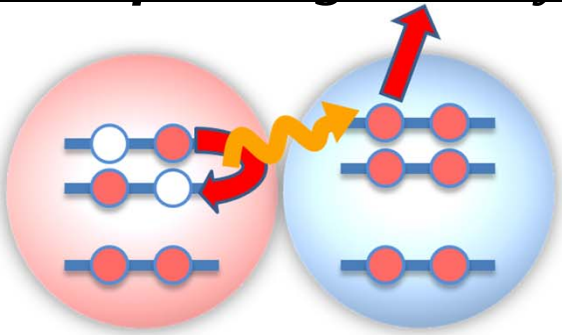

Morishita et al.
Phys. Rev. Lett. ***96****, 243402 (2006).*

<u>'3-electrons' ICD</u>

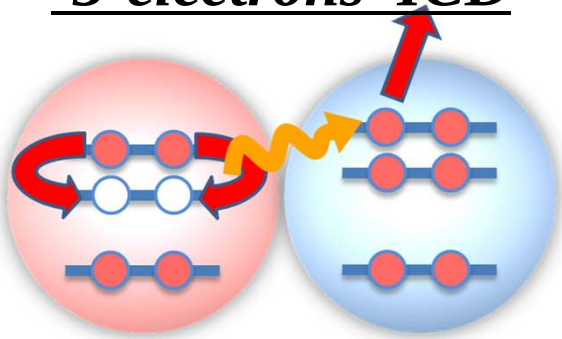

Oichi et al.
Phys. Rev. Lett. ***107****, 053401 (2011).*

ICD gangs in Germany and Japan !

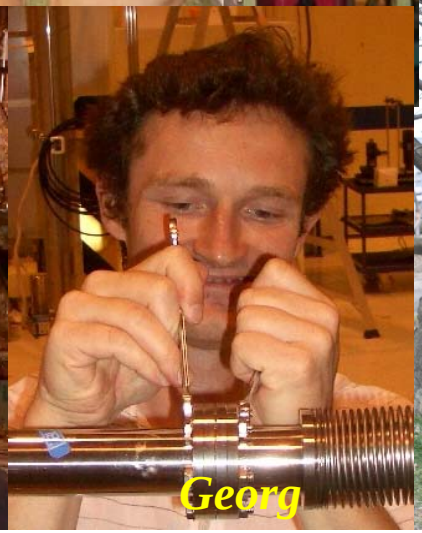

EUV-X FELs in the world

Swiss FEL (2016), Korean FEL, Shanghai FEL, etc., are coming!

Characteristic properties of FEL pulses

Coherent, intense, and ultra-short pulses at short wavelengths (EUV to X –rays)

Coherent X-ray imaging of non-crystalized samples

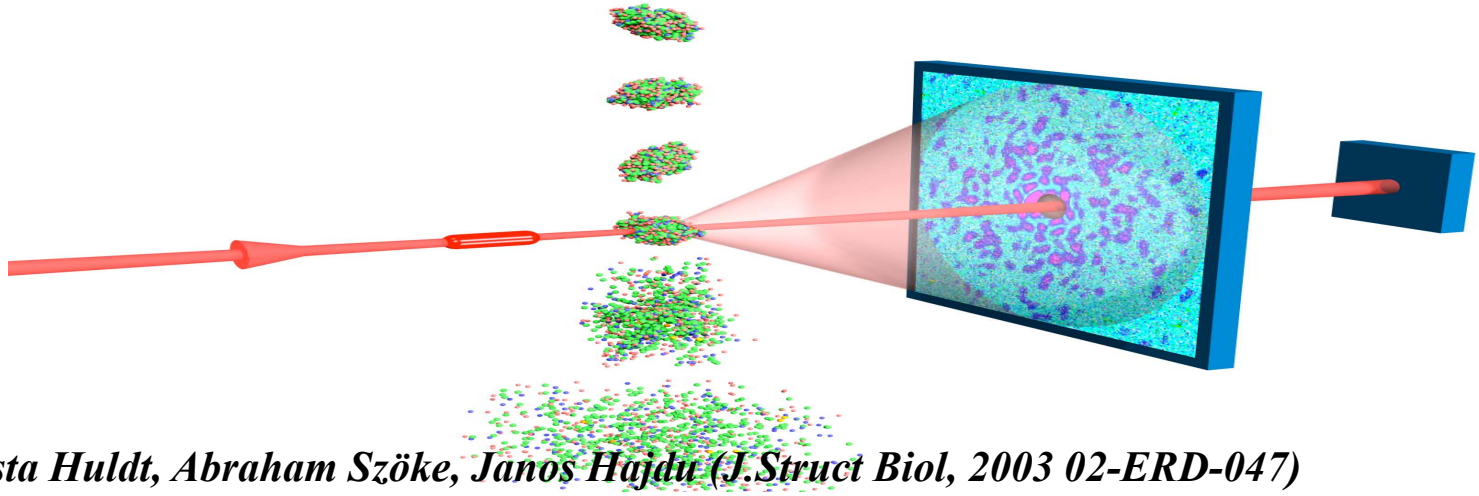

Gösta Huldt, Abraham Szöke, Janos Hajdu (J.Struct Biol, 2003 02-ERD-047)

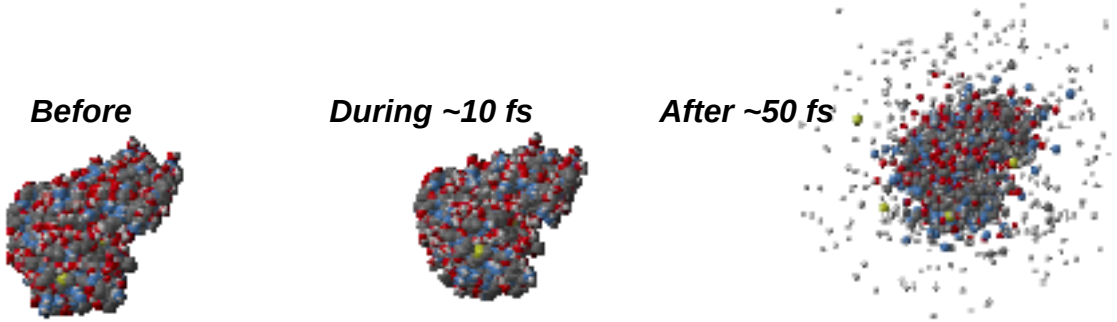

Neutze, Wouts, van der Spoel, Weckert, Hajdu Nature 406, 752 (2000)

Single Mimivirus Particles Intercepted and Imaged with an X-ray laser

Seibert et al. *Nature* ***470****, 78–81 (2011)*

Characteristic properties of FEL pulses

Intense and ultra-short pulses at ***X –rays***

Why X-rays? structure determination at atomic resolution

Femtosecond X-ray Protein Nanocrystallography, Chapman et al., Nature 470, 73–77 (2011).

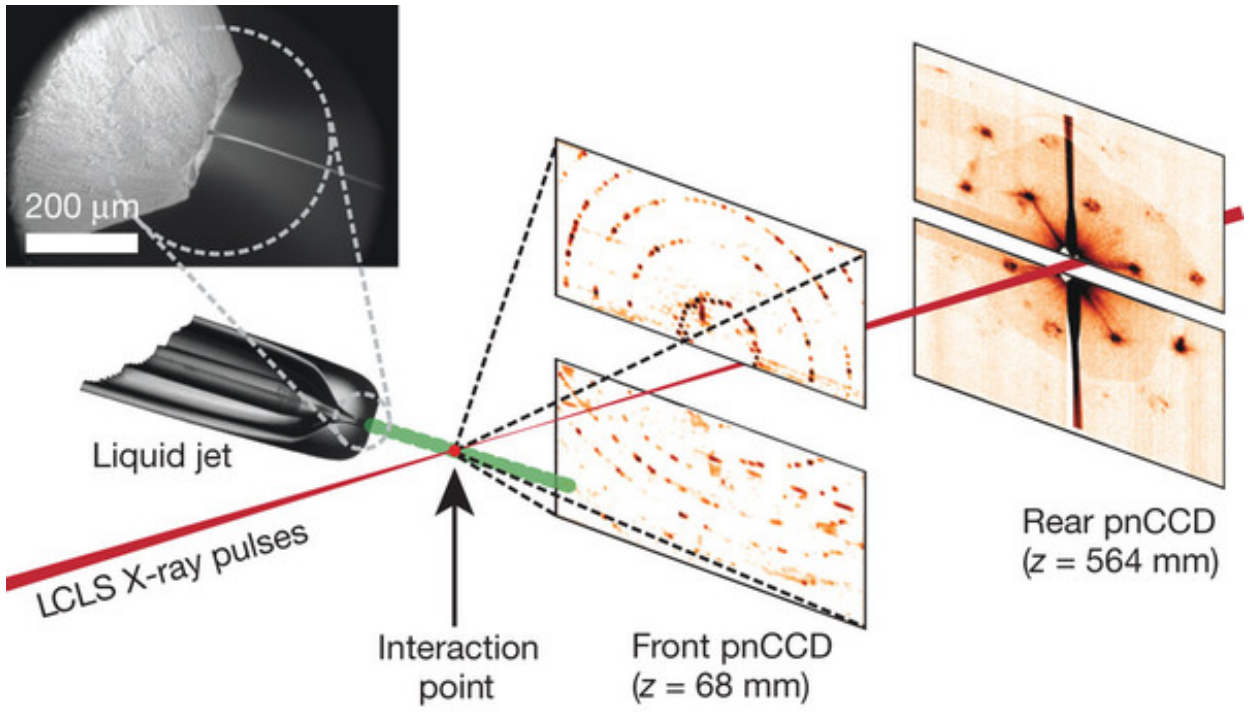

*High-Resolution Protein Structure Determination by Serial Femtosecond Crystallography, Boutet et al. Science **337** (6092) 362 (2012).*

Characteristic properties of FEL pulses

ultra-short (100 – 10 fs)

Attosecond dynamics

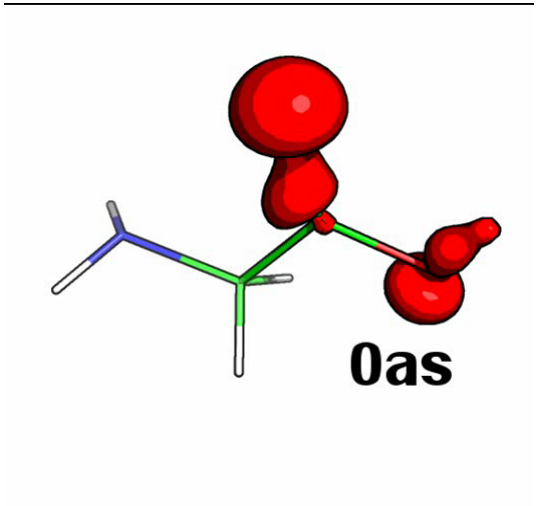

0 – 0.5 fs

Femtosecond dynamics

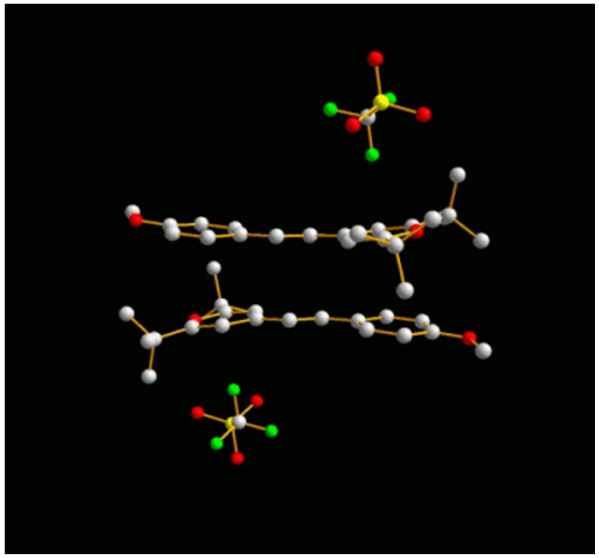

0 – 10 ps

Mili-second mechanics

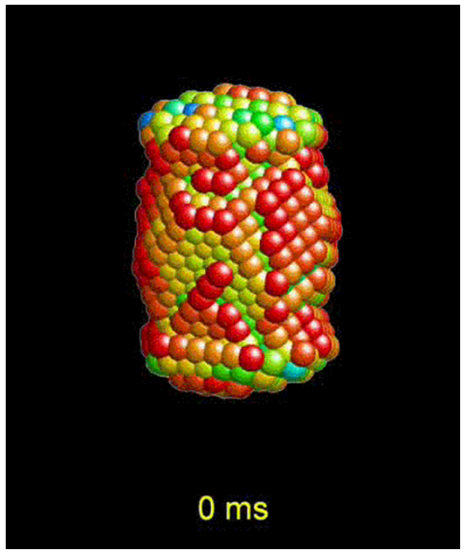

0 – 200 ms

Courtesy of Simone Techert

Characteristic properties of FEL pulses

ultra-short (100 – 10 fs)

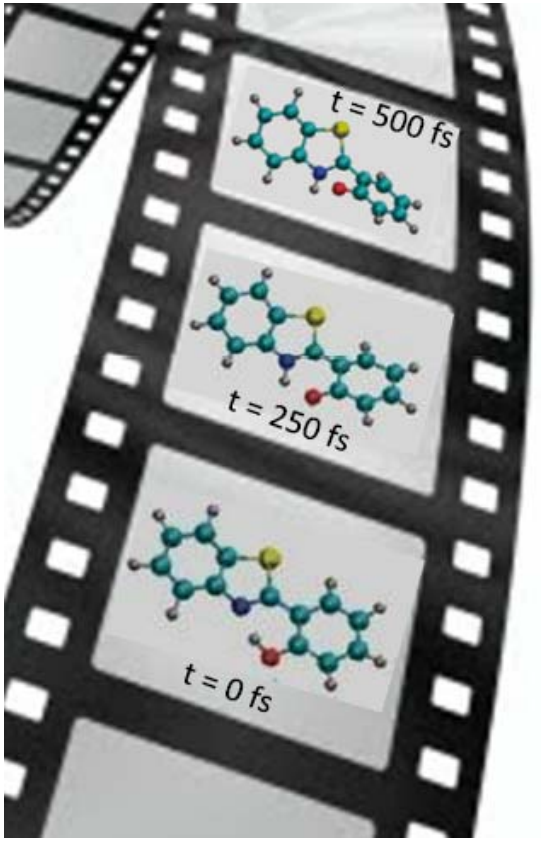

Femtosecond dynamics

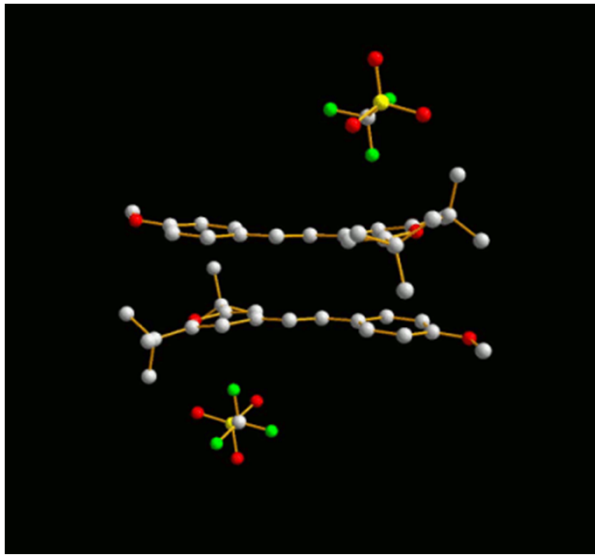

0 – 10 ps

Courtesy of Simone Techert

Catching atomic motion in reaction (molecular movie)

Characteristic properties of FEL pulses

Intense

10^{14} W/cm^2 (EUV) - 10^{20} W/cm^2 (X)

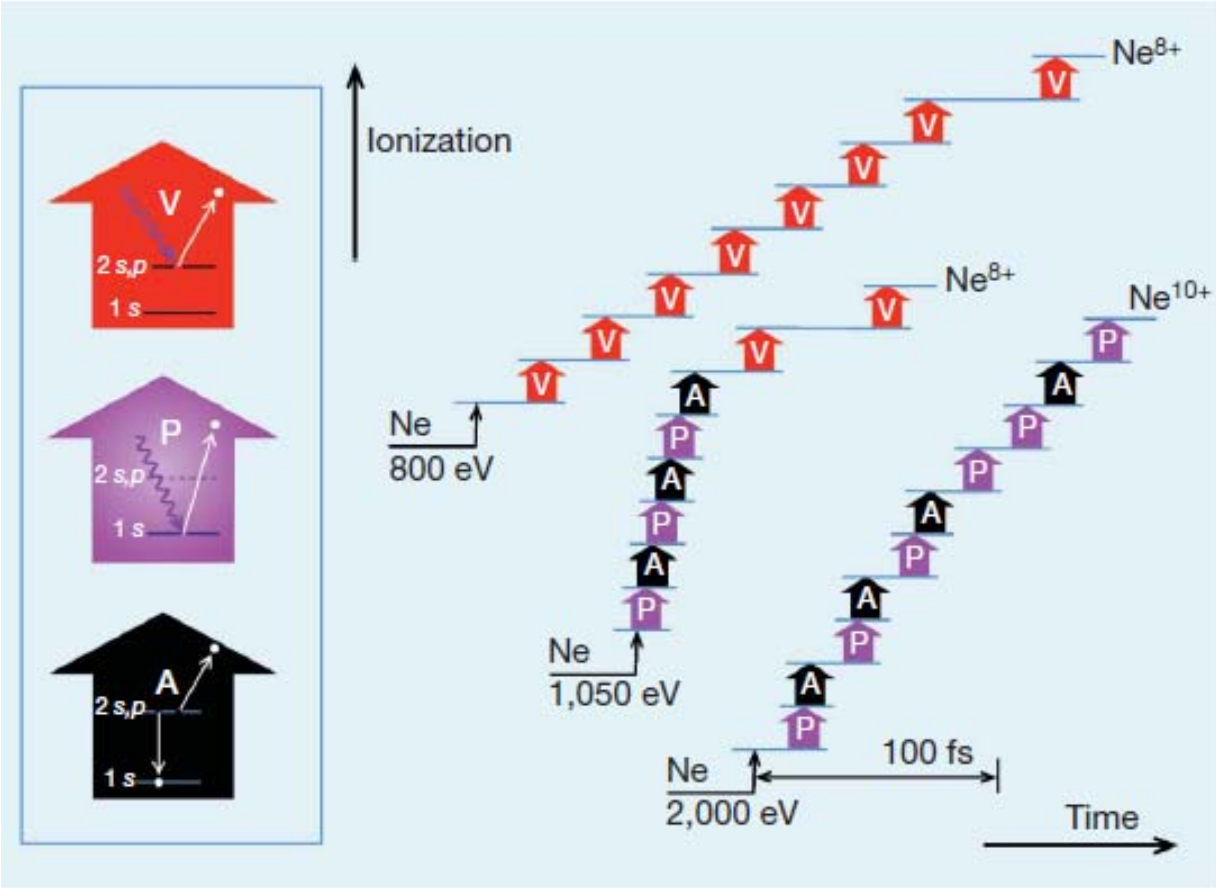

One LCLS pulse at 2 keV can remove all ten electrons from the neon atom.

The pulse is so intense that it causes electronic damage to the sample.

Femtosecond electronic response of atoms to ultra-intense x-rays

*L. Young et al., Nature **466**, 56 (2010).*

Characteristic properties of FEL pulses

○ ***Short wave-length: toward Hard X-rays***

structure determination at atomic resolution

○ ***Coherent***

Coherent X-ray imaging of non-crystalized samples

○ ***Ultrafast*** *100 -10 fs: resolving atomic motion*

-> ~ 200 as: resolving electron wave-packet motion

○ ***Intense*** *10^{14} W/cm^2 (EUV) - 10^{20} W/cm^2 (X)*

Light matter interaction *Non-linear response*

Electronic damage

Warm (Hot) dense matter science

SACLA (XFEL lased on 7 June 2011)

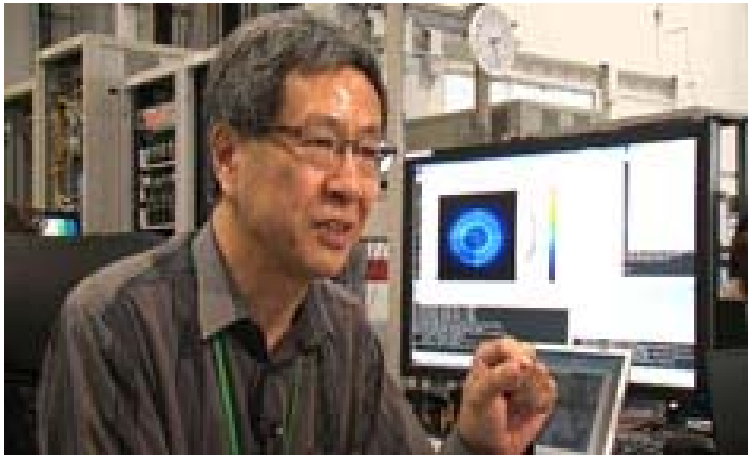

on air!

SACLA XFEL

Photon energy range: 4-20 keV

Photon numbers: ～10^{11} photon/pulse (5-15 keV)

Repetition rate: 10~60 Hz

Pulse width 10 ~ 15 fs

Focusing optics: ~1 μm (1.5 m) *→ 50 nm (0.5 m)*

First round user beam time: March – July 2012

My first beam time: 30 May – 4 June 2012
Atoms and atomic clusters

Second round beam time: September 2012-March 2013

My second beam time: 2–5 December 2012
Molecules

SCSS test accelerator : EUV-FEL (20-24 eV)

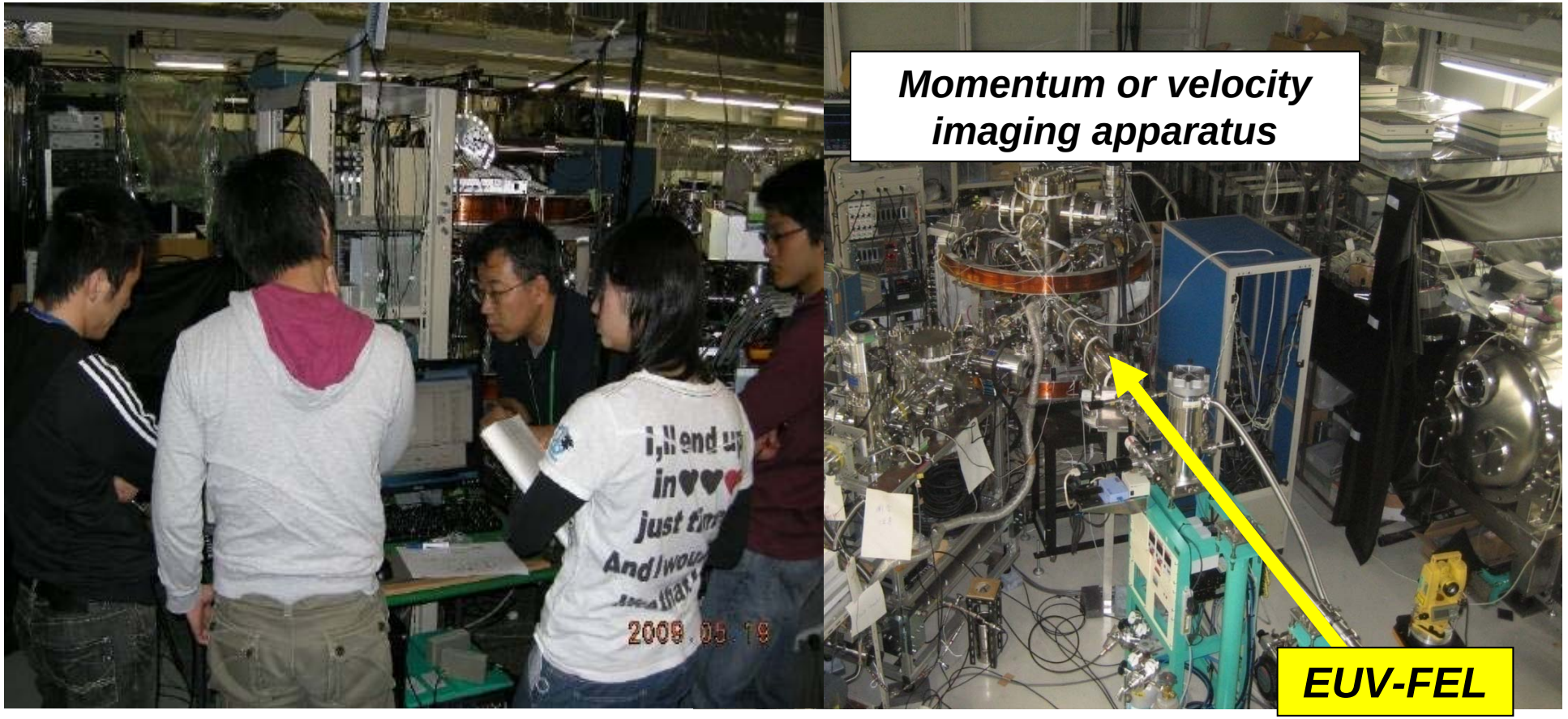

Multiple ionization of rare gas atoms and clusters: with M. Yao's group

VMI: with help of M. Vrakking's group

Autocorrelation: with J. Ullrich's group

Multi-photon ionization of atoms

● Second-order autocorrelation of **SCSS** EUVFEL pulses via time-resolved two-photon single ionization of He

– Characteristics of SASE-FEL

● Photoelectron angular distributions for two-photon Ionization of He atoms by **SCSS** EUVFEL pulses

– Potential of coherent control via seeded FEL

● Deep inner-shell multi-photon absorption of Ar and Xe atoms by **SACLA** XFEL pulses

– Relevance to the electronic radiation damage

Second-order autocorrelation of EUV FEL pulses via time resolved two-photon single ionization of He

R. Moshammer, Th. Pfeifer, A. Rudenko, Y.H. Jiang, L. Foucar, M. Kurka, K.U. Kuhnel, C.D. Schroter, J. Ullrich, O. Herrwerth, M.F. Kling, X.-J. Liu, K. Motomura, H. Fukuzawa, A. Yamada, K. Ueda, K. L. Ishikawa, K. Nagaya, H. Iwayama, A. Sugishima, Y. Mizoguchi, S. Yase, Yao, N. Saito, A. Belkacem, M. Nagasono, A. Higashiya, M. Yabashi, T. Ishikawa, H. Ohashi, H. Kimura, and T. Togashi, *Optics Express **19**, 21698 (2011).*

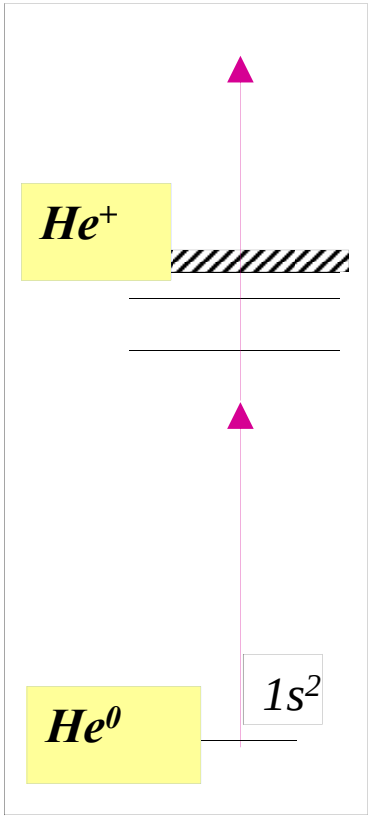

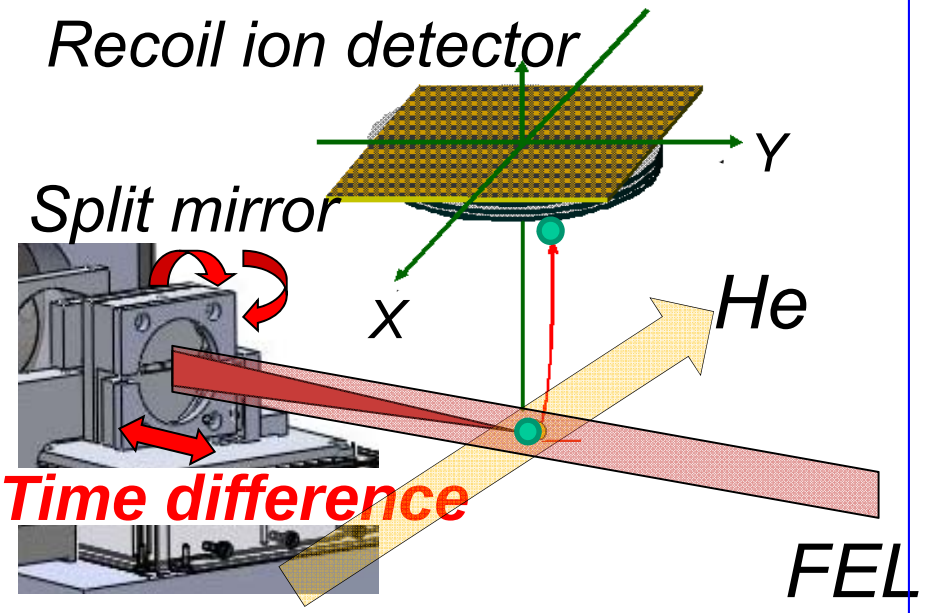

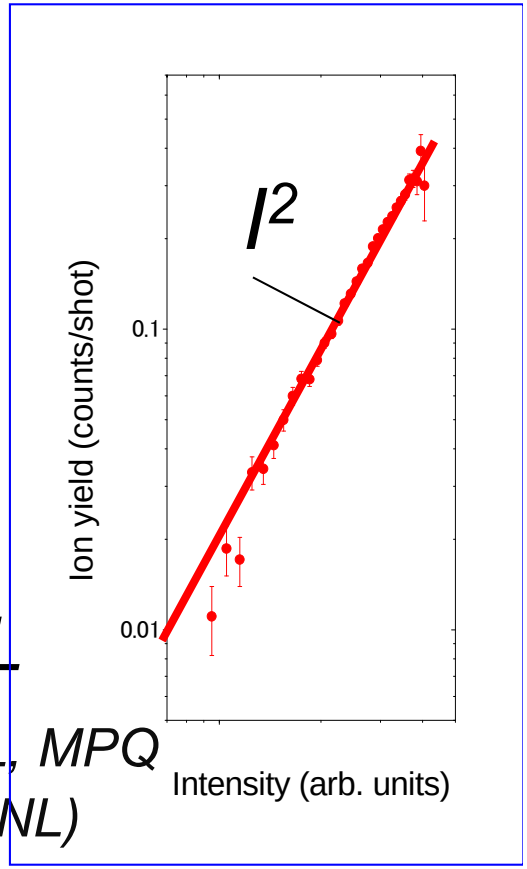

Split mirror assembly: MPI-K, ASG-CFEL, MPQ

Mirror: Mg/Si multilayer (f=600 mm, LBNL)

Autocorrelation measurement with He two photon ionization

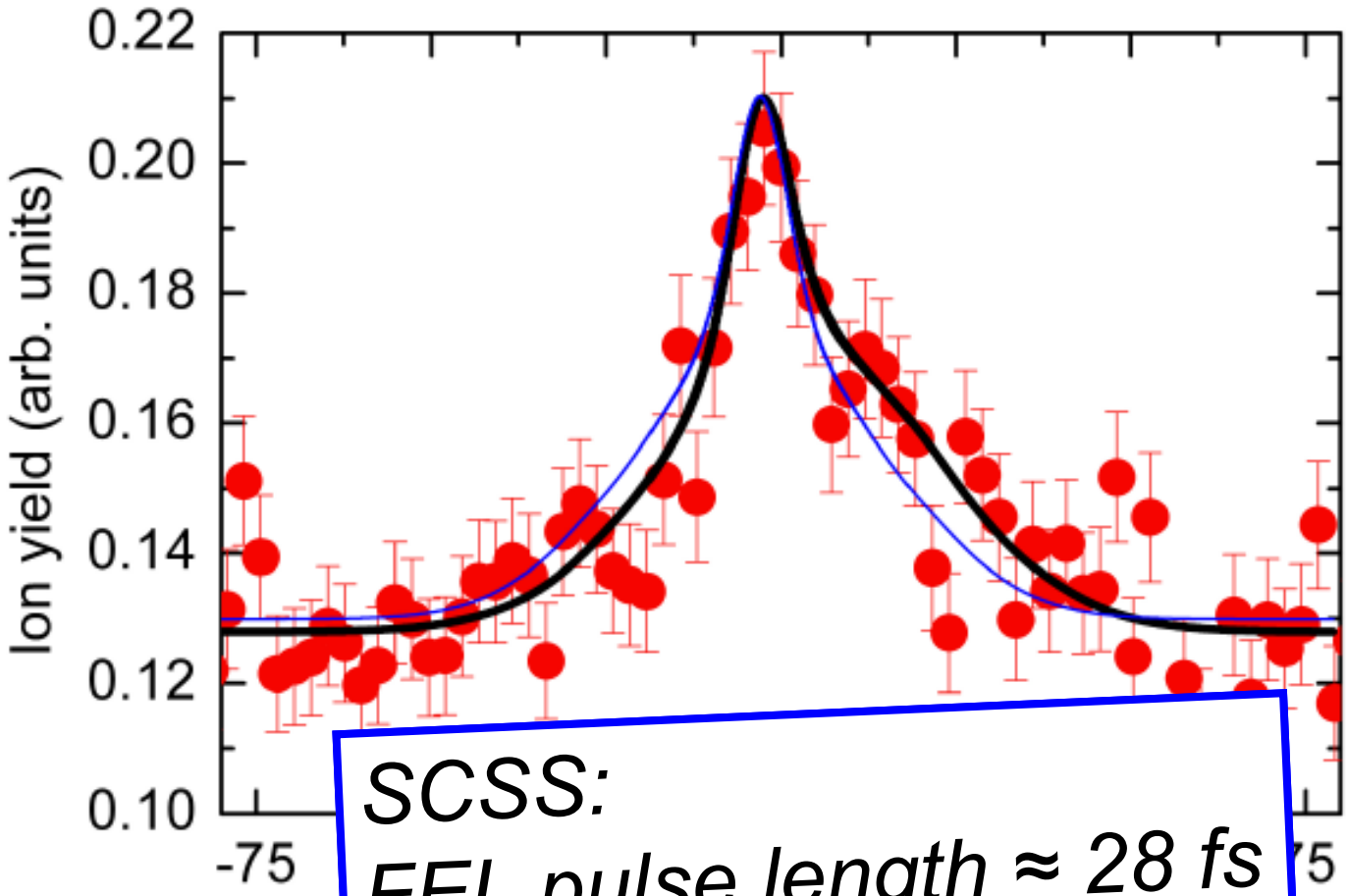

SCSS:
FEL pulse length ≈ 28 fs
coherence length ≈ 8 fs
Pulse-front tilt ≈ 5 fs

*Optics Express **19**, 21698 (2011).*

SCSS Sample Pulse Shapes

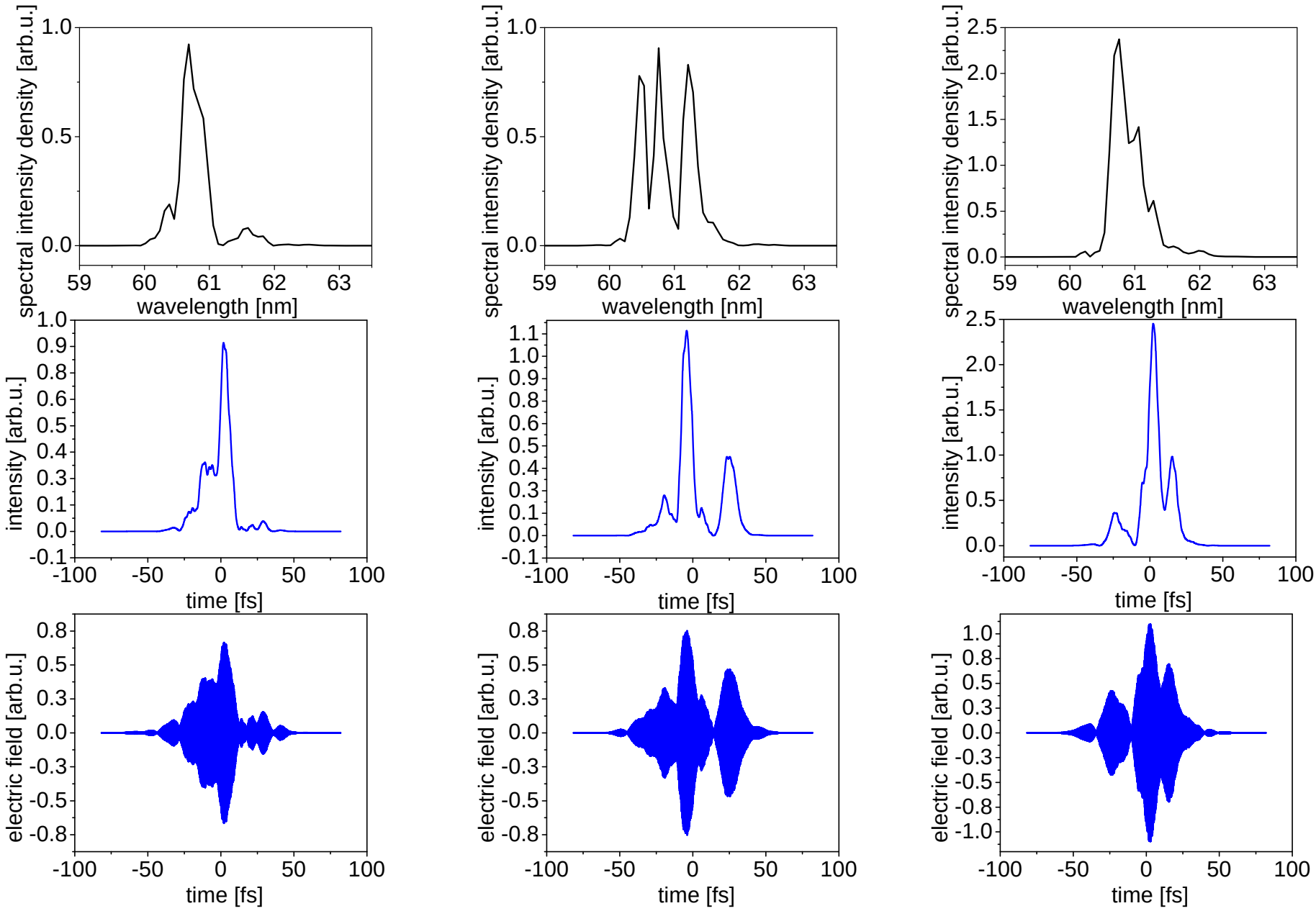

Experimental evidence for competition between the resonant and non-resonant two-photon ionization

R. Ma, K. Motomura, ***K.L. Ishikawa****, H. Fukuzawa, A. Yamada,*
K. Ueda*, K. Nagaya, S. Yase, Y. Mizoguchi,* ***M. Yao****, A. Rouzee,*
A. Hundermark, ***M. Vrakking, P. Johnsson****, M. Nagasono, K. Tono,*
T. Togashi, Y. Senba, H. Ohashi, M. Yabashi, and ***T. Ishikawa***

Photoelectron angular distribution for two-photon single ionization of He

Direct numerical simulation of the two-electron time-dependent Schrödinger equation (TDSE)

vs

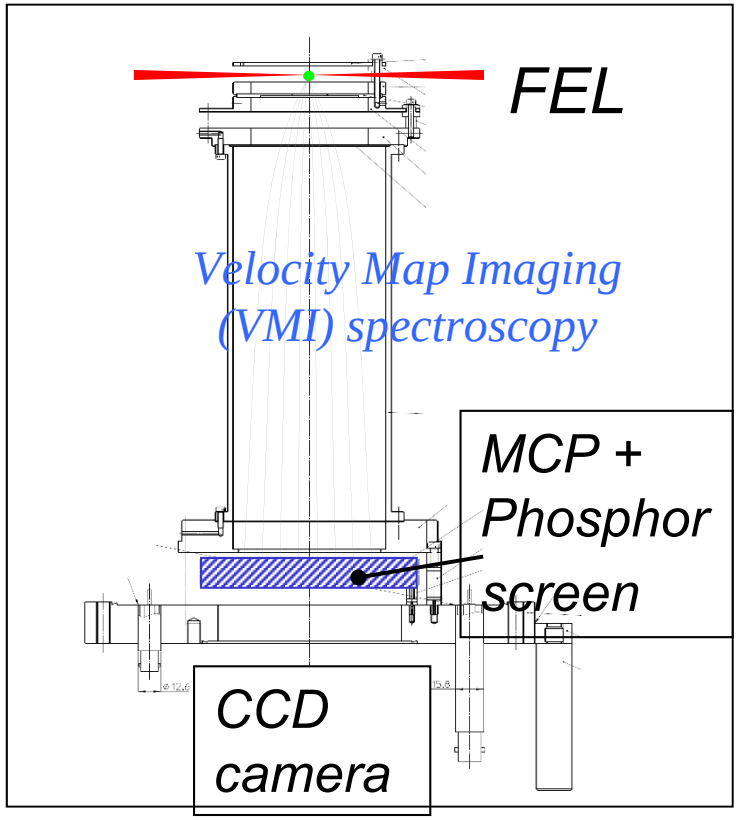

Excitation energies for two-photon ionization of He

Photon energy range available at SCSS test accelerator

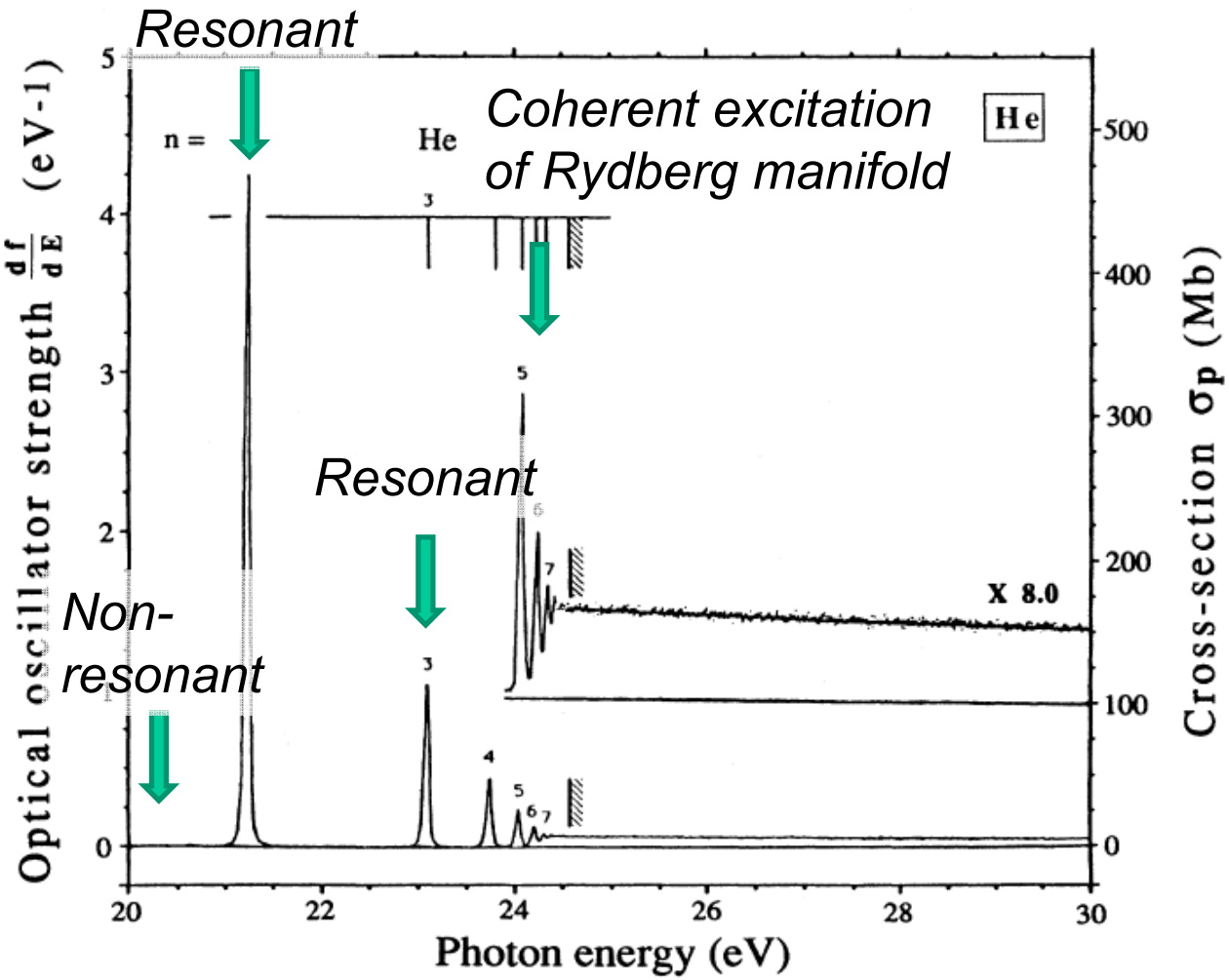

*W. F. Chan et al., Phys. Rev. A **44**, 186 (1991).*

Photoelectron angular distribution for two-photon ionization of He

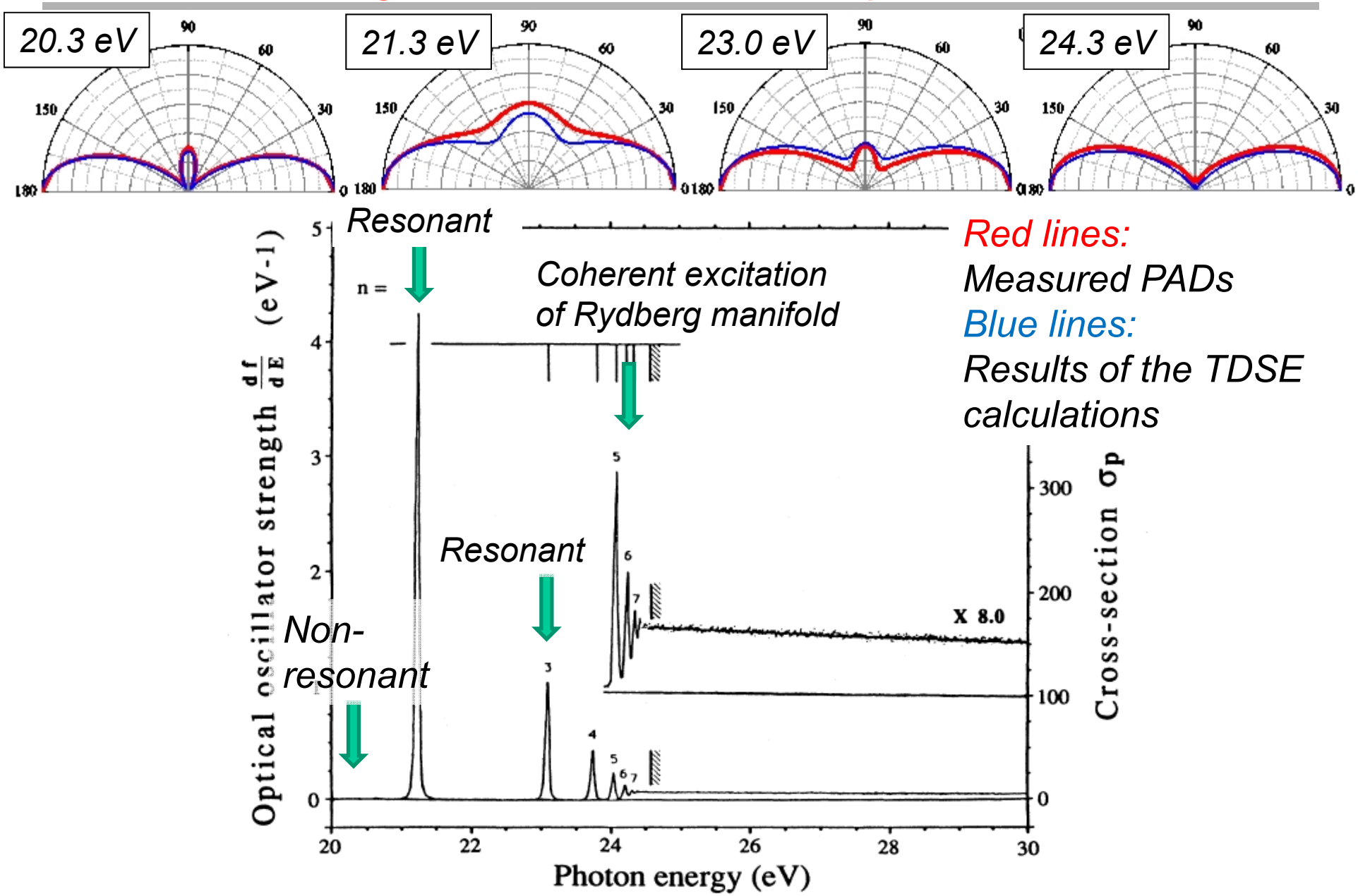

Red lines:
Measured PADs
Blue lines:
Results of the TDSE calculations

R. Ma, K. Motomura, K. L. Ishikawa, H. Fukuzawa *et al*., submitted.

Photoelectron angular distribution for two-photon ionization of He

$$I(\theta) = \frac{\sigma}{4\pi}\left[1 + \beta_2 P_2(\cos\theta) + \beta_4 P_4(\cos\theta)\right]$$

The outgoing photoelectron wave is a superposition of s and d waves.

Anisotropy parameters

$$\beta_2 = \frac{10}{W^2+1}\left[\frac{1}{7} - \frac{W}{\sqrt{5}}\cos\delta\right], \quad \beta_4 = \frac{18}{7(W^2+1)}$$

see:
*K. L. Ishikawa and K. Ueda, Phys. Rev. Lett., **108**, 033003 (2012).*

$W = |c_0 / c_2|$: *Amplitude ratio* , $\delta = \delta_0 - \delta_2$: *Phase difference*

c_l : *complex amplitude of a final state with an angular momentum l*
δ_l : *phase of each partial wave*

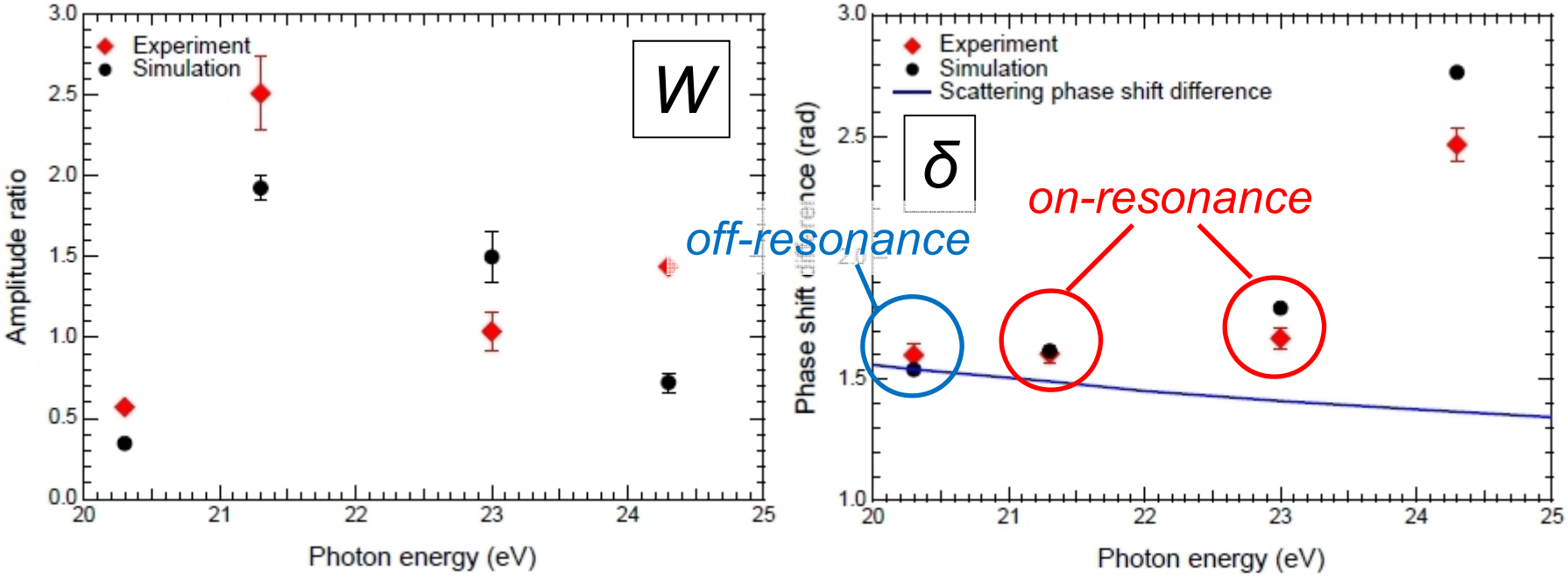

Deviation from scattering phase shift difference

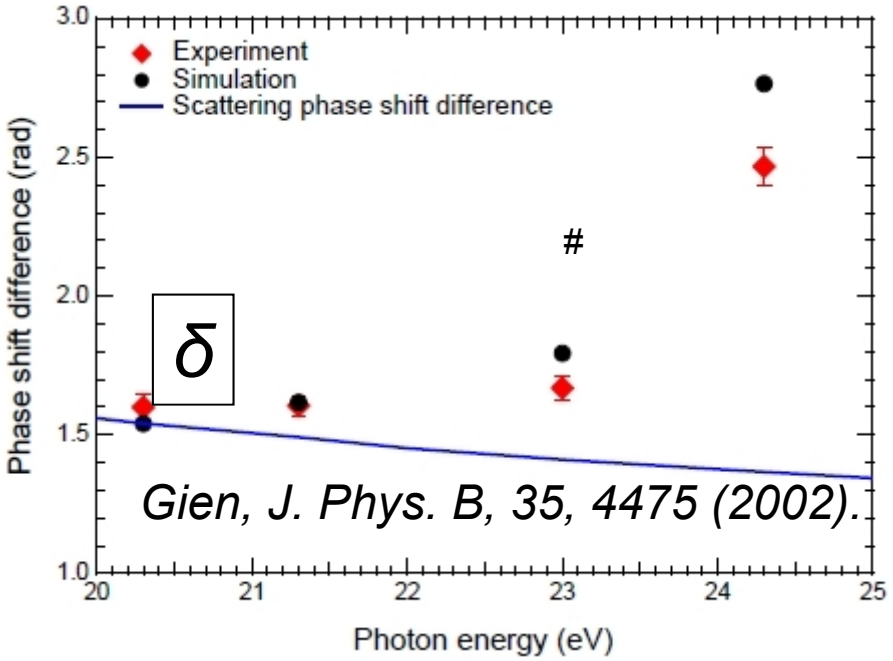

Gien, J. Phys. B, 35, 4475 (2002).

The excitation laser is a short pulse with finite width in both energy and time!
Taking it into account, we have

$$\delta = \delta_{\mathrm{SC}} + \mathrm{Arg}\, c_0 / c_2$$

Additional phase shift

δ_{SC} *: scattering phase shift difference*

K. L. Ishikawa and K. Ueda,
Phys. Rev. Lett., ***108***, *033003 (2012).*

$$c_f = \pi E_0^2 T^2 \sum_m \mu_{fm}\mu_{mi}\left[e^{-\Delta_m^2 T^2} - i\frac{2}{\sqrt{\pi}} F\left(\Delta_m T\right)\right]$$

$\Delta_m = \omega_m - (\omega_i + \omega)$ T: the pulse width

Deviation from δ_{SC} *is evidence of competition between resonant and non-resonant paths*

Tailoring continuum wavepacket controlling the additional phase shift by the short EUV pulses !

Dependence of W and δ on the pulse width of the Fourier transform limited pulse

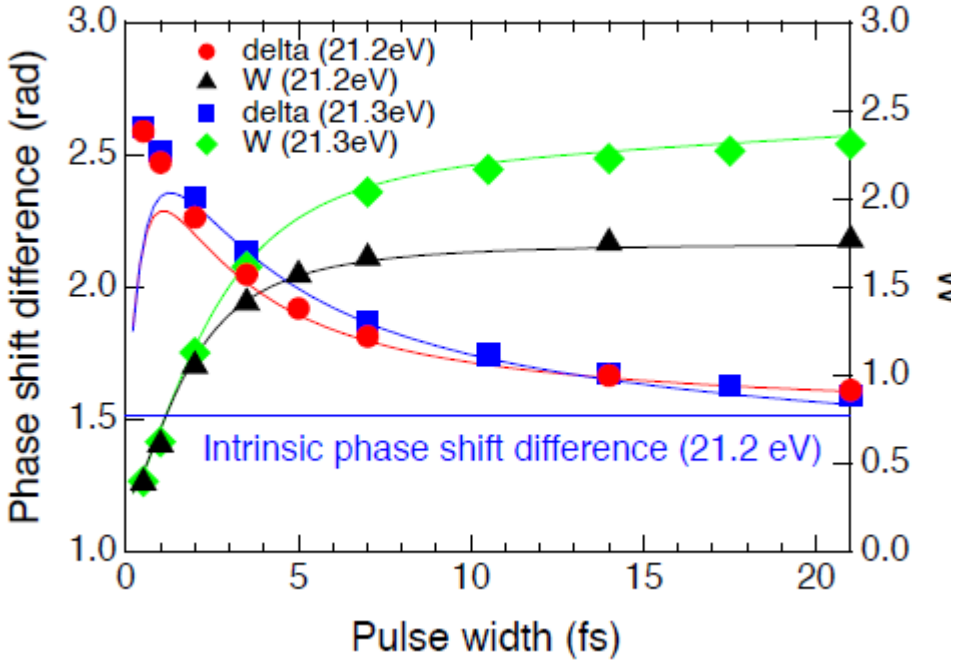

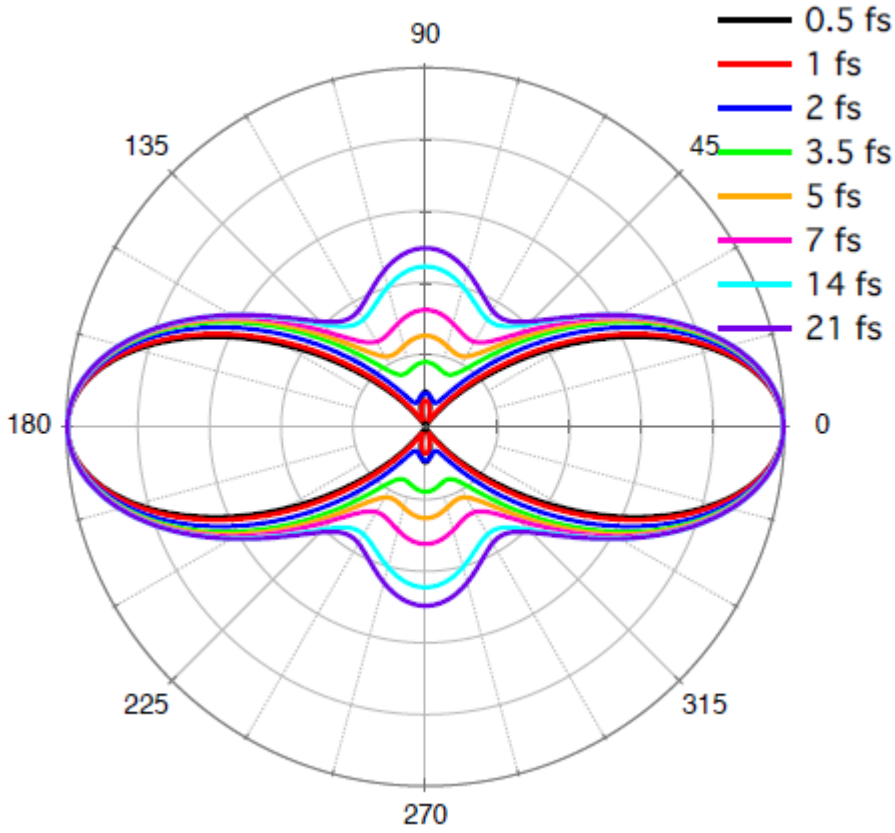

$$\frac{c_S}{c_D} = \frac{\mu_{Sr}}{\mu_{Dr}} \frac{\sqrt{\pi} T e^{-\Delta_r^2 T^2} - i[a_S + 2F(\Delta_r T)T]}{\sqrt{\pi} T e^{-\Delta_r^2 T^2} - i[a_D + 2F(\Delta_r T)T]}$$

$$\Delta_m = \omega_m - (\omega_i + \omega)$$

T: the pulse width

Chirping the pulse width from 500 as to 20 fs, we can control the contributions of direct and non-direct contributions

Tailoring the continuum wave packet (wave function)!

*Ishikawa and Ueda, PRL **108**, 033003 (2012).*

Multiple ionization of rare gas atoms irradiated by EUV free-electron laser pulses at 51 nm

K. Motomura, H. Fukuzawa, K. Papamihail, M. Kurka, A. Rudenko, L. Foucar, H. Iwayama, K. Nagaya, X.-J. Liu, H.-U. Kühnel, G. Prümper, P. Labropoulos, J. Ullrich, K. Ueda, N. Saito, H. Murakami, M. Yao, A. Belkacem, R. Feifel, M. Nagasono, A. Higashiya, T. Togashi, H. Ohashi, and H. Kimura, M. Yabashi, and T. Ishikawa

Ar $^{7+}$ > 434 eV
> 18 photons

Kr $^{8+}$ > 508 eV
> 21 photons

Mirror:
Mg/Si multilayer
f=250 mm,
made by LBNL

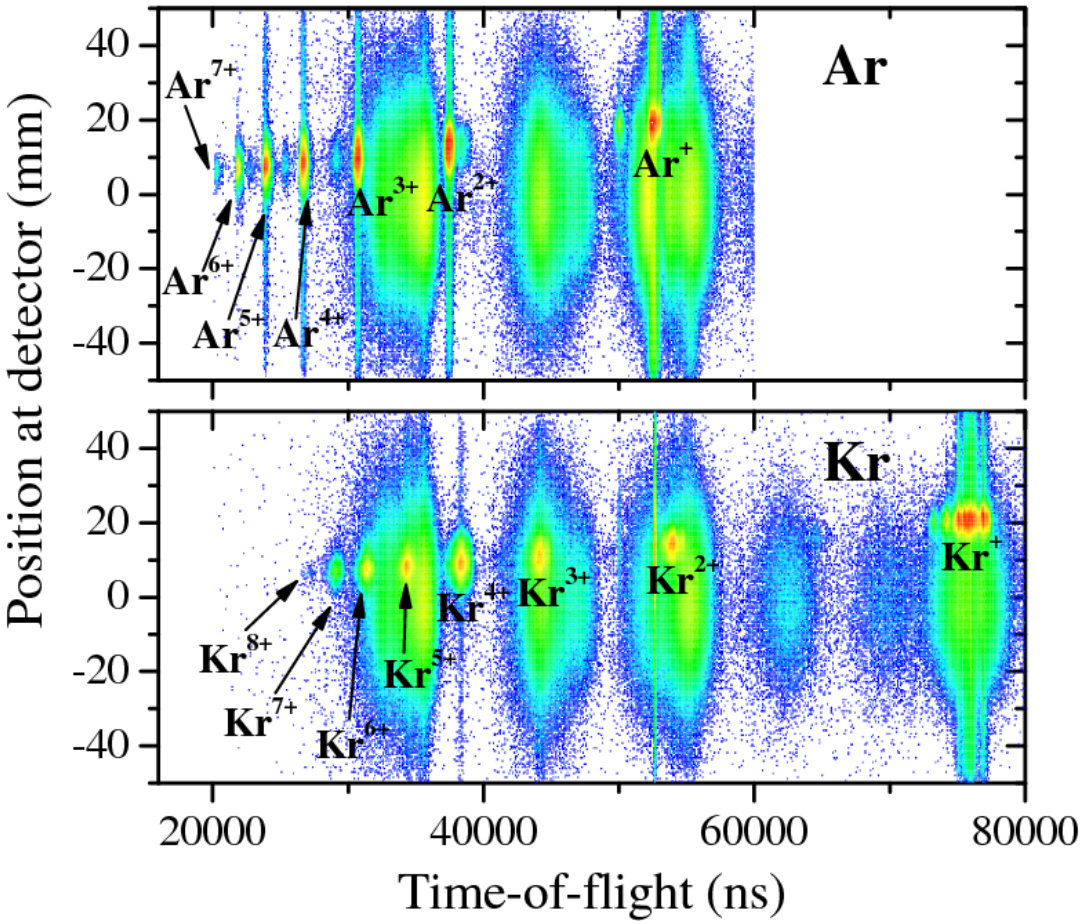

Deep inner-shell multiphoton absorption of Ar and Xe by SACLA XFEL pulses

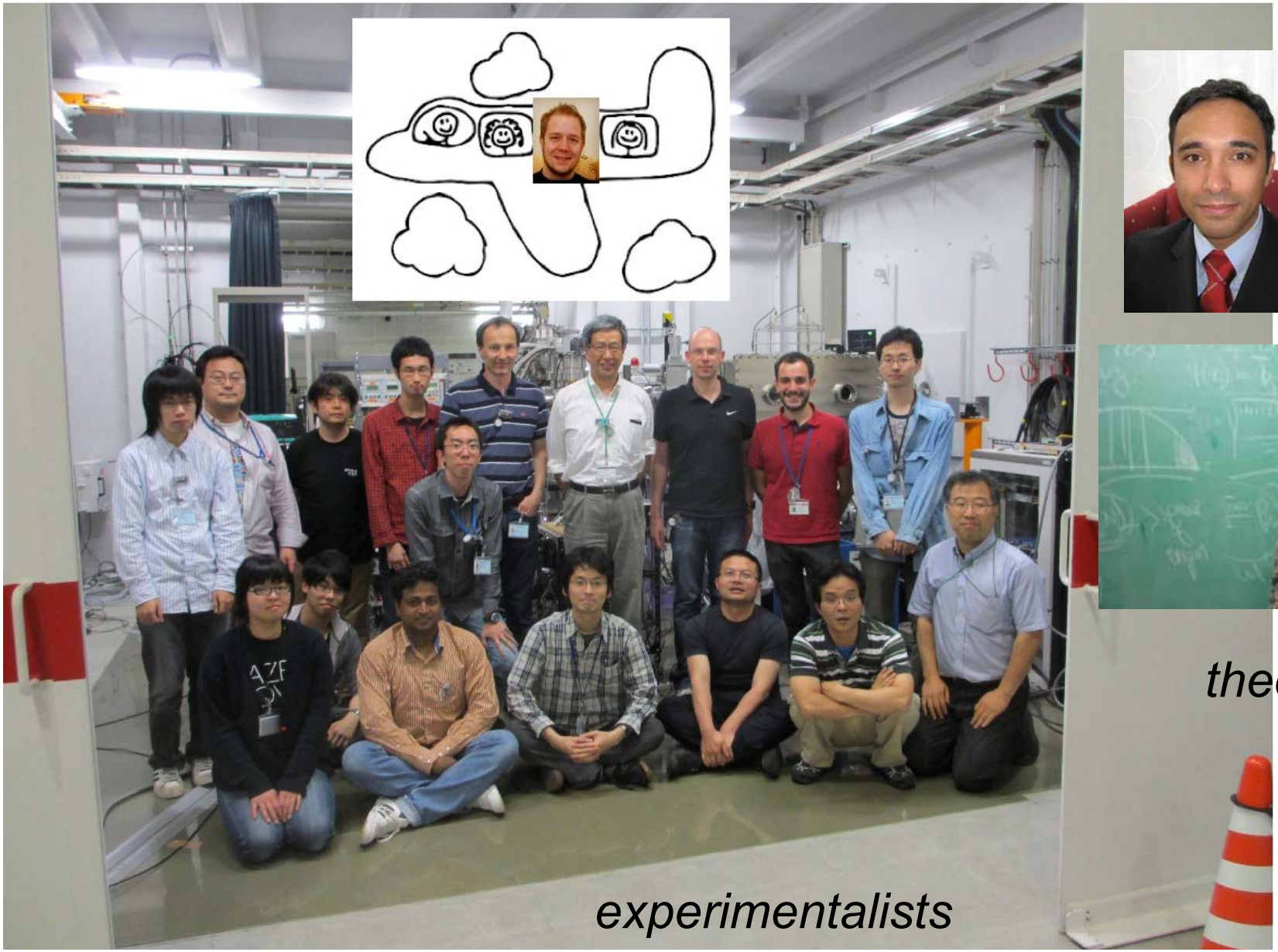

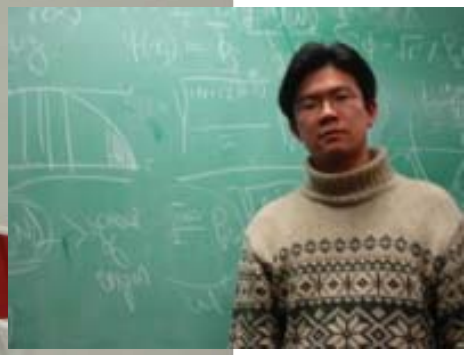

theorists

experimentalists

Time of Flight spectrum of argon ions

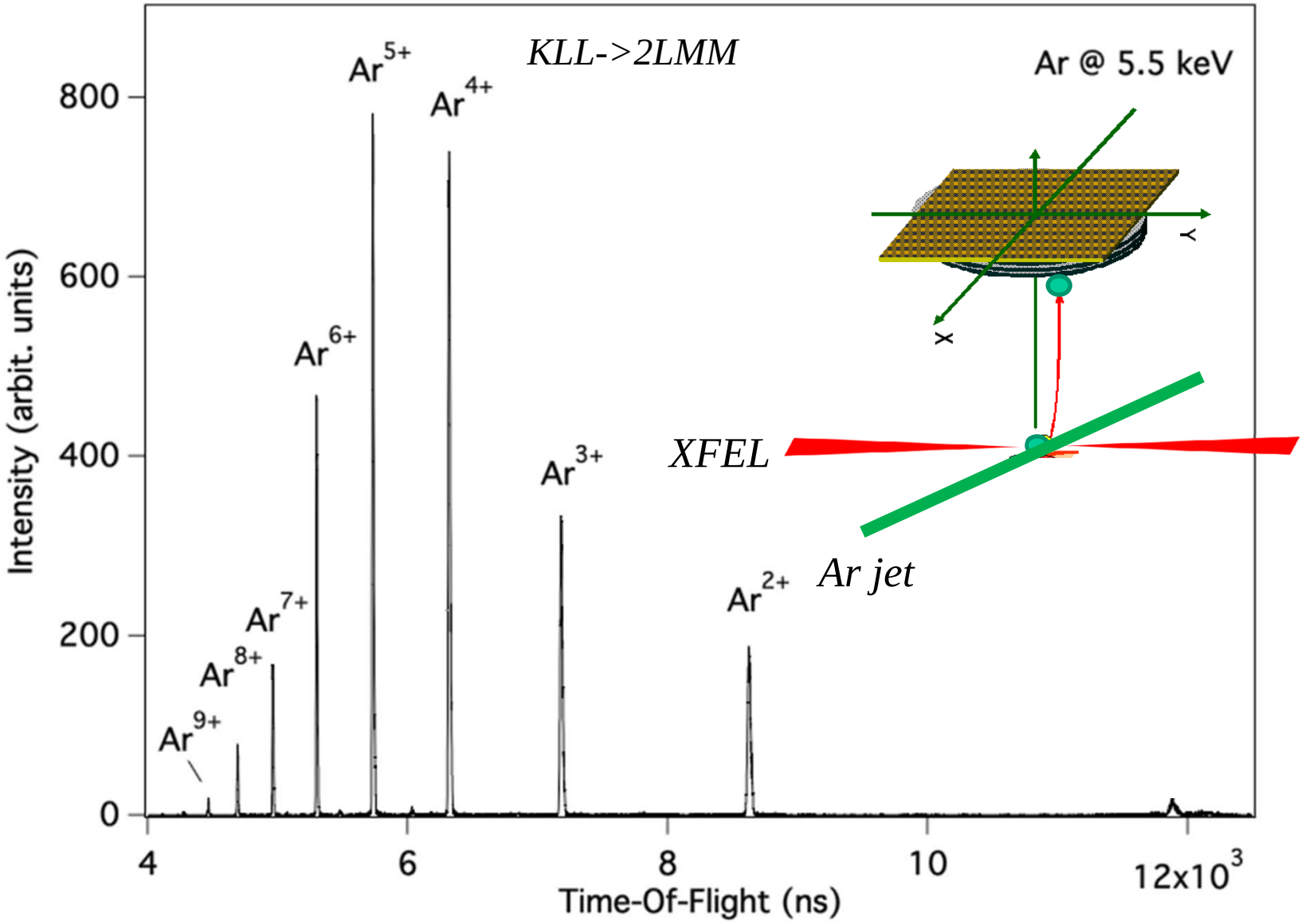

XFEL fluence dependence for Ar^{n+} yields

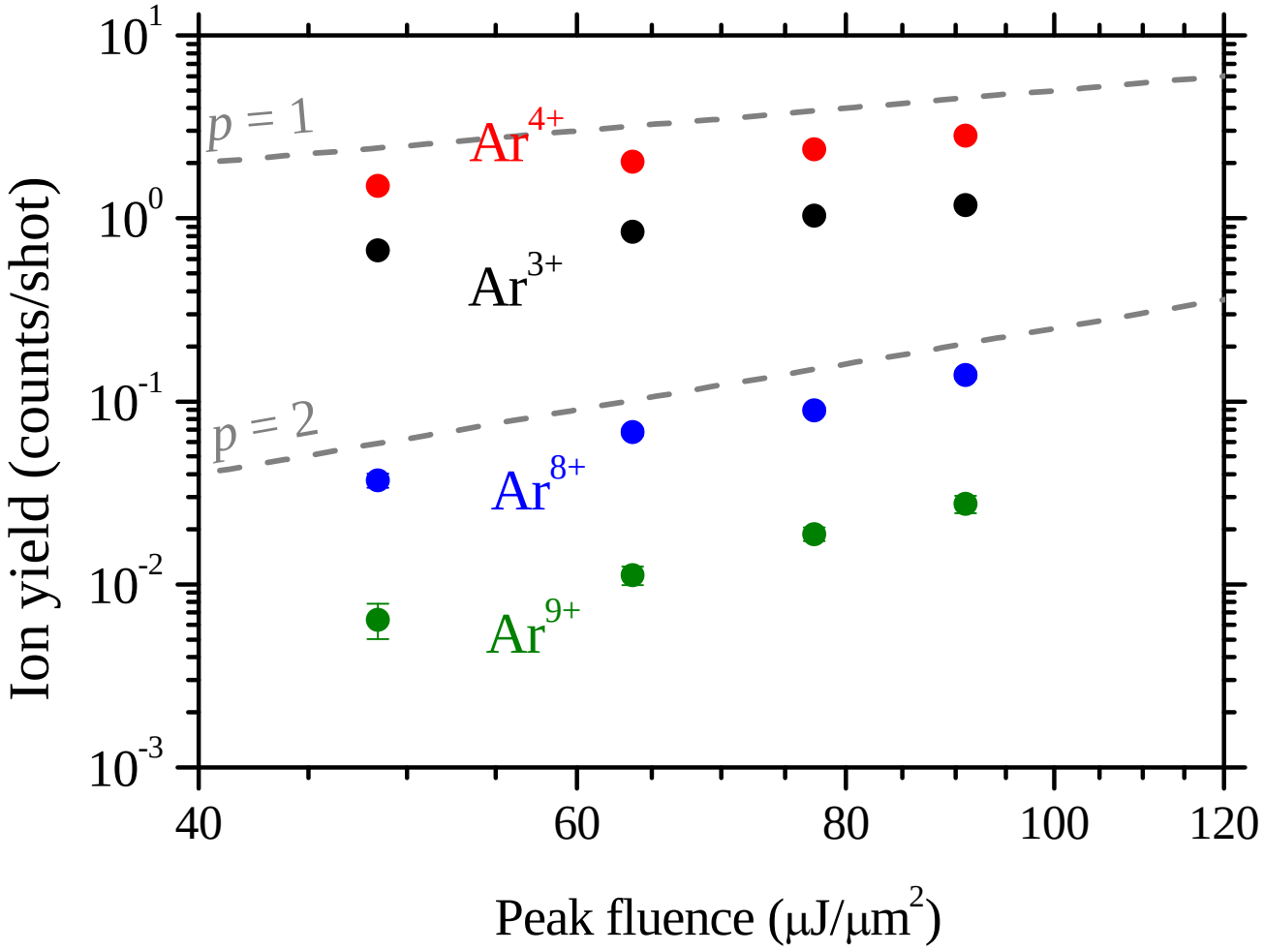

Charge state distribution of Ar: experiment and theory

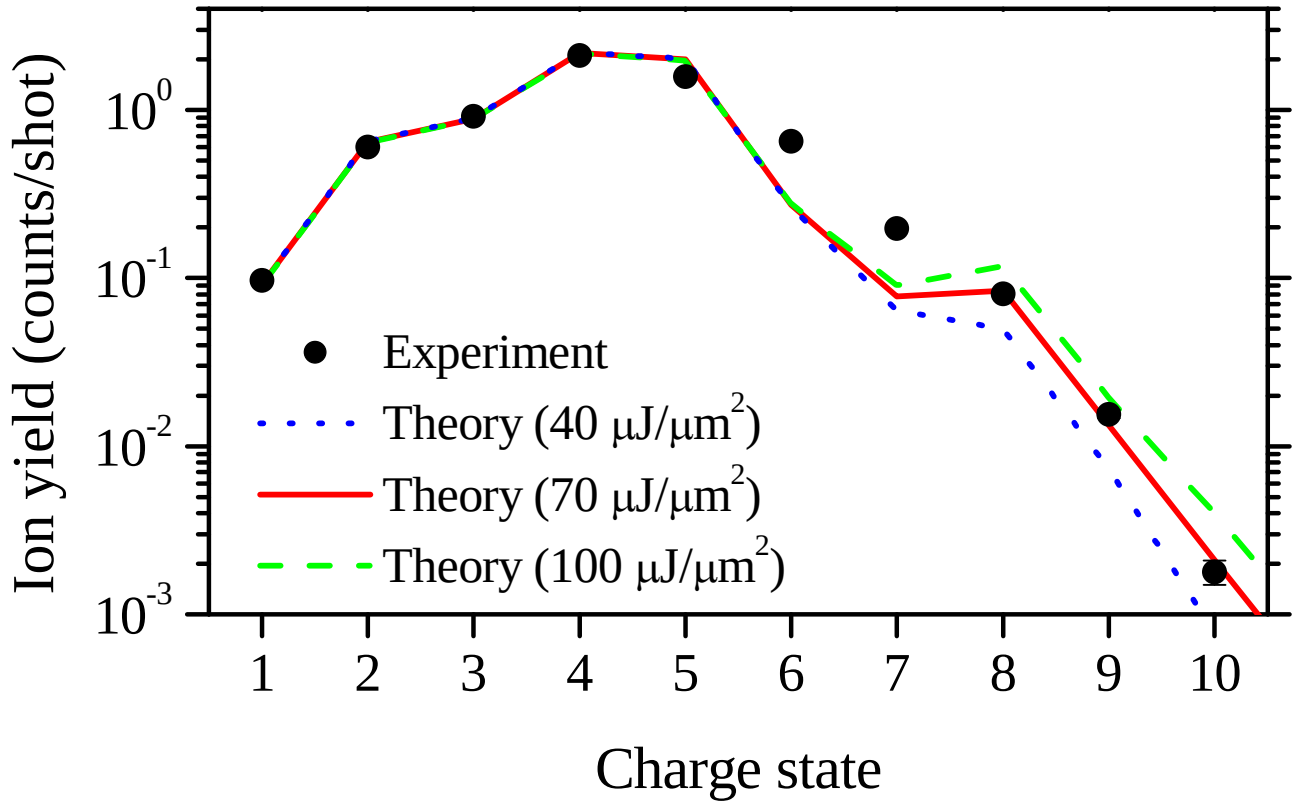

In the theory, the pulse shape of Gaussian of 30 fs (FWHM), and Gaussian focal shape of 1 μm (FWHM) × 1 μm (FWHM) are assumed.

By comparison with theory, we obtained peak fluence of 70 μJ/μm² in the experiment.

Time of Flight spectrum of xenon ions

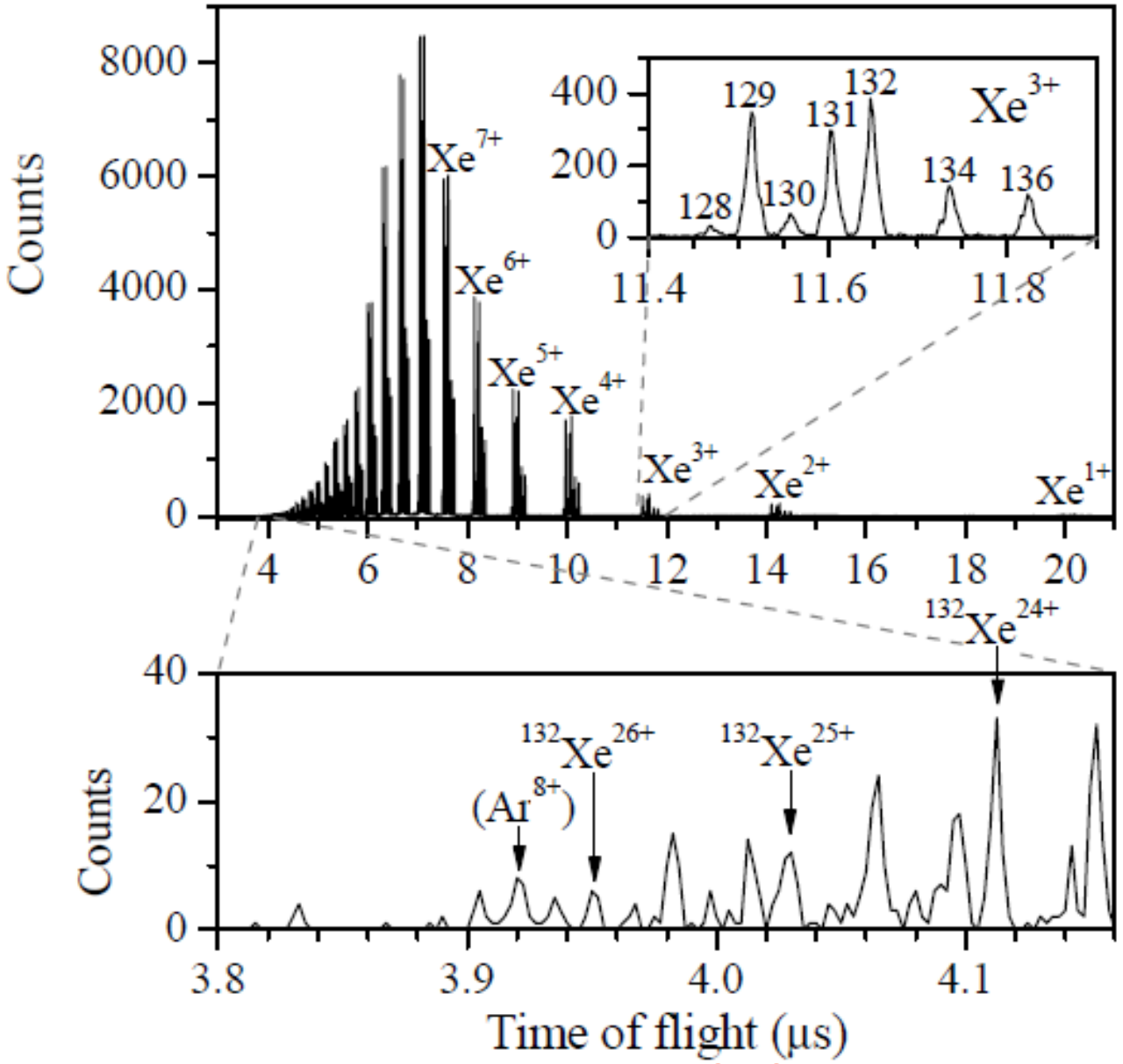

Experiment done at 5.5 keV, at SACLA !

Xenon ion charge distributions (exper. vs theory)

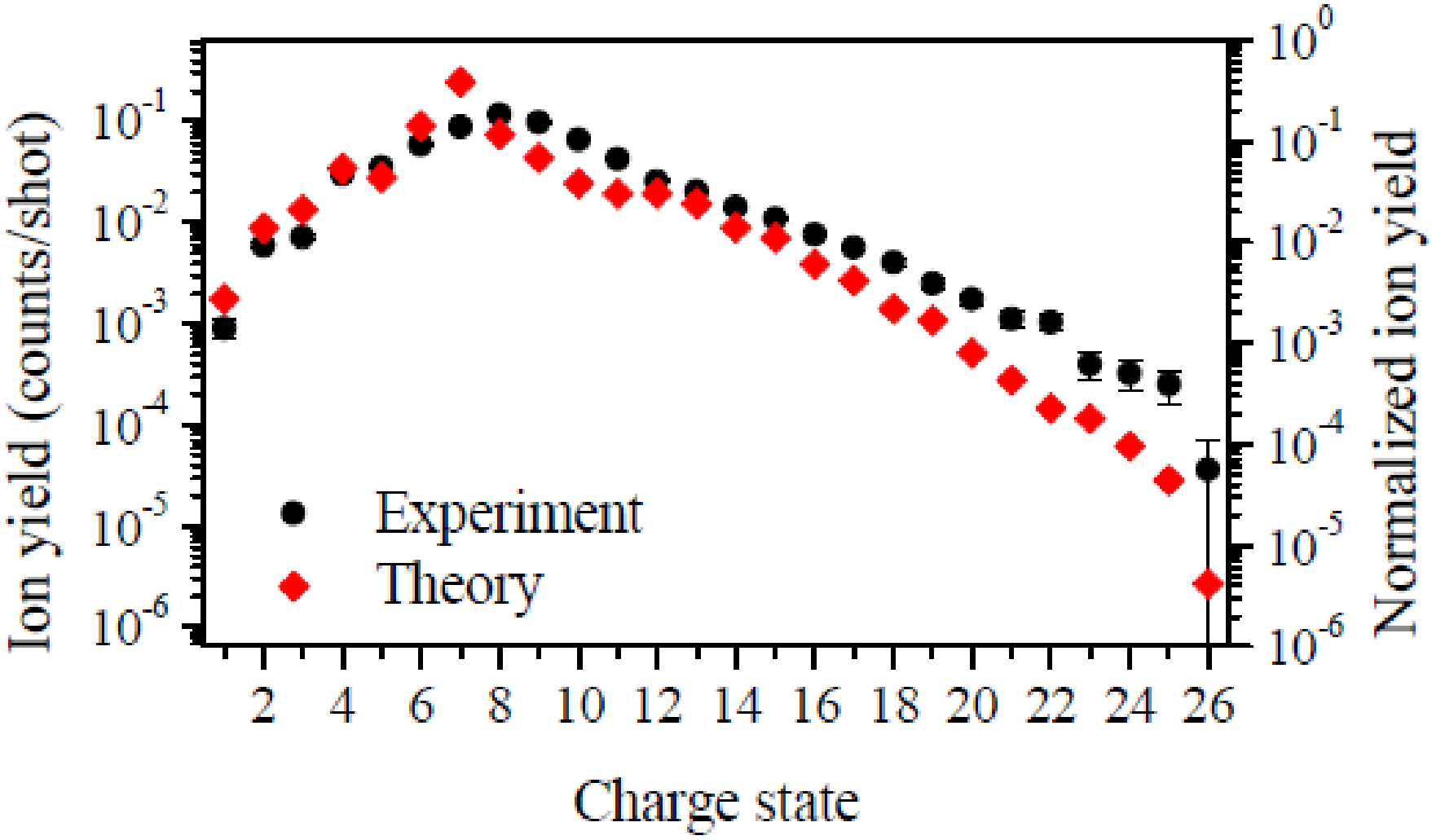

Experiment done at 5.5 keV, at SACLA !

XFEL fluence dependence for Xe^{n+} yields

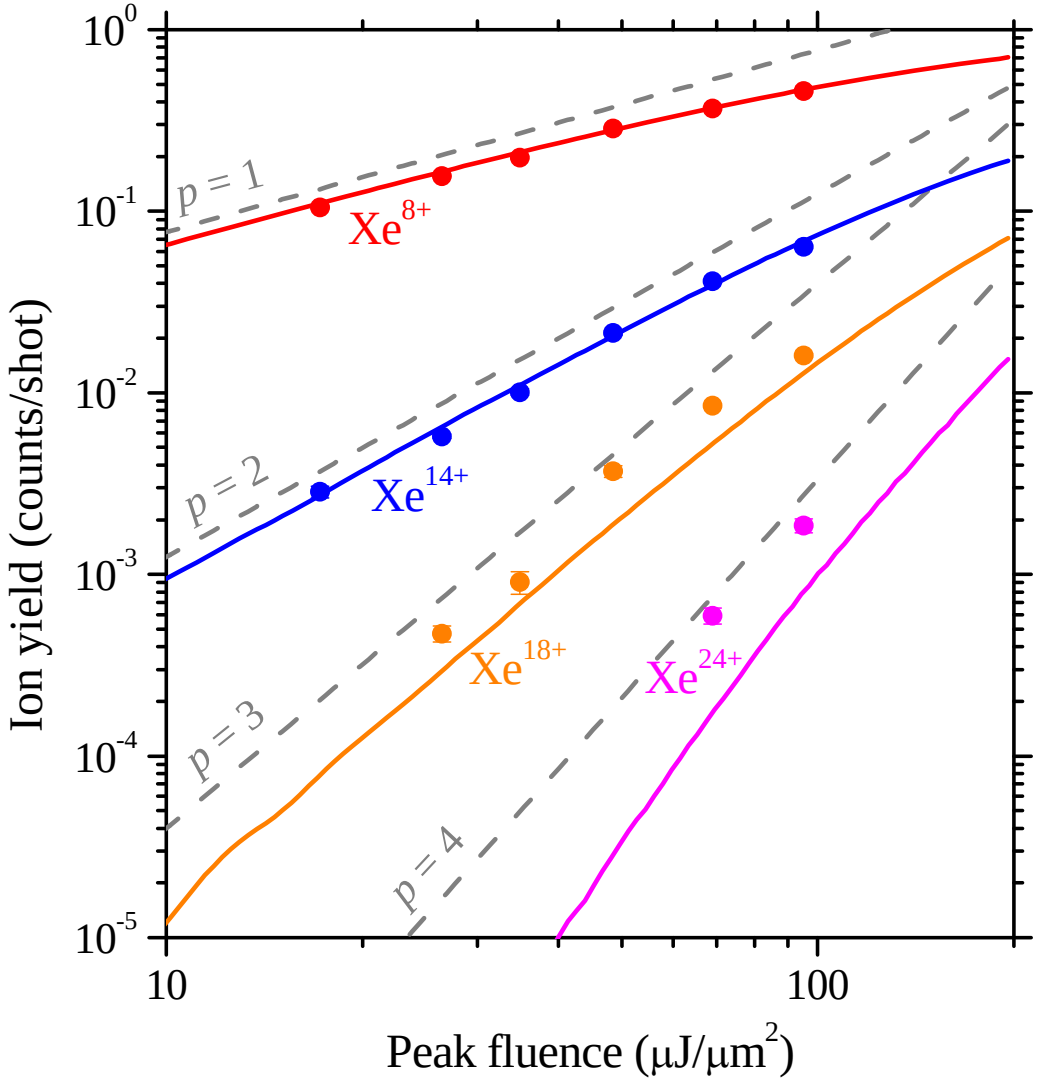

Xenon ion charge distributions (exper. vs theory)

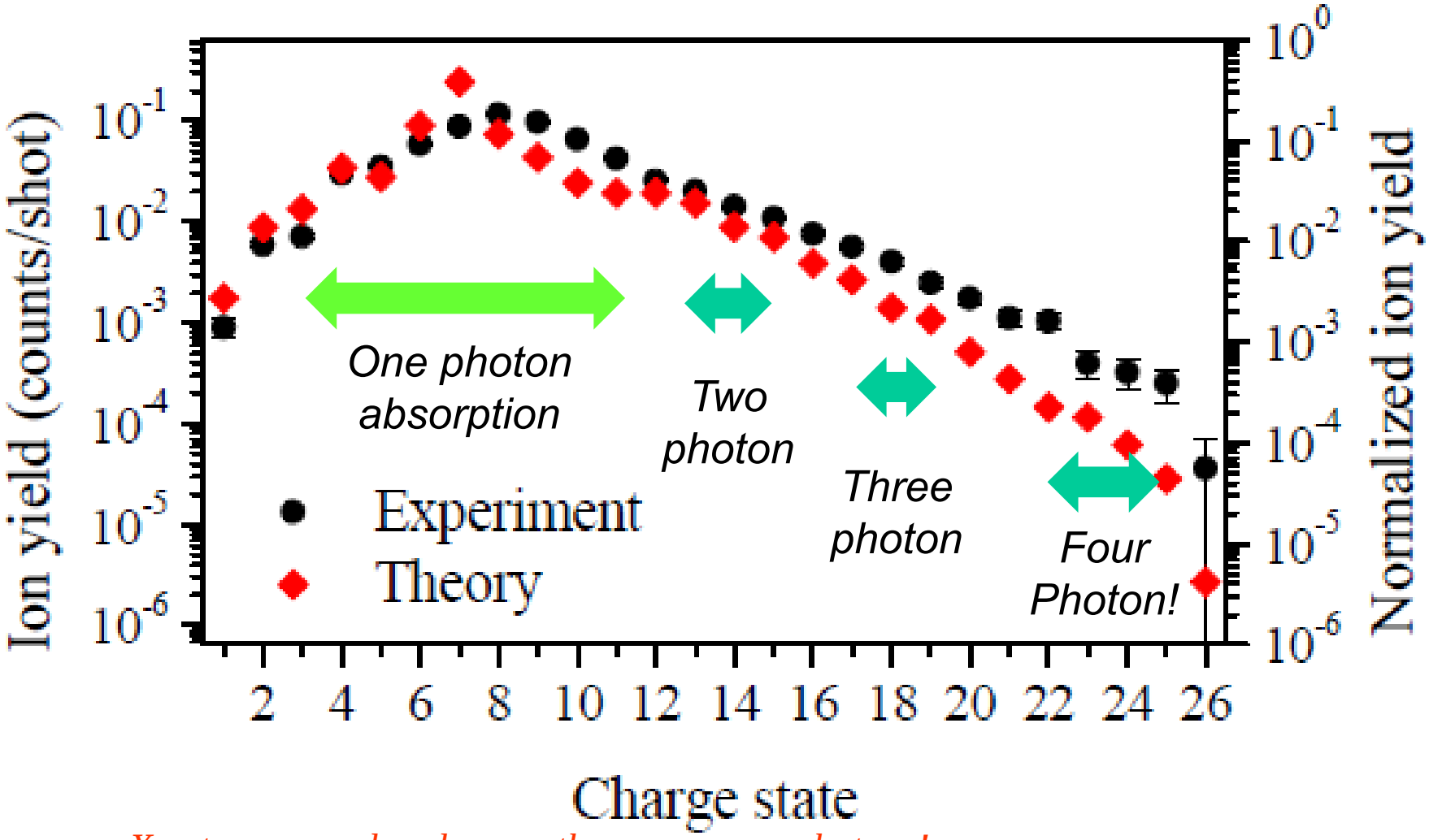

Xe atoms can absorb more than one x-ray photons!

Experiment done at 5.5 keV, at SACLA !

Relevance to other fields: Radiation damage

Radio-sensitizer

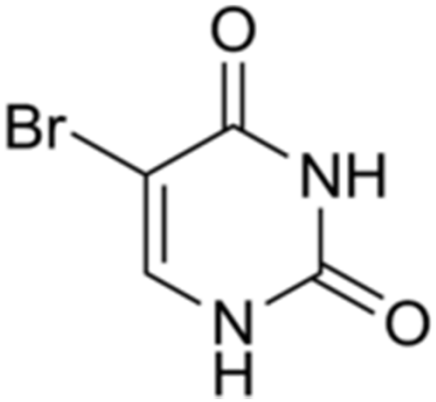

5Br-Uracil

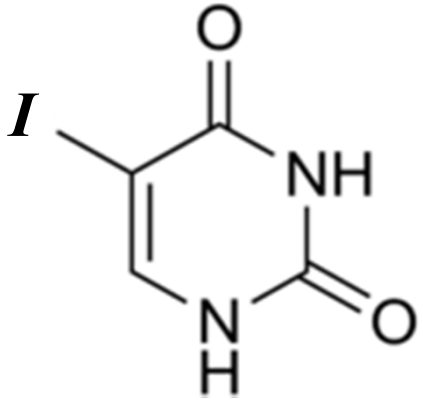

5I-Uracil

Anomalous X-ray scattering

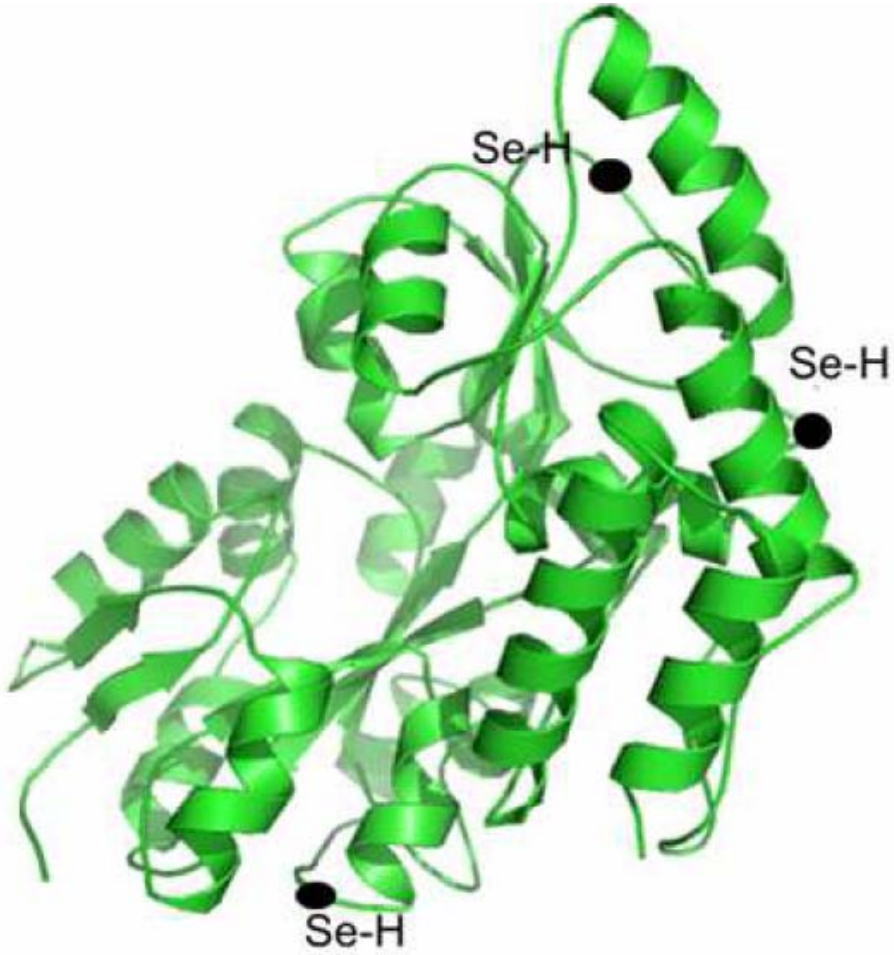

Multiwavelength anomalous diffraction at high X-ray intensity

S.-K. Son, H. N. Chapman, and R. Santra,
Phys. Rev. Lett. 107, 218102 (2011).

Deep inner-shell multiphoton ionization by intense x-ray free-electron laser pulses

H. Fukuzawa, S.-K. Son, K. Motomura, S. Mondal, K. Nagaya,
S. Wada, X.-J. Liu, R. Feifel, T. Tachibana, Y. Ito, M. Kimura,
T. Sakai, K. Matsunami, H. Hayashita, J. Kajikawa, P. Johnsson, M. Siano, E. Kukk, B. Rudek, B. Erk, L. Foucar, E. Robert,
C. Miron, K. Tono, T. Togashi, Y. Inubushi, T. Sato, T. Katayama,
T. Hatsui, T. Kameshima, M. Yabashi, M. Yao, R. Santra,
and K. Ueda (submitted)

A couple postdoc positions are open at Tohoku University for SACLA project!